# *Real-time Safety and Mobility-optimized Signalized Intersections*

DRAFT REPORT

for:

TRANSLINK New Mobility Research Grant (NMRG) Program 2019
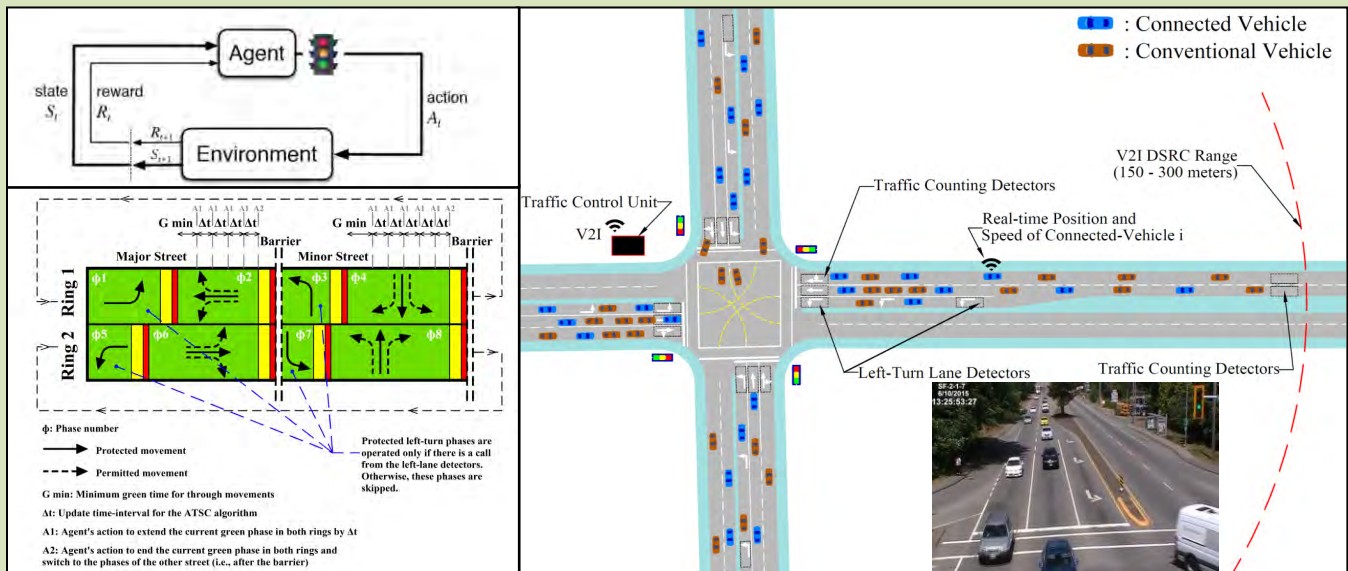
Prepared by:

Mohamed Essa, M.Sc., EIT.
PhD Candidate & Research Assistant

Tarek Sayed, PhD, P.Eng., FCAE, FEIC, FCSCE
Professor & Distinguished University Scholar

Department of Civil Engineering, University of British Columbia

February 2020

TABLE OF CONTENTS

University of British Columbia
Department of Civil Engineering

LIST OF FIGURES

LIST OF TABLES

EXECUTIVE SUMMARY

E.1   Introduction

One of the promising solutions to improve the safety and mobility of signalized intersections is the emerging Connected-Vehicles (CVs) technology. The concept of CVs refers to the capability of various elements of the transportation system (vehicles, bicycles, pedestrians, road infrastructure, traffic control, management centers, etc.) to electronically communicate with each other continuously in real-time (U.S. Department of Transportation, 2015). In such an environment, drivers can be supported with advisories and warnings to avoid collisions or unnecessary delays. In addition, traffic control devices, such as traffic signals and variable message signs, can be adapted in real-time to relieve congestion and improve safety. Existing research has demonstrated that CVs can potentially have considerable mobility, safety, and environmental benefits to road networks (Olia et al. 2016).

In the era of CVs, an enormous amount of high-resolution data on vehicle positions and trajectories will be generated in real-time. These data can potentially be used for real-time safety and mobility optimization of traffic signals. Using CVs data for *mobility* optimization at signalized intersections has been investigated in several studies (Lee et al., 2013; Guler et al., 2014; Feng et al., 2015). Various procedures have been proposed to minimize delays by adapting traffic signal controllers in real-time given data from vehicle-to-infrastructure (V2I) and vehicle-to-vehicle (V2V) communications. However, existing research has not considered the real-time *safety* optimization of traffic signals. This is mainly because safety optimization is more complicated than mobility optimization. Unlike vehicle delay and travel time, the safety level of signalized intersections is difficult to be directly estimated in real-time from CVs data. The main challenge is the lack of tools to evaluate the real-time safety of signalized intersections.

Traditionally, the safety of signalized intersections has often been evaluated at an aggregate level by relating historical collision records to the annual traffic volume and the geometric characteristics of the intersection. Relying on collision data in modelling real-time safety is very difficult for several reasons. First, the use of the historical collision data in safety analysis requires collisions to occur and be recorded over an adequately long period (usually years) to conduct a statistically sound safety diagnosis (Sayed and Zein, 1999; Chin and Quek,1997). Second, the use of several years of collisions requires reliance on aggregate exposure measures such as the annual average daily traffic (AADT) which does not explicitly account for the fact that not all vehicles are interacting unsafely and does not represent the variation of traffic flow within shorter periods. Third, important signal cycle-related variables that can affect intersection safety such as the arrival type and the shock wave characteristics are usually omitted due to the traffic data aggregation.

Therefore, there is an important need to develop safety models that can be used to evaluate the safety of signalized intersections in real time. Specifically, there is a need for models that can consider the effects of dynamic traffic parameters (e.g., traffic volume, shock waves, queue length, platoon ratio) on safety within short time periods (e.g., the signal cycle). These safety models could then be incorporated into an adaptive traffic signal control (ATSC) algorithm to optimize both

University of British Columbia
Department of Civil Engineering

traffic safety and traffic mobility using real-time CVs data. The feasibility of such an ATSC algorithm should also be investigated under various market penetration rates of CVs to represent the transition period that predates the full deployment of the CVs technology.

E.2   Research Objectives

Toward optimizing safety and mobility of signalized intersections in real time using CVs data, this research has the following key objectives:

1. To develop, using real-world traffic data, safety models for signalized intersections at the signal cycle level that can be used to evaluate safety in real time based on various dynamic traffic parameters, such as traffic volume, queue length, shock waves, and platoon ratio
2. To investigate the transferability of the developed real-time safety models across different locations/jurisdictions
3. To develop, using traffic microsimulation models, a practical ATSC algorithm that can utilize CVs data to optimize safety of signalized intersection in real time
4. To test and validate the developed ATSC algorithm using real-world traffic data
5. To investigate the safety and mobility performances of the developed ATSC algorithm under various market penetration rates of CVs

E.3   Real-Time Safety Models

The first objective of this research is to develop real-time safety models for signalized intersections at the signal cycle level. The models relate the number of rear-end conflicts occurring in each signal cycle to dynamic traffic variables such as traffic volume (V), maximum queue length (Q), shock wave characteristics [e.g. shock wave speed (S_{12}) and shock wave area (A)], and the platoon ratio (P) (**FIGURE E.1**). The models were developed using real-world traffic data obtained from six signalized intersections located in Surrey, British Columbia, and Edmonton, Alberta (**TABLE E.1**). The approach that we followed in this research to develop these models provides several advantages as follows:

- The use of real-world traffic data, obtained from video recordings at six different intersections, which reflects actual driving behavior (i.e. the results are not based on microsimulation models).
- Proposing a video analysis procedure to collect data at the cycle level.
- The use of traffic conflicts as a measure of safety. Conflicts are extracted automatically and quantified using a conflict indicator (e.g. Time to collision). Also, the actual conflict location is determined.
- The proposed approach allows for the extraction of various traffic parameters including: the traffic volume, the maximum queue length, the shock wave characteristics, and the platoon ratio.
- The traffic conflict data and the traffic parameters are measured directly from the recorded video data and evaluated at the signal cycle level. As such, no hourly aggregation is needed.

FIGURE E.1: Traffic Parameters for Real-time Safety Models

TABLE E.1: Description of the Study Locations

Site #	City	Roads	Selected approaches	Number of Lanes	Video scene
1	Edmonton (AB)	Stony Plain Rd & 170 St	170 St (Northbound)	1 (Right) 1 (Left) 4 (Through)	
2	Edmonton (AB)	Gateway Blvd & 34 Ave	Gateway Blvd (Northbound)	1 (Right) 1 (Left) 4 (Through)	
3	Surrey (BC)	72 Ave & 128 St	72 Ave (Eastbound)	1 (Left) 2 (Through)	
4	Surrey (BC)	72 Ave & 132 St	72 Ave (Westbound)	1 (Left) 2 (Through)	

University of British Columbia
Department of Civil Engineering

3

Site #	City	Roads	Selected approaches	Number of Lanes	Video scene
5	Surrey (BC)	64 Ave & King George Blvd	King George Blvd (Southbound)	1 (Right) 1 (Left) 2 (Through)	
6	Surrey (BC)	Fraser Highway & 168 A St	Fraser Highway (Southbound)	1 (Bike lane) 1 (Left) 2 (Through)	

The models were developed using the generalized linear models (GLM) approach. Six different real-time safety models were developed using different combinations of the explanatory variables (**V**, **A**, **Q**, **S12**, and **P**). **TABLE E.2** provides a summary of the developed real-time safety models.

TABLE E.2: Real-time Safety Models

Base models developed from the base jurisdiction dataset (Canada)								
Model# * $E(Y) =$	**Variables**	**Error Structure**	**K**	**SD**	**df**	**χ²**	**AIC**
One Variable (Exposure only): **Model 1:** $V^{1.563}exp(-3.231)$	V	NB	3.05	249	220	356	775
(Exposure + One Variable): **Model 2:** $V^{0.706}exp(-1.797 + 0.501\,A)$	V, A	NB	14.9	244	219	241	702
Model 3: $V^{0.65}exp(-2.046 + 0.0122\,Q)$	V, Q	NB	8.73	243	219	253	716
Model 4: $V^{1.637}exp(-3.316 + 0.05\,S_{12})$	V, S_{12}**	NB	3.10	248	219	347	775
Model 5: $V^{1.571}exp(-1.768 - 1.266\,P)$	V, P	Poisson	---	276	219	281	706
Combined Model: **Model 6:** $V^{1.239}exp(-1.624 + 0.294\,A - 0.828\,P + 0.119\,S_{12})$	V, A, P, S_{12}	Poisson	---	240	217	215	674

K: Shape parameter for Negative Binomial family
All variables are significantly different from zero at 95% confidence level
*Y: Number of rear-end conflicts per cycle with TTC equal or less than 1.50 seconds
**Significantly different from zero at 90% confidence level

The results show that all models have good fit and almost all the explanatory variables are statistically significant leading to better prediction of conflict occurrence beyond what can be expected from the traffic volume only. The developed models can give insight about how real-time changes in the signal cycle design affect the safety of signalized intersections. The developed real-time safety models can have the following potential applications:

- Safety evaluation using field-observed data
- The real-time safety optimization of signalized intersections

E.4   Transferability of Real-time Safety Models

After developing the real-time safety models for signalized intersections, the second objective of this research is to investigate the transferability of these models across various locations/jurisdictions. Two different datasets, from two corridors of signalized intersections in California and Atlanta in USA, were used as destination jurisdictions for the transferability analysis (**FIGURE E.2**). For each corridor, detailed traffic data was obtained from the NGSIM vehicle trajectories and supporting data provided online by the United States Department of Transportation (US DOT, 2018).
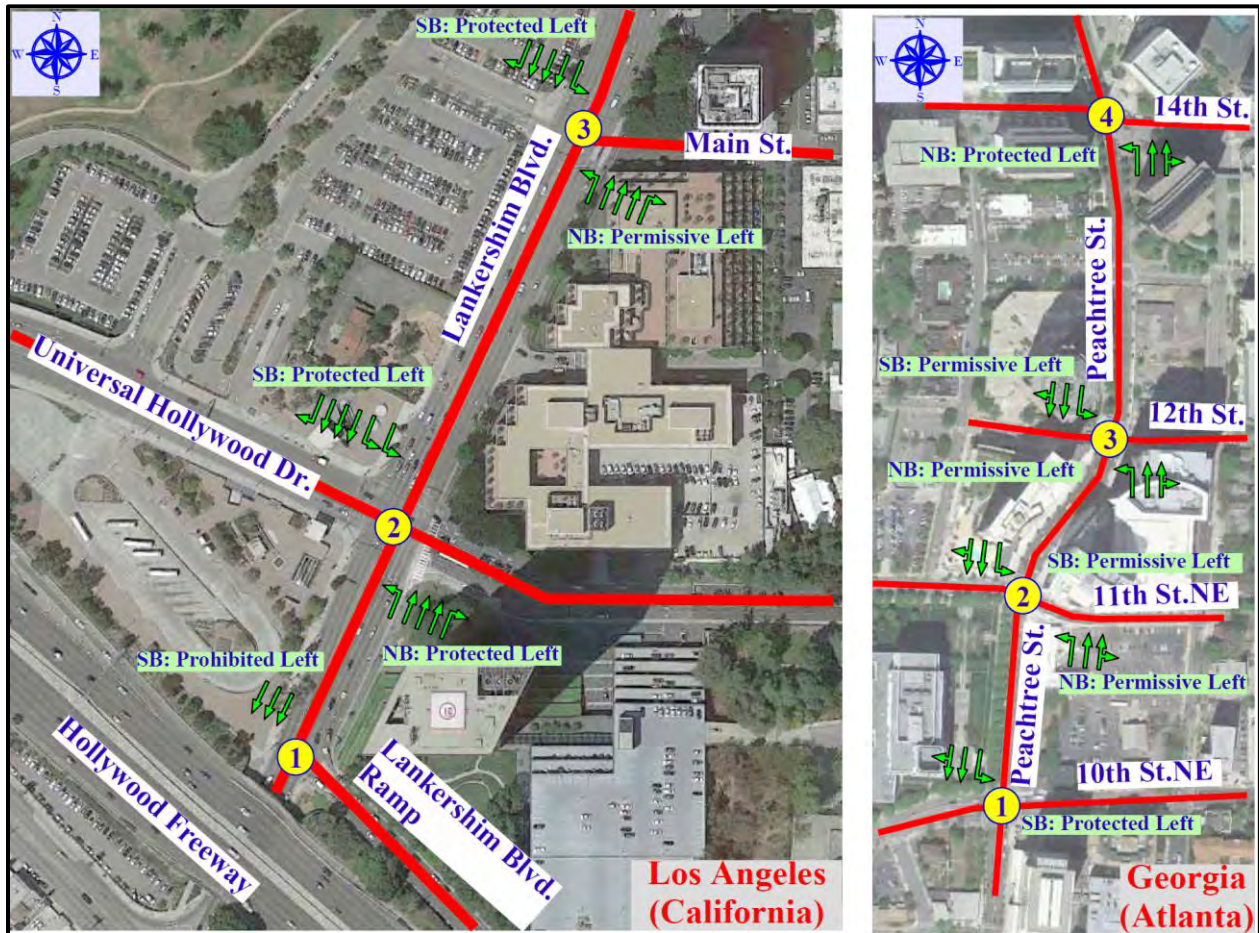
- The left image shows the first destination Jurisdiction (Lankershim Blvd., Los Angeles, California, USA)
- The right image shows the second destination jurisdiction (Peachtree St., Georgia, Atlanta, USA)
FIGURE E.2: Destination Jurisdictions

Several conventional measures of transferability and goodness-of-fit (GOF) were estimated to assess the ability of the transferred models to predict traffic conflicts at the new jurisdictions (the application jurisdictions). These measures are: Transfer Index (TI); Akiake's Information Criterion (AIC) (Akaike, 1974); Pearson's product moment correlation coefficient (r); Mean prediction bias (MPB); Mean absolute deviation (MAD); Mean absolute percentage error (MAPD); Pearson chi-squared (χ^2) (Pearson, 1900); Z-score (Vogt and Bared, 1998), and the highway safety manual calibration factor (C) (AASHTO, 2010). All of these measures compare the predicted conflicts obtained from the model with the observed ones at the new jurisdictions.

To analyze the transferability of the developed models, two transferability approaches were applied: 1) the application-based approach, and 2) the estimation-based approach. In the application-based approach, the base model developed from the base jurisdiction (Canada) is applied with no change (without calibration) to the destination jurisdiction (California and Atlanta) to assess how well the model predicts at the new region. In the estimation-based approach, the base model parameters estimated from the base jurisdiction data are recalibrated using the destination jurisdiction data. Two methods of calibration were considered herein. The first method comprises the calibration of the model intercept and the shape parameter only, while the second method considers the calibration of all the model parameters.

Overall, the results showed that the real-time safety models are fairly transferable among different sites. The transferred models generally, with and without calibration, were shown to have a good fit for the destination jurisdiction datasets. However, there was a notable improvement in the GOF measures for all models in general after calibrating the intercept and the shape parameter. This is expected as the local calibration of the intercept and the shape parameter allows the transferred models to better suit local conditions at the destination jurisdictions. The GOF measures were further improved after redeveloping the models in the second calibration method. This is reasonable because the new models are locally developed by maximizing the likelihood function using the new data from the destination jurisdictions, which leads to a better fit. However, comparing to the first calibration method, the improvement in the GOF measures was slight. This means that calibrating only the intercept and the shape parameter seems sufficient to transfer the base safety models to new jurisdictions.

Based on the transferability analysis results and considering the base jurisdiction as well as the two destination jurisdictions, the model that combined the traffic volume and the shock wave area was the most recommended model due to several reasons. First, the inclusion of the shock wave area as an explanatory variable in the safety model is logically valid. The covariate shock wave area enables the model to discriminate between different cycles even at the same traffic volume, and describes indirectly the maximum queue length and the vehicle arrival pattern. Most importantly, the effects of real-time signal changes on traffic conflicts can be captured in the real-time safety model through the shock wave area. Second, the recommended model showed a good fit at the three studied jurisdictions. Finally, the regression results of the recommended model are consistent at the three jurisdictions in terms of the sign and the value of each model parameter.

E.4   Self-Learning Adaptive Traffic Signal Control for Real-Time Safety Optimization

The third contribution of this research is to develop a novel self-learning adaptive traffic signal control algorithm to optimize traffic safety in real time using CVs data. The developed algorithm is referred to as RS-ATSC (*Real-time Safety-optimized Adaptive Traffic Signal Control"*. The RS-ATSC algorithm is based on the real-time safety models presented earlier in this report (**TABLE E.2**). To the best of our knowledge, the RS-ATSC is the first self-learning ATSC algorithm that uses CVs data to optimize traffic safety in real time.

The RS-ATSC algorithm was developed using the Reinforcement Learning (RL) technique (**FIGURE E.3**). Specifically, the Q-learning off-policy method was applied. In the developed Q-learning algorithm, the state is defined using vehicle speeds and positions upstream all approaches within a specific Vehicle-to-infrastructure Dedicated Short-range Communications (V2I DSRC) domain. The action space includes only two actions representing the fixed phasing sequence. Thus, every time step, the RL agent decides whether to extend the current green time or to switch the green light to the next phase (**FIGURE E.4**). The reward function is defined by the shock wave area between consecutive time steps as a penalty. In addition, several constraints are considered to ensure the safety and feasibility of implementing the proposed algorithm in real-world. This includes accommodating the yellow time, the all-red time, the minimum green time, and the maximum green time, whenever they are necessary.
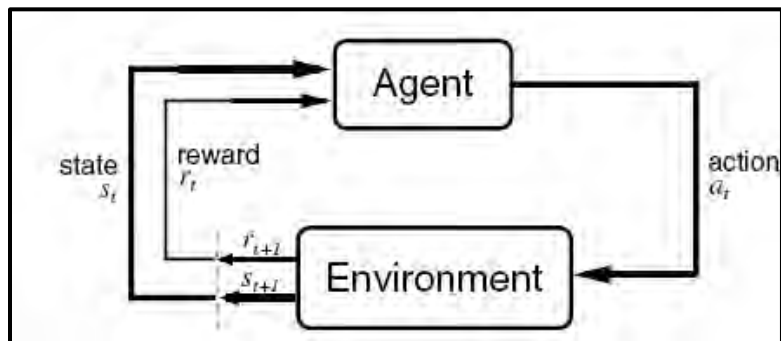
FIGURE E.3: The Agent–environment Interaction in Reinforcement Learning (Sutton and Barto 1998)
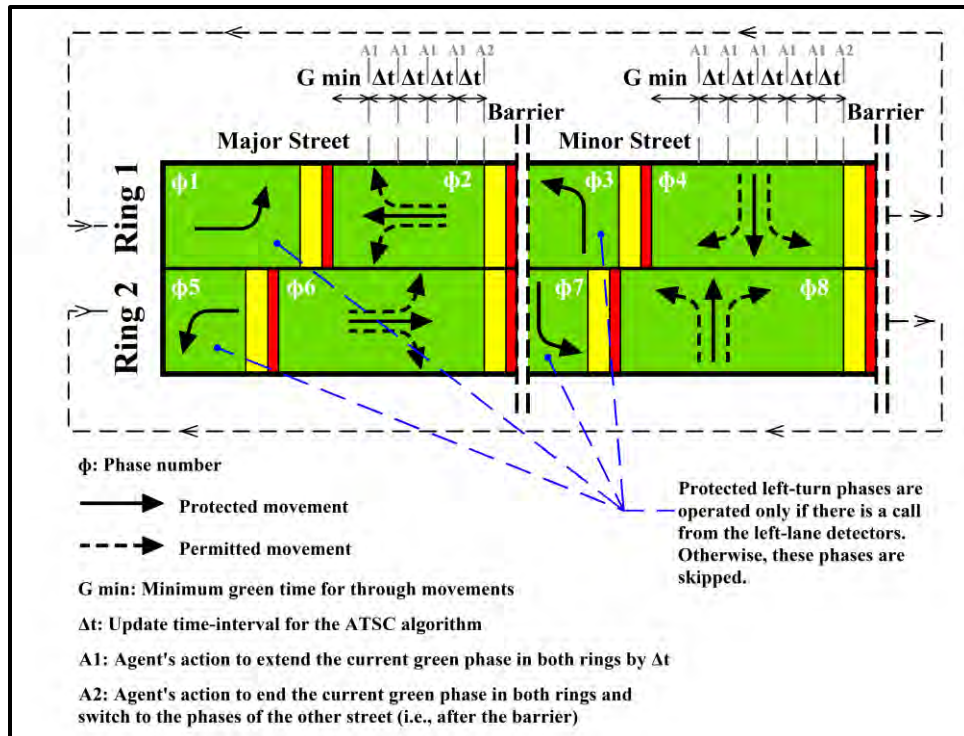
FIGURE E.4: Phasing Sequence and Possible Actions of the RL Agent in the Proposed RS-ATSC Algorithm for 4-leg Intersections with Protected-permissive Left-turns

To train the RS-ATSC algorithm, an isolated intersection was modelled in the simulation platform VISSIM. The VISSIM model was controlled by an external program to emulate the CVs environment as well as real-time signal changes. In the learning process, the simulation model was run using random traffic volumes for 633 episodes, each includes 20,000 seconds. The RS-ATSC agent converged to the optimal policy after about 550 episodes. The average shock wave area was reduced from approximately 0.11 km. s/vehicle at the beginning of the learning process to 0.02 km. s/vehicle when the convergence was reached.

The trained RS-ATSC algorithm was validated using real-world traffic data of two signalized intersections in the City of Surrey, British Columbia (**FIGURE E.5**). The algorithm's performance was compared with the performance of the existing fully-actuated traffic signal control (ASC). Various measures of performances were considered, including the shock wave area, the platoon ratio, and the number of traffic conflicts.
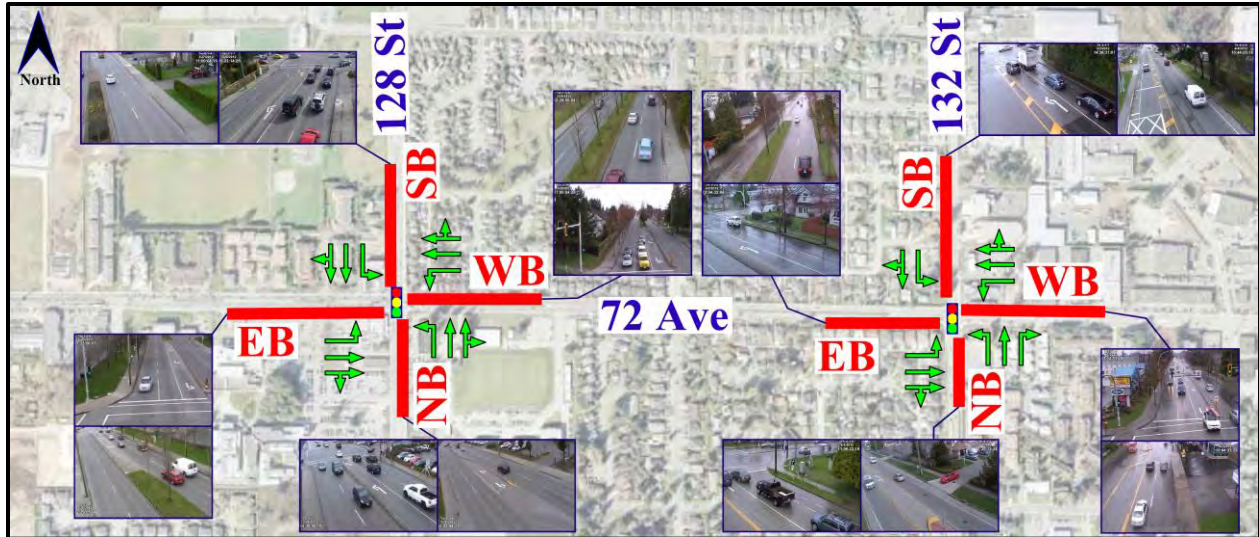
FIGURE E.5: Study Locations and Video Scenes*
(EB: eastbound, WB: westbound, NB: northbound, SB: southbound)

Overall, the validation results showed that the proposed RS-ATSC algorithm outperforms the real-world ASC. When implementing the RS-ATSC, the total shock wave area was reduced by 71% at each intersection (**FIGURE E.6**). Most importantly, the overall rate of rear-end conflicts (i.e., the total number of conflicts normalized by the exposure) was decreased by 31% and 36% at the first and second intersection, respectively (**FIGURE E.6**). In addition to these safety benefits, the RS-ATSC has positive mobility impacts. Compared to the benchmark ASC, the RS-ATSC reduced the average delay time by 44% and 61% for the first and second intersection, respectively. This is reasonable because reducing shock waves most likely decreases vehicle delays and improves mobility. However, this cannot be considered the optimum mobility performance, since the RS-ATSC is a safety-oriented algorithm whose optimal policy is minimizing shock waves to optimize safety.
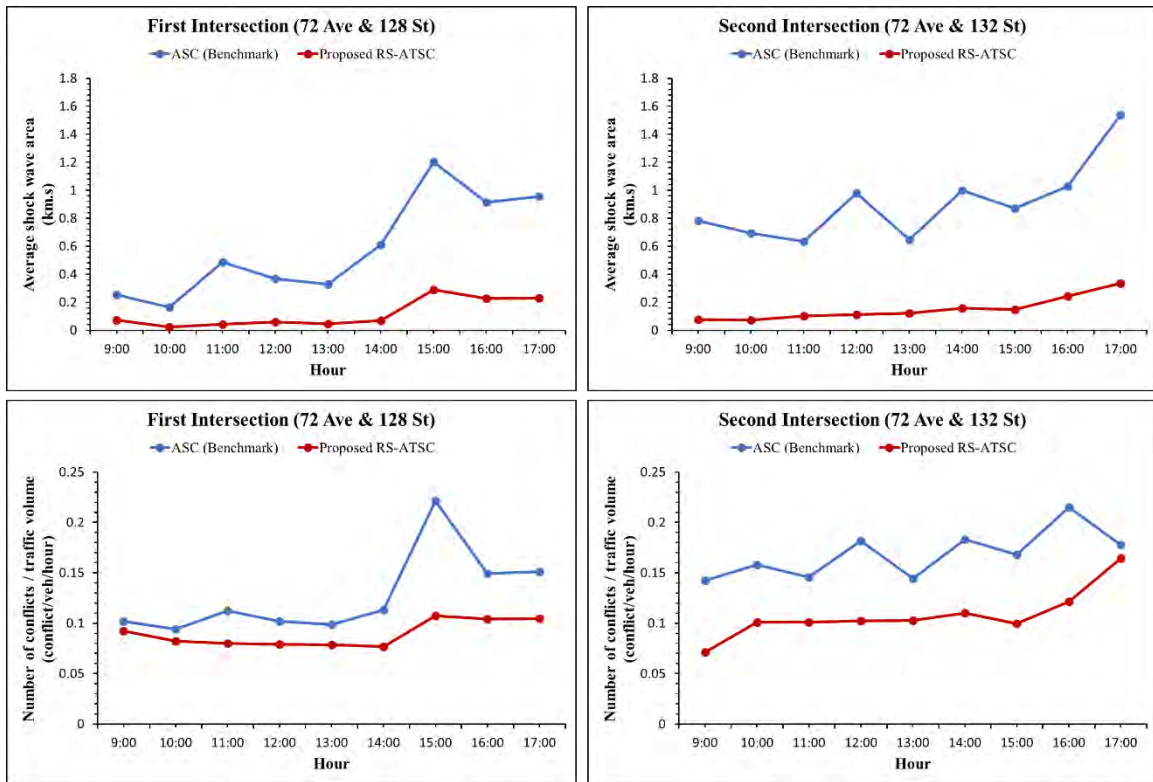
FIGURE E.6: Average shock wave area and the number of conflicts at the selected intersections before and after implementing the proposed RS-ATSC

Moreover, the RS-ATSC algorithm was tested under various market penetration rates of CVs. Although the maximum safety benefit is corresponding to the MPR of 100%, the results showed that 98% of this benefit can be achieved when the MPR value is 50% (**FIGURE E.7**). Moreover, the MPR of 20% seems sufficient to achieve more than 60% of the maximum safety benefit. MPR values less than 20% may not lead to significant safety benefits, since the algorithm cannot define the environment state with a reasonable accuracy due to the lack of real-time information on vehicle positions and speeds.

University of British Columbia
Department of Civil Engineering

10
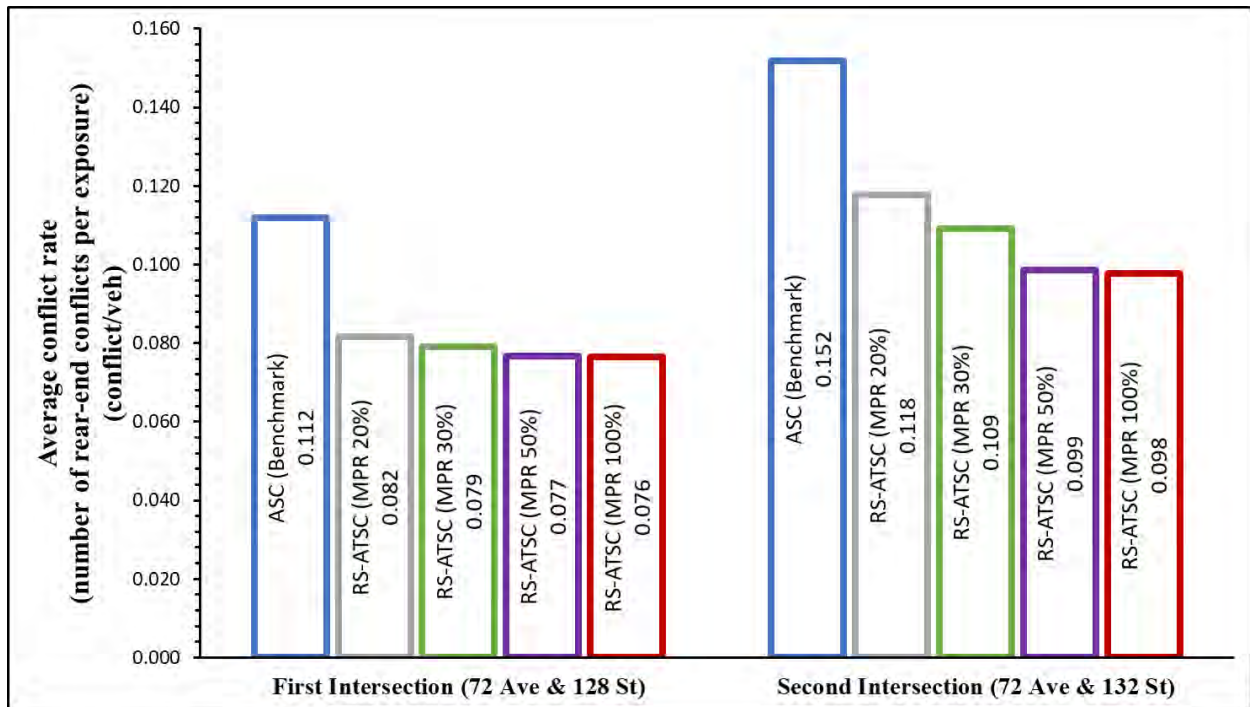
FIGURE E.7: The effect of the CVs MPR value on the average conflict rate at the selected intersections when implementing the proposed RS-ATSC

In conclusion, the proposed RS-ATSC is a promising and feasible algorithm that can adapt traffic signals to optimize real-time safety in the CVs environment. The algorithm outperforms the traditional actuated traffic signal control in terms of the resulted shock waves and the produced number of traffic conflicts. The proposed RS-ATSC algorithm can be very effective when the MPR of CVs is equal to or higher than 20%. The higher the MPR value, the more the safety effectiveness of the algorithm. More important, when implemented to a specific intersection, the RS-ATSC algorithm can be designed to continue learning itself using real-world traffic and geometric data of this intersection. Considering these site-specific data can potentially lead to better safety and mobility performances.

CHAPTER 1: INTRODUCTION

1.1 Motivation

In Canada, traffic collisions result in about 1,900 fatalities and 165,000 injuries annually (Transport Canada 2016), and the annual cost of road collisions to the Canadian economy is estimated at $CDN 62.7 billion. In many jurisdictions such as British Columbia (BC), insurance premiums are spiraling ever higher as auto insurance companies face considerable losses (ICBC 2018). Therefore, the importance of research into reducing the social and economic costs of crashes cannot be overstated. Approximately 60% of all collisions in BC occur at intersections especially in urban areas; with more than 50 percent of collisions occurring in urban areas are at signalized intersections. For many intersections, especially those among urban corridors, collision frequencies and severities remain high despite the implementation of various geometric and traffic measures. In addition to being hazard locations, signalized interactions are considered one of the main contributors to road network delays, likely due to inadequate capacity or poor signal control.

In the existing practice, the management of traffic flow (aimed at improving mobility and level of service of traffic facilities) and road safety (aimed at reducing crashes) have largely been considered independently despite the clear relationship between them. This can mainly be attributed to the availability of numerous traffic micro-simulation tools that can simulate traffic flow. However, most existing traffic flow models only focus on evaluating the level of service. They usually assume a crash-free environment and ignore violating road user behavior that can lead to crashes. As well, collecting data on important traffic control-related variables that can affect safety, such as shock waves at signalized intersections, is difficult and needs special advanced algorithms.

One of the promising solutions to improve safety and mobility of signalized intersections is the emerging Connected-Vehicles (CVs) technology. The concept of CVs refers to the capability of various elements of the transportation system (vehicles, bicycles, pedestrians, road infrastructure, traffic control, management centers, etc.) to electronically communicate with each other continuously in real-time (U.S. Department of Transportation, 2015). In such an environment, drivers can be supported with advisories and warnings to avoid collisions or unnecessary delays. In addition, traffic control devices, such as traffic signals and variable message signs, can be adapted in real-time to relieve congestion and improve safety. Existing research has demonstrated that CVs can potentially have considerable mobility, safety, and environmental benefits to road networks (Olia et al. 2016).

In the era of CVs, an enormous amount of high-resolution data on vehicle positions and trajectories will be generated in real-time. These data can potentially be used for real-time safety and mobility optimization of traffic signals. Using CVs data for *mobility* optimization at signalized intersections has been investigated in several studies (Lee et al., 2013; Guler et al., 2014; Feng et al., 2015). Various procedures have been proposed to minimize delays by adapting traffic signal controllers in real-time given data from vehicle-to-infrastructure (V2I) and vehicle-to-vehicle (V2V) communications. However, existing research has not considered the real-time *safety* optimization

of traffic signals. This is mainly because safety optimization is more complicated than mobility optimization. Unlike vehicle delay and travel time, the safety level of signalized intersections cannot be directly estimated in real-time from CVs data. The main challenge is the lack of tools to evaluate the real-time safety of signalized intersections.

Traditionally, the safety of signalized intersections has often been evaluated at an aggregate level by relating historical collision records to the annual traffic volume and the geometric characteristics of the intersection. Relying on collision data in modelling real-time safety is very difficult for several reasons. First, the use of the historical collision data in safety analysis requires collisions to occur and be recorded over an adequately long period (usually years) to conduct a statistically sound safety diagnosis (Sayed and Zein, 1999; Chin and Quek,1997). Second, the use of several years of collisions requires reliance on aggregate exposure measures such as the annual average daily traffic (AADT) which does not explicitly account for the fact that not all vehicles are interacting unsafely and does not represent the variation of traffic flow within shorter periods. Third, important signal cycle-related variables that can affect intersection safety such as the arrival type and the shock wave characteristics are usually omitted due to the traffic data aggregation.

Therefore, there is an important need to develop safety models that can be used to evaluate the safety of signalized intersections in real time. Specifically, there is a need for models that can consider the effects of dynamic traffic parameters (e.g., traffic volume, shock waves, queue length, platoon ratio) on safety within short time periods (e.g., the signal cycle). These safety models could then be incorporated into an adaptive traffic signal control (ATSC) algorithm to optimize both traffic safety and traffic mobility using real-time CVs data. The feasibility of such an ATSC algorithm should also be investigated under various market penetration rates of CVs to represent the transition period that predates the full deployment of the CVs technology.

1.2   Research Objectives

Toward optimizing safety and mobility of signalized intersections in real time using CVs data, this research has the following key objectives:

1. To develop, using real-world traffic data, safety models for signalized intersections at the signal cycle level that can be used to evaluate safety in real time based on various dynamic traffic parameters, such as traffic volume, queue length, shock waves, and platoon ratio
2. To investigate the transferability of the developed real-time safety models across different locations/jurisdictions
3. To develop, using traffic microsimulation models, a practical ATSC algorithm that can utilize CVs data to optimize safety of signalized intersection in real time
4. To test and validate the developed ATSC algorithm using real-world traffic data
5. To investigate the safety and mobility performances of the developed ATSC algorithm under various market penetration rates of CVs

1.3   Report Structure

This report is divided into five chapters. **Chapter one** includes an introduction to the presented research project, including the motivation, the research objectives, and the structure of this report. **Chapter two** provides a brief review of existing studies related to this research. **Chapter three** describes the development of real-time safety models for signalized intersections using real-world traffic data. **Chapter four** explains the transferability of the developed models to new jurisdictions. **Chapter five** presents a practical real-time ATSC algorithm to optimize safety of signalized intersections in the CVs environment. Finally, **chapter six** contains the report summary, the key findings of this research, and the suggested future research areas.

CHAPTER 2: BACKGROUND AND LITERATURE REVIEW

This chapter provides a background of the relevant previous research, to date, to develop a foundation on which this study is based. Four main topics are covered in this chapter. First, different approaches of evaluating safety of signalized intersection in the literature are reviewed. Second, background on connected-vehicles (CVs) technology is provided. Third, the differences between automated vehicles and connected vehicles are defined. Fourth, previous studies that utilized traffic microsimulation models to mimic road facilities under the CVs environment are discussed. As a considerably high number of previous studies related to safety of signalized intersections or CVs was found; the literature review in this chapter focuses on a reduced list of selected key studies that are highly cited or recently published in top-ranked journals.

2.1 Safety Evaluation of Signalized Intersections

2.1.1 Collision-based SPFs at Signalized Intersections

Collision prediction models, or SPFs, of signalized intersections have been widely developed, investigated and calibrated in the literature. The highway safety manual (AASHTO 2010) provides SPFs that estimate the average crash frequency for signalized intersections on different road classes including rural two-lane roads, rural multi-lane roads, urban and suburban arterials. Also, several studies locally developed, adopted and calibrated SPFs for signalized intersections to local conditions of specific zones (Poch and Mannering, 1996; Miaou and Lord, 2003; Lyon et al., 2005; Wang et al., 2006; Sayed and de Leur, 2007; Wong et al., 2007; Wang and Abdel-Aty, 2008; El-Basyouny and Sayed, 2009c; Guo et al., 2010; Persaud et al., 2012; Lee et al., 2017). The traffic exposure measure used in most of these studies was an aggregation of the traffic volume (e.g. AADT) and the predicted number of collisions was aggregated to several years.

2.1.2 Conflict-based SPFs at Signalized Intersections

Relying on collision data in safety analysis is associated with several limitations. First, collisions have to occur and be recorded for a long period (usually years) to obtain statistical reliability (Sayed and Zein, 1999; Ismail et al., 2010; Chin and Quek, 1997). Second, there are well-recognized availability and quality problems associated with collision data. To overcome these limitations, traffic conflict technique has been advocated as a proactive approach to study road safety from a broader perspective than relying only on collision data analysis (Sayed and Zein, 1999; Songchitruksa and Tarko, 2006). Traffic conflicts are more frequent than collisions, can be clearly observed, and can provide insight into the failure mechanism that leads to collisions. Previous research showed that reducing traffic conflicts can lead to reducing the frequency of road collisions (Ismail et al., 2011; Sacchi et al., 2013). The use of traffic conflicts for safety diagnosis has been recently gaining acceptance among road safety researchers as a surrogate or a complementary approach to the collision data analysis approach. A traffic conflict is defined as "*an observable situation in which two or more road users approach each other in space and time to such an extent that there is a risk of collision if their movements remained unchanged*"

(Amundsen and Hydén, 1977). Previous studies attempted to develop SPFs for signalized intersections based on field-observed traffic conflicts (Sayed and Zein, 1999; El-Basyouny and Sayed, 2013; Zhang et al., 2014; Sacchi and Sayed, 2016a; Sacchi and Sayed, 2016b). The exposure measure in theses SPFs is represented by the average hourly traffic volume, while the traffic conflicts are aggregated to hours (i.e. number of conflicts/hour).

2.1.3   Safety of Signalized Intersection Using Microsimulation Models

The use of traffic simulation models for conducting conflict-based safety evaluations has also been recently proposed (Gettman et al., 2003; 2008). There is a growing interest in using simulation models for the safety assessment of road facilities by analyzing simulated vehicle trajectories and estimating conflict indicators. The main advantages of this approach are: 1) the ability to evaluate the safety of various design and traffic management options of road facilities before making changes and 2) the ease of estimating simulated conflicts without actually observing them.

The Surrogate Safety Assessment Model (SSAM) was recently proposed by (Siemens Energy & Automation, Inc.) and was sponsored by the Federal Highway Administration (FHWA) of the United States. The SSAM was developed to estimate traffic conflicts using simulated vehicle trajectories exported from four commonly-used microscopic simulation models: VISSIM, AIMSUN, PARAMICS, and TEXAS. Several traffic conflict indicators can be calculated including the time to collision (TTC), post-encroachment time (PET), deceleration rate (DR), maximum speed (MaxS), and speed differential (DeltaS). In SSAM, conflicts are classified into three maneuver types: rear-end; lane-change; and crossing. Conflicts are identified based on conflict angle and specific thresholds for TTC and PET, which are predetermined by the user (Gettman et al., 2003; 2008).

Using simulated conflicts extracted from traffic microsimulation models and processed in SSAM tool in safety evaluation has been widely investigated in the literature. Several studies proposed a calibration procedure of microsimulation models for safety analysis of signalized intersections (Essa and Sayed, 2015a; 2015b; 2016; Gettman et al., 2008; Cunto and Saccomanno, 2008; Dijkstra et al., 2010; Huang et al., 2013; Shahdah et al., 2014; among others). However, most of these studies aggregated the simulated results into larger time periods such as hours and did not consider the traffic variation between signal cycles. In addition, the use of microsimulation models in safety evaluation has been generally criticized for two main reasons. First, vehicles in the simulation models are programmed to follow specific rules which are aimed at avoiding collisions. Therefore, it is very difficult to represent unsafe vehicle interactions and near misses. Second, there are several parameters and several ways to model traffic in simulation models, which means that the simulation results can vary significantly depending on the input values.

2.1.4   Dilemma Zone and Red-light-runner Violations

Safety analysis of signalized intersections considering dilemma zone and red-light-runners has also been introduced. A dilemma zone is defined as the area upstream of signalized intersections in which drivers have to decide whether to continue through the intersection or to stop at the

beginning of the yellow time. Different decisions in dilemma zone for a couple of consecutive vehicles may lead to a risk of rear-end collision. Papaioannou (2007) developed a binary choice model relating the probability of stopping at the stop line or crossing it as a function of approach speed, distance from intersection, gender, age group and the existence or not of a dilemma zone. The results showed that a large percentage of drivers facing the yellow signal are caught in a dilemma zone and exercise an aggressive behavior (Papaioannou 2007). Elmitiny et al. (2010) used a video-based system to observe driver's behavior associated with the signal change at high-speed signalized intersections. A model was developed to predict stop/go decisions and red-light-runner violations based on many factors such as the vehicle speed at yellow-onset and the vehicle distance from the intersection (Elmitiny et al., 2010). Machiani and Abbas (2016) developed a new surrogate safety measure that captures the degree and frequency of rear-end conflicts in the dilemma zone at signalized intersections (Machiani and Abbas, 2016). Jahangiri et al. (2016) developed models to predict red-light-runner violations before they occur using observational and simulator data. Ren et al. (2016) identified factors that can significantly affect red-light-runner behavior using high-resolution traffic data collected by loop detectors from three signalized intersections. Wu et al. (2017a) proposed a new warning system that integrates the pavement marking and flashing yellow system to reduce the dilemma zone and enhance the traffic safety at signalized intersections. The system can provide drivers with better suggestions about stop/go decisions based on their arriving time and speed (Wu et al., 2017a).

2.1.5 Real-time Crash Prediction

Although many previous studies has focused on freeways in terms of real-time crash risk analysis (Lee et al., 2003; Pande and Abdel-Aty, 2006; Hossain and Muromachi, 2012; Ahmed and Abdel-Aty, 2013; Xu et al., 2013; Shi and Abdel-Aty, 2015; Wu et al., 2017b; among others), a few studies have considered signalized intersections and urban arterials. Theofilatos (Theofilatos 2017) investigated accident likelihood and severity using real-time traffic and weather data collected from two urban arterials in Athens, Greece. However, the traffic data were aggregated to one-hour interval which might not capture the variations in traffic parameters within shorter time periods (such as the traffic signal cycle).

Although there are several studies developing SPFs or other safety measures for signalized intersections, to the best of our knowledge, no studies have attempted to develop SPFs at the cycle level. The first phase of the proposed research aims to fill this research gap by relating the number of traffic conflicts at each signal cycle to various traffic parameters such as traffic volume, queue length, shock wave characteristics (the area and the speed of the shock wave), and the platoon ratio (the arrival pattern) in order to develop various conflict-based SPFs at cycle level that can be useful for futuristic real-time safety optimization of signalized intersections.

2.2 Connected Vehicles Technology

Generally, the concept of CVs refers to the capability of the various elements of the transportation system (vehicles, transit, bicycles, pedestrians, road infrastructures, traffic control/management

centers, etc.) to electronically communicate with each other rabidly and continuously (U.S. Department of Transportation, 2015).

In the CVs environment, vehicles use wireless technology to connect with other vehicles (i.e. vehicle to vehicle communication or V2V) and/or with transportation infrastructures (i.e. vehicle to infrastructure or V2I). The two communication types V2V and V2I can be generally denoted as V2X. V2X means a communication between a connected vehicle and any other device (vehicle, infrastructure, smart phone, etc.). V2V connectivity allows vehicles to share their position, speed, brake status and other information in real-time with other similar connected vehicles (Harding et al., 2014). V2I connectivity allows real-time exchange of different information between the connected vehicles and the transportation infrastructures (Such as traffic signals, roadway signage) that equipped by CV technology.

Both V2V and V2I communications occur over dedicated short-range communications (DSRC) systems. DSRC is a wireless technology that allows rapid communications (up to 10 times per second) between connected vehicles within a distance ranges from 300 to 500 meters (U.S. Department of Transportation, 2015). The DSRC network primarily communicates using a language dictionary standardized by the Society of Automotive Engineers (SAE) International in SAE J2735. The most common data element is called a basic safety message (BSM). The BSM contains a vehicle's location, speed, direction, brake-status, and other information (Chong, 2016; Center for Automative Research, 2017). Cellular phone technology is also expected to facilitate the use of many connected vehicle concepts (U.S. Department of Transportation, 2015).

Recently, CVs has a grown interest among researchers, and expected to be the next generation of intelligent transportation systems. The CVs concept is moving rapidly from the experimental phase into real-world deployments (U.S. Department of Transportation, 2015). Via real-time connectivity and data transmissions, CVs are supposed to have potential safety, mobility and environmental benefits to transportation networks. CVs can play an important role in decreasing traffic collisions and improving road safety. CVs safety applications can provide drivers with 360-degree awareness of hazards and situations they cannot see. V2V communications can provide drivers with awareness of imminent crash situations such as a sudden stop by a vehicle ahead, an icy road, a dangerous curve, or a car exists in the driver's blind spot. Also, V2I communications can provide drivers with awareness in different situations such as when the traffic light is about to change or when the driver is entering a school zone or a construction zone (U.S. Department of Transportation, 2017). In addition, V2I communications can be used to perform a real-time optimization for different road-side infrastructures design such as electronic signs (Variable message signs (VMS)) and traffic signals. The optimization can be performed to avoid crashes and minimize traffic conflicts by changing the signal design or changing the contents of the VMS in real-time.

Regarding mobility, CVs could help in reducing both recurrent and non-recurrent congestions. Via real-time communications, CVs mobility applications can provide drivers with information necessary to navigate roads more efficiently, which could lead to fewer delays. In addition, CVs could help transportation system operators improve the functioning of the overall system (Chong

2016). Real-time communications can be used to perform a real-time mobility optimization for different road-side infrastructures design, such as VMS and traffic signals, to minimize traffic delays. In addition, providing travelers with real-time information could make public transportation more appealing. For example, travelers will have a realistic idea of when transit vehicles will arrive; they will also be able to improve bus and train connections. Overall, the data-rich environment of the CVs will be the genesis for a multitude of new mobility applications that will help to keep traffic flowing, reduce congestion, and make it easier for people to plan their travel experience (U.S. Department of Transportation, 2017).

Furthermore, CVs could have potential environmental benefits to the transportation networks. CVs technologies will generate real-time data that drivers and transportation managers can use to make transportation networks more ecofriendly. For example, CVs applications could help in reducing congestion, improving lane management, eliminating unnecessary stop, and subsequently improving fuel efficiency and reducing emissions. In addition, using real-time data, travelers may also be encouraged to make green transportation choices such as avoiding congestion by taking alternate routes or public transit, or rescheduling their trip (U.S. Department of Transportation, 2017).

2.3   Difference between Automated Vehicles (AVs) and Connected Vehicles (CVs)

The two terms AVs and CVs are not synonymous, although they can share some of the same technology. According to the Ontario Centers of Excellence, the connected and automated vehicles can be defined as follows "*Connected vehicles use wireless technology to connect with other vehicles, transportation infrastructure and mobile devices to give motorists the information they need to drive more safely. Automated vehicles, also known as self-driving vehicles, rely on sensors and computer analytics to sense their environments and navigate without human input*" (The Ontario Centers of Excellence, 2017). **FIGURE 2.1** illustrates the difference between the automated and the connected vehicles (Chong 2016).
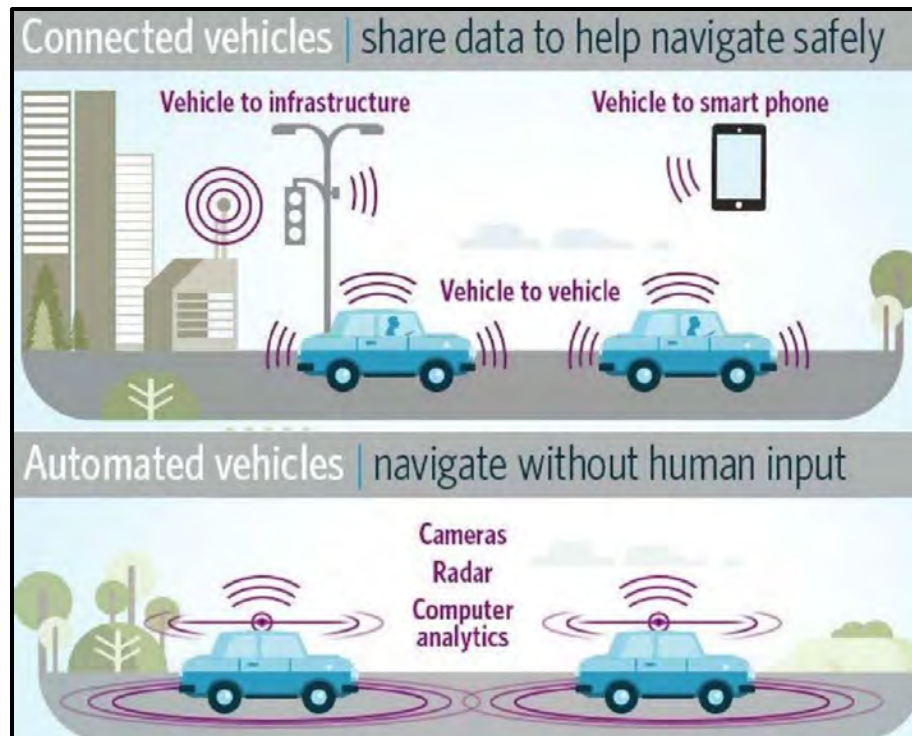
FIGURE 2.1: Automated and Connected Vehicles (Source: (Chong 2016))

However, there are many types of connectivity and automation, as well as there are many ways to combine them. Therefore, a vehicle can be in one of the following cases: 1) conventional (non-automated and non-connected); 2) connected and non-automated; 3) automated and non-connected; 4) connected and automated.

Furthermore, both CVs and AVs are often combined with intelligent transportation system (ITS). According to ITS Canada, ITS can be defined as "*the application of advanced and emerging technologies (computers, sensors, control, communications, and electronic devices) in transportation to save lives, time, money, energy and the environment.*" (ITS Canada, 2017). ITS represents the much wider concept that includes CVs and AVs in addition to a variety of advanced applications that are beyond the vehicle system such as remote traffic monitoring, adaptive signal control, etc. **FIGURE 2.2** (Center for Automative Research, 2017) identifies the three categories: CVs, AVs, and ITS.
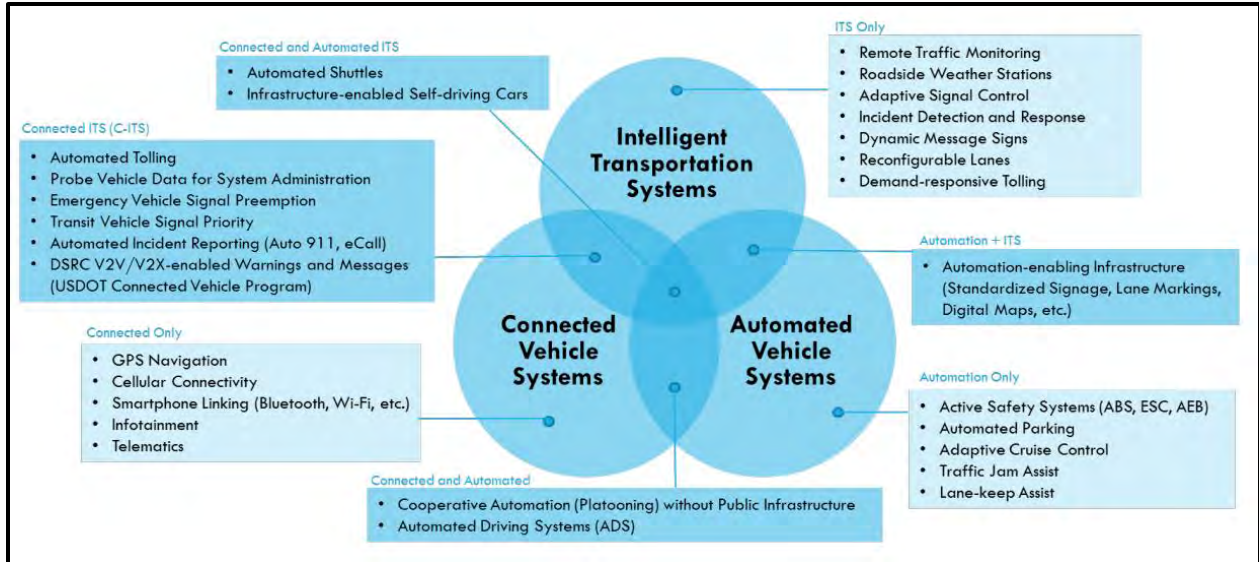
FIGURE 2.2: Advanced Transportation Technology (Source: (Center for Automative Research, 2017))

Regarding the automated vehicles, the vehicle relies on information from its sensors (such as camera, radar, etc.) to perceive the external environment and navigate. There are different levels of automation. According to the Society of Automotive Engineers (SAE) international's standard J3016 (SAE International 2014), there are 6 levels of automations starting from level 0, which represents no automation level, to level 5, which represents the full automation level. **FIGURE 2.3** (SAE International 2014) provides more description for the different automation levels.

SAE level	Name	Narrative Definition	Execution of Steering and Acceleration/ Deceleration	Monitoring of Driving Environment	Fallback Performance of Dynamic Driving Task	System Capability (Driving Modes)
Human driver monitors the driving environment						
0	No Automation	the full-time performance by the *human driver* of all aspects of the *dynamic driving task*, even when enhanced by warning or intervention systems	Human driver	Human driver	Human driver	n/a
1	Driver Assistance	the *driving mode*-specific execution by a driver assistance system of either steering or acceleration/deceleration using information about the driving environment and with the expectation that the *human driver* perform all remaining aspects of the *dynamic driving task*	Human driver and system	Human driver	Human driver	Some driving modes
2	Partial Automation	the *driving mode*-specific execution by one or more driver assistance systems of both steering and acceleration/deceleration using information about the driving environment and with the expectation that the *human driver* perform all remaining aspects of the *dynamic driving task*	System	Human driver	Human driver	Some driving modes
Automated driving system ("system") monitors the driving environment						
3	Conditional Automation	the *driving mode*-specific performance by an *automated driving system* of all aspects of the dynamic driving task with the expectation that the *human driver* will respond appropriately to a *request to intervene*	System	System	Human driver	Some driving modes
4	High Automation	the *driving mode*-specific performance by an automated driving system of all aspects of the *dynamic driving task*, even if a *human driver* does not respond appropriately to a request to intervene	System	System	System	Some driving modes
5	Full Automation	the full-time performance by an *automated driving system* of all aspects of the *dynamic driving task* under all roadway and environmental conditions that can be managed by a *human driver*	System	System	System	All driving modes

FIGURE 2.3: Automation Levels According to SAE J3016 (Source: (SAE International 2014))

2.4   Connected Vehicles in Microsimulation Models

Several studies in the literature have investigated the mobility, safety and environmental impacts of the CVs technology. Since this technology is still under development, most of the previous research utilized microsimulation models to analyze the performance of different road facilities in the CVs environment. This section summarizes some of these studies.

Lee and Park (2012) proposed a Cooperative Vehicle Intersection Control (CVIC) algorithm that enables cooperation between vehicles and infrastructure for effective intersection operations without traffic signal controller. The developed algorithm was tested on a hypothetical four-way single-lane approach intersection modeled using the microsimulation model VISSIM. The results indicated that the CVIC system significantly improved the intersection performance in terms of the delay time, the air quality, and the energy saving. However, this study focused only on the mobility and the environmental performance. Safety performance was not considered, except one constraint in the algorithm that aims at avoiding collisions between vehicles in the absence of the traffic signal. Lee et al. (2013) expanded the previous study and implemented the CVIC algorithm to a corridor that consists of multiple intersections. Also, the safety and environmental impact of the implementation of the CVIC algorithm were investigated. The safety was evaluated using the SSAM tool (Gettman et al., 2008). Nevertheless, the two previous studies assumed that all vehicles

are fully automated and connected. Different market penetration rates and the transition period before the full deployment of the CVs and AVs were not considered.

Lee et al. (2013) proposed a cumulative travel-time responsive (CTR) algorithm that optimizes traffic signals in real time to minimize the total delay at signalized intersections in the CVs environment. The simulation test bed that incorporated the simulations of the CVs environment was developed with VISSIM. The update interval used in the algorithm was assumed to be 5 seconds. Multiple market penetration rates of the CVs technology were considered. Also, the environmental impacts of the proposed algorithm were evaluated. However, the safety of signalized intersections was neither considered in the optimization process nor in the evaluation process.

Goodall et al. (2013) developed a traffic control algorithm to adapt traffic signals in real-time in the CVs environment. The developed algorithm was tested using VISSIM with 15-seconds update interval. Multiple objective functions were considered in the optimization process, including delay time, number of stops, and decelerations. Also, multiple CVs market penetration rates were investigated. However, safety of signalized intersections was not considered.

Paikari et al. (2014) used the traffic microsimulation model PARAMICS to evaluate the safety and mobility impacts of the CVs in freeways. V2V and V2I systems were implemented in the simulation model to represent rerouting guidance and advisory speed using variable message signs (VMS). Five scenarios were tested to reflect different CVs market penetration rates. The mobility measure was the point-to-point travel time along the freeway section. The safety measure was the crash probability estimated from the crash likelihood model that was earlier presented in (Abdel-Aty et al., 2006).

Li et al. (2014) developed a signal control optimization algorithm to minimize delay time assuming a signalized intersection with two single-lane approaches. The algorithm optimizes vehicle trajectories based on the assumption that all vehicles are automated and connected to the signal controller. The delay results were compared to the traditional actuated signal control. The simulation model CORSIM was used to develop the traditional signal control. The results indicated that the optimization algorithm reduced the average travel time delay by 16.2–36.9%. The safety of the intersection was not investigated.

Guler et al. (2014) developed an intersection traffic control algorithm to adapt traffic signals to minimize the total delay using information obtained from CVs. The developed algorithm considers vehicles within a certain radius of the intersection, enumerates the possible discharge sequences for these vehicles and picks the best strategy. The developed algorithm was tested at different CVs market penetration rates using a simulation model. A hypothetical intersection of two one-way streets was modeled. The objective function was to minimize the total delay time. The results indicated that the algorithm can reduce the total delay time up to 60%. Yang et al. (2016) extended the aforementioned algorithm by including a certain percentage of automated vehicles. Considering a percentage of automated vehicles enables bidirectional V2I communications in the signal control scheme and allows the central controller to optimize the automated vehicle

trajectories for further improvement in the intersection performance. The Intelligent Driver Model (IDM) (Treiber et al., 2000) was used as the basic car following model; and a Java script was used to model a simulation platform. The results indicated improvement in both the delay time and the number of stops. However, safety of the signalized intersection was not considered in both studies.

Feng et al. (2015) proposed a real-time adaptive signal phase allocation algorithm using CVs data. The developed algorithm optimizes the phase sequence and duration by considering two objective functions: minimization of total vehicle delay, and minimization of queue length. The developed algorithm was developed and tested using the simulation model VISSIM. Different CVs market penetration rates were investigated. The results indicated that the developed algorithm outperformed the traditional actuated signal controller by reducing the total delay by 16.33%. Most importantly, the results showed that different objective functions can result in different signal timing design. The minimization of total vehicle delay usually generates lower total vehicle delay, while the minimization of the queue length serves all phases in a more balanced way (Feng et al., 2015). The safety of the signalized intersection was neither optimized nor evaluated.

Kamal et al. (2015) presented a coordination scheme for an intersection without using any traffic lights. It was assumed that all vehicles are automated and connected using two-way communication network. Approaching vehicles from all sections were globally coordinated to achieve smooth traffic flows. Firstly, vehicles were assumed to follow the Intelligent Driver Model (IDM) (Treiber et al., 2000) as the basic car-following model. Next, the vehicle trajectories were optimized to avoid any cross-collision risks around the intersection. The proposed scheme prevents any each pair of conflicting vehicles from approaching their cross-collision point at the same time, instead of reserving the whole intersection area for the conflicting vehicles one after another (Kamal et al., 2015). The simulator model AIMSUN was used to test the coordination scheme. Unlike the earlier studies (Lee and Park, 2012; Li et al., 2014), the proposed scheme was evaluated using simulation in a hypothetical intersection with multi-lanes approaches and with left and right-turn movements. Compared to the traditional signalized intersection, the proposed scheme significantly improves the intersection performance in terms of delay time, capacity, and fuel consumption.

So et al. (2015) adopted an integrated simulation approach to assess the safety impact of CVs applications by considering potential positioning errors and communication delays which are likely to occur in reality. In their study they considered safety applications (driver warnings) based on Global Position System (GPS) devices and V2V/V2I communications. The simulation model VISSIM was used as the basic traffic simulator. Next, the safety was evaluated based on the number of conflicts obtained from the SSAM tool (Gettman et al., 2008). The results showed that the V2V/V2I communication delays reduced the safety effectiveness (i.e., reduction in traffic conflicts) of driver warnings by 3-13%. In addition, for CVs safety applications, the GPS/INU device showed the highest accuracy, while the autonomous GPS showed the lowest accuracy (So et al., 2015). Different market penetration rates were not considered in this study.

Stevanovic et al. (2015) proposed a method to optimize traffic signal considering three objective functions: mobility, safety, and environment. The multi-objective optimization algorithm was

based on 3-dimensional Pareto fronts (i.e., the set of Pareto optimal solutions that are not dominated by any other feasible solutions) of signal timing. Genetic Algorithm (GA) was applied to get the Pareto fronts by evaluating several signal timing plans. Different types of signal controller were considered, including fixed and actuated signals. Some of the signal timing scenarios were combined with a Connected-vehicle application called the green light optimized speed advisory (GLOSA) (Stevanovic et al., 2013) that guides drivers (through infrastructure-to-vehicle communication) with speed advice for a more uniform commute with less stopping time through traffic signals. To test the multi-objective optimization algorithm, five signalized intersections were used as a test bed. The simulation model VISSIM was used to simulate the selected intersections, while SSAM (Gettman et al., 2008) and Comprehensive Modal Emission Model (CMEM) (Barth et al., 2000) were used to evaluate safety and environmental impacts, respectively. The results showed that the optimal balance between mobility, safety and environmental impacts does not seem to produce very different signal timings. However, future studies were recommended to test the hypothesis that such differences may get pronounced when tested in the stochastic traffic flows (Stevanovic et al., 2015). In addition, this study did not consider real-time optimization; rather, previously developed signal timing plans were simulated and tested. Thus, the optimization process aimed only to select the optimum signal plan, not to adapt the traffic signals in real-time.

Olia et al. (2016) assessed the potential safety, mobility and environmental benefits of the CVs deployment. In their study, a real network located in the City of Toronto was simulated using the PARAMICS microsimulation model. A combination of CVs and non-CVs was considered. Real-time routing guidance and advisory warning messages for CVs were emulated in the simulation model. Other sources of information were also considered for non-CVs such as GPS, and variable message signs. The mobility measure was the total travel time estimated from PARAMICS. The safety of the traffic network was assessed using the number of traffic conflicts obtained from the SSAM tool (Gettman et al., 2008). The Comprehensive Modal Emission Model (CMEM) (Barth et al., 2000) was used to evaluate the environmental impacts. Different CVs market penetration rates were investigated. The results showed that the market penetration rate of CVs and the level of information among non-CV vehicles can play an essential role in improving congestion, enhancing safety, and reducing emissions of transportation networks (Olia et al., 2016).

Li et al. (2017) presented a CV application called the high-speed differential warning (HSDW). The main goal of this application is to improve road safety through the wireless communication. The application identifies potential hazards resulting from high-speed differentials and then provides alerts to drivers to help them take appropriate actions. A traffic network was developed using the PARAMICS simulation model. The average speed was used as a mobility measure. The Motor Vehicle Emission Simulator (MOVES) (MOVES) was used to estimate the energy consumption and emissions. The safety of the traffic network was assessed using the number of rear-end traffic conflicts obtained from the SSAM tool (Gettman et al., 2008). Different CVs market penetration rates were considered. The results indicated that the proposed application can improve the safety performance without compromising the mobility and environmental sustainability performance of the overall traffic.

Al Islam and Hajbabaie (2017) presented a real-time distributed-coordinated technique for signal timing optimization on urban street networks. The main objective of the optimization technique is to find the signal timing parameters that maximize the traffic throughput values and control the queue length by preventing queue spillbacks. The traffic simulation model VISSIM was utilized to test the proposed technique on two case studies: 1) network with two intersections, and 2) network with nine intersections. The main assumption was that all vehicles and intersections are connected and intersections can share information with each other. The results showed that the proposed algorithm controls queue length and maximizes intersection throughput between 1% and 5% increase compared to the actuated coordinated signals. Also, the algorithm reduces the travel time by (17% to 48%) compared to the actuated coordinated signals. Safety of signalized intersections was neither optimized nor evaluated.

Jiang et al. (2017) proposed an eco-driving system for an isolated signalized intersection under partially connected and automated vehicles environment. A certain percentage of vehicles were assumed to be connected and automated (CAVs). The proposed system optimizes speed profiles of the CAVs to improve mobility and fuel efficiency. The simulation model VISSIM was utilized to test the proposed system. Different CAV's market penetration rates were considered. The results indicated that the system can improve the traffic throughput up to 10.80%. Fuel consumption benefits ranged from 2.02% to 58.01%. The results also showed that the proposed system can smooth out the shock wave caused by signal controls and is robust over the impedance from conventional vehicles and randomness of traffic (Jiang et al., 2017). Safety of signalized intersections was not considered in this study.

Xu et al. (2017) proposed an optimization algorithm based on the V2I cooperation between the traffic signal and approaching automated vehicles (CTV). The proposed algorithm optimizes traffic signal and vehicles' trajectories concurrently to minimize the travel time and the fuel consumption. All vehicles were assumed to be automated and connected. The algorithm was tested using the simulation model VISSIM. The results indicated that, compared with the actuated signal control, the proposed algorithm can improve travel time and fuel consumption by 19.7% and 23.7% respectively. Safety of signalized intersections was not considered except some constraints in the optimization process that aim to provide a minimum safe distance and avoid collisions.

Khazraeian et al. (2017) investigated the accuracy and the safety benefits of the Queue warning systems (QWS) in the CVs environment. The main concept of the QWS is to increase traffic safety by informing drivers about queued traffic ahead so they can time-properly react to the queue. In their study, Khazraeian et al. (2017) simulated freeway sections with CVs and QWS using the simulation model VISSIM. Different CVs market penetration rates were investigated. The safety benefits were evaluated using the number of traffic conflicts obtained from the SSAM tool. The results showed that from this study indicate that low market penetration rates (3% to 6%) are enough for an accurate estimation of the queue length. The results also indicated that CV data allowed faster detection of the bottleneck and queue formation. Safety effects were shown to be dependent on the driver compliance to the queue warning messages.

Although several studies have focused on the mobility and the safety evaluation of different road facilities in the CVs environment, a few of them have considered both safety and mobility of signalized intersections. Also, a few studies considered improving safety and minimizing traffic conflicts as an optimization objective. Unlike the optimization process for mobility, the optimization process of safety in real-time seems to be complicated and not straight forward. In addition, most of the previous studies that evaluated safety of signalized intersections in the CVs environment utilized the SSAM tool to estimate the total number of traffic conflicts. However, using SSAM to analyze the simulated trajectories and evaluate safety is generally criticized due to two main reasons. First, vehicles in the simulation models are programmed to follow specific rules which are aimed at avoiding collisions. Therefore, it is very difficult to represent unsafe vehicle interactions and near misses. Second, there are several parameters and several ways to model traffic in simulation models, which means that the simulation results can vary significantly depending on the input values. This study uses real-time SPFs developed from real traffic data to evaluate safety. Unlike SSAM, the SPFs can be used to estimate the traffic conflicts using macroscopic traffic characteristics at the signal cycle level. Instead of producing microscopic trajectories to be analyzed in SSAM, the role of the simulation model will be to estimate macroscopic traffic characteristics to be used in evaluating safety.

2.5 Implemented ATSC Algorithms

Over the past few decades, several ATSC algorithms have been implemented around the world. The earliest two algorithms were the Sydney Coordinated Adaptive Traffic System (SCATS) (Sims 1979), and the Split Cycle Offset Optimization Technique (SCOOT) (Hunt et al. 1981). After that, Federal Highway Administration (FHWA) adaptive control systems were developed and used, including the Optimization Policies for Adaptive Control (OPAC) (Gartner 1983), the Real Time Hierarchical Optimized Distributed Effective System (RHODES) (Head et al. 1992), and, more recently, the ACS Lite (Luyanda et al. 2003). These algorithms differ in operation, but they share a common objective of accommodating current traffic demands to maximize throughput capacity and minimizing traffic delays (Sabra et al. 2010). However, these ATSC systems generally suffer from several operational limitations, such as handling several intersections at the same time, using a centralized control system, and relying on loop detectors for detection and estimation (Abdulhai and Kattan 2003; El-Tantawy et al. 2014). Besides, these systems do not consider optimizing traffic safety as an objective.

2.6 Self-learning ATSC Algorithms

Self-learning ATSC algorithms are emerging methods that rely on learning the control policy from the direct interaction with the traffic environment without needing a predefined model for the environment nor human intervention. A significant amount of research has been conducted on developing self-learning ATSC algorithms with the goal of improving traffic efficiency and optimizing mobility using real-time traffic data. The Reinforcement Learning (RL) technique seems to be the most attractive approach in the literature to develop self-learning ATSC algorithms. Several RL methods have been applied, including model-based Q-learning (Wiering 2000), Q-learning (Abdulhai et al. 2003; Camponogara and Kraus 2003; Shoufeng et al. 2008;

Salkham et al. 2008; Balaji et al. 2010; Arel et al. 2010; El-Tantawy et al. 2014), State-Action-Reward-State-Action (SARSA) (Thorpe and Anderson 1996; El-Tantawy et al., 2014; Brys et al. 2014), Multiagent Reinforcement Learning (Wiering 2000; El-Tantawy et al. 2013), and, more recently, Deep Q-Network (DQN) (Shabestary and Abdulhai 2018; Gong et al. 2019). Various objectives have been considered to optimize mobility, including minimizing queue length, minimizing travel time, minimizing total delay, and maximizing vehicle throughput.

Although these RL-based ATSC algorithms have shown a significant improvement in traffic mobility, they have not considered evaluating or optimizing traffic safety. The safety regard in these studies is limited to avoiding crashes between simulated vehicles, providing standard signal times (e.g., yellow time, all-red time, minimum green time), and prohibiting conflicting signal phases from being operated simultaneously.

CHAPTER 3: REAL-TIME SAFETY MODELS

The safety of signalized intersections has often been evaluated at an aggregate level relating historical collision records to annual traffic volume and the geometric characteristics of the intersection. The collision-based safety evaluation is very useful in several applications such as identifying and ranking hazardous locations, and conducting before-and-after safety studies. However, collisions at signalized intersections can occur for several reasons, including drivers' behavior in dilemma zones, approach queues, and shock waves (Papaioannou 2007; Machiani and Abbas 2016). For safety solutions that target these collisions, it is essential to understand how changes in traffic parameters and signal control affect safety at the signal cycle level. Unfortunately, modeling the safety of signalized intersections using collisions at the cycle level can be difficult for several reasons:

- The use of the historical collision data in safety analysis requires collisions to occur and be recorded over an adequately long period (e.g. years) in order to conduct a statistically sound safety diagnosis (Sayed and Zein 1999; Chin and Quek 1997).
- The use of several years of collisions requires reliance on aggregate exposure measures such as the annual daily traffic (AADT) which does not explicitly account for the fact that not all vehicles are interacting unsafely (El-Basyouny and Sayed 2013) and does not represent the variation of traffic flow between cycles.
- Collecting data on important traffic parameters such as delay, queue length, and traffic volume at each cycle is difficult and requires special sensing needs.
- Important cycle-related variables that can affect the intersection safety, such as the arrival type and the shock wave characteristics, are difficult to collect and need special advanced algorithms.

In this chapter, we present real-time safety models for signalized intersections at the signal cycle level. These models relate the number of rear-end conflicts occurring in each cycle to dynamic traffic parameters, such as traffic volume, maximum queue length, shock wave characteristics (e.g. shock wave speed and shock wave area), and the platoon ratio. The models were developed using real-world traffic data. The developed models can give insight about how changes in the signal cycle design affect the safety of signalized intersections. The overall goal is to use the developed models for real-time safety optimization of signalized intersections. The approach that we followed in this research to develop these models provides several advantages as follows:

- The use of real-world traffic data, obtained from video recordings at six different intersections, which reflects actual driving behavior (i.e. the results are not based on microsimulation models).
- Proposing a video analysis procedure to collect data at the cycle level.
- The use of traffic conflicts as a measure of safety. Conflicts are extracted automatically and quantified using a conflict indicator (e.g. Time to collision). Also, the actual conflict location is determined.

- The proposed approach allows for the extraction of various traffic parameters including: the traffic volume, the maximum queue length, the shock wave characteristics, and the platoon ratio.
- The traffic conflict data and the traffic parameters are measured directly from the recorded video data and evaluated at the signal cycle level. As such, no hourly aggregation is needed.

3.1   Study Locations and Data Collection

Data from six signalized intersections in in the City of Edmonton, Alberta, and the City of Surrey, British Columbia, were used in this study. For all six sites, video cameras were installed to record traffic movements. The camera scenes were mainly focused on the intersection's approaches, where most of rear-end conflicts occur. To enable accurate analysis of rear-end conflicts and shock waves, two issues were considered during the camera installation process. First, the camera scenes must cover a sufficient length of the intersection's approach upstream the stop line. Second, the stop line and the traffic signal lights must be clearly captured in the video recordings. **TABLE 3.1** provides more details on the selected intersections, including the intersection location, the selected approaches, and the number of lanes per approach.

TABLE 3.1: Description of the Study Locations

Site #	City	Roads	Selected approaches	Number of Lanes	Video scene
1	Edmonton (AB)	Stony Plain Rd & 170 St	170 St (Northbound)	1 (Right) 1 (Left) 4 (Through)	
2	Edmonton (AB)	Gateway Blvd & 34 Ave	Gateway Blvd (Northbound)	1 (Right) 1 (Left) 4 (Through)	
3	Surrey (BC)	72 Ave & 128 St	72 Ave (Eastbound)	1 (Left) 2 (Through)	
4	Surrey (BC)	72 Ave & 132 St	72 Ave (Westbound)	1 (Left) 2 (Through)	

Site #	City	Roads	Selected approaches	Number of Lanes	Video scene
5	Surrey (BC)	64 Ave & King George Blvd	King George Blvd (Southbound)	1 (Right) 1 (Left) 2 (Through)	
6	Surrey (BC)	Fraser Highway & 168 A St	Fraser Highway (Southbound)	1 (Bike lane) 1 (Left) 2 (Through)	

3.2 Video Data Processing

The video data were analyzed to extract various traffic parameters and the number of traffic conflicts at each signal cycle. The video analysis process was based on a set of MATLAB codes and included several steps. First, traffic signal cycles for each intersection was identified automatically by detecting changes in the signal lights from video scenes. Second, moving vehicles in through lanes were tracked and the space-time diagram for each cycle was plotted. Third, using the space-time diagram for each cycle, various traffic parameters were extracted (figure 1). The extracted traffic parameters include: traffic volume (V), shock wave area (A), queue length (Q), platoon ratio (P). Finally, the number of rear-end conflicts per each cycle was estimated. To estimate the number of conflicts, the Time-to-Collision (TTC), with a threshold of 1.5 s, was selected as a traffic conflict indicator. The TTC is generally recognized as the most frequently used indicator to identify rear-end conflicts and is defined as "the time required for two vehicles to collide if they continue at their present speeds and on the same path" (Hayward, 1972).
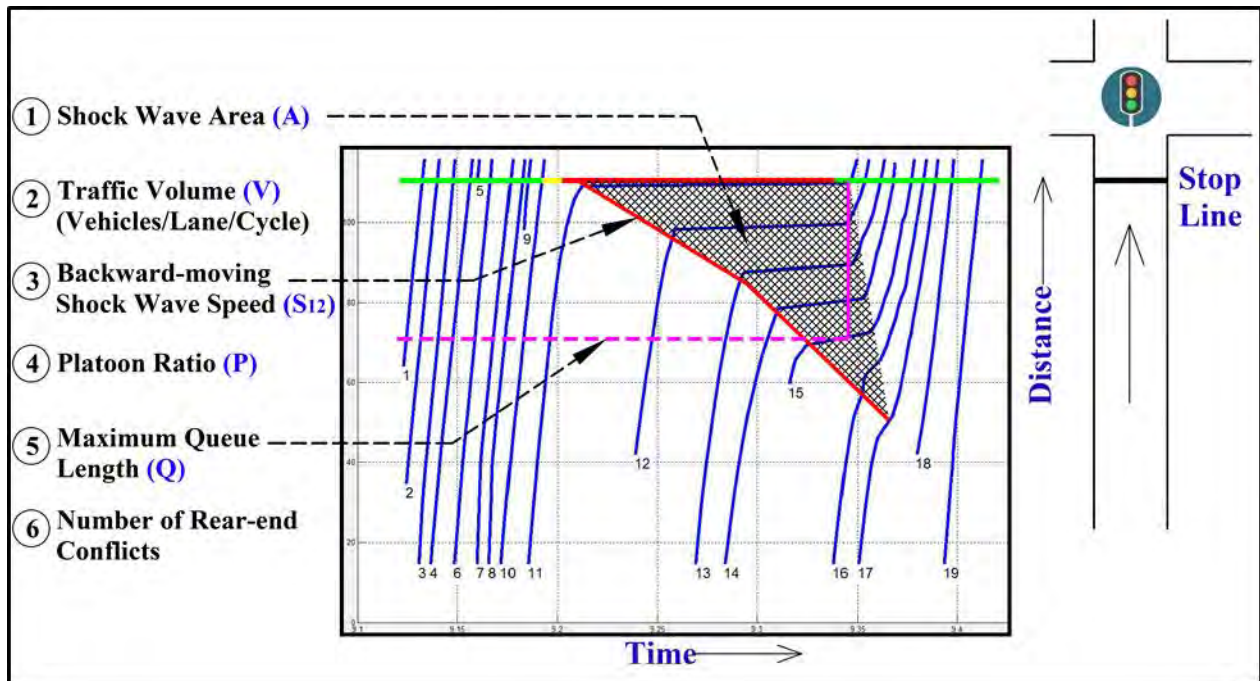
FIGURE 3.1: Traffic Parameters for Real-time Safety Models

Detailed trajectories of more than 2500 vehicles were extracted. **TABLE 3.2** provides a summary of statistics for the data extracted from the video analysis process.

TABLE 3.2: Summary of Data Statistics

Variable	Description	Unit	Mean	SD	Min	Max
V	Traffic Volume per lane per cycle	---	11.58	3.56	2	22
A	Shock wave area	km. seconds	1.05	0.96	0	3.93
Q	Maximum queue length	meter	40.42	24.54	0	97.46
P	Platoon ratio	---	1.26	0.40	0	2.27
$TTC_{1.5}$	Number of rear-end conflicts (TTC≤ 1.5 s)	---	1.88	1.88	0	7

3.3   Real-time Safety Models Development

3.3.1   *Explanatory Variables*

The explanatory variables of the developed models represent dynamic traffic characteristics that can affect the occurrence of traffic conflicts at the signal cycle level. The traffic variables described in the following paragraphs were determined for each signal cycle. It is noteworthy to mention that only through-lanes were considered in the analysis. Exclusive left-turn and right-turn lanes were excluded. Also, all of these traffic characteristics were measured only for cycles that are under-saturated. Over-saturated cycles, where a vehicle can stay in the same approach for more than one cycle, were not included in this study.

The first two explanatory variables of the developed models are the exposure measure represented by the traffic volume (**V**) per cycle per lane and the maximum queue length (**Q**) at each cycle. The

third explanatory variable is the platoon ratio (**P**). The platoon ratio is defined in the Highway Capacity Manual (AASHTO, 2000) as the proportion of all vehicles arriving during green multiplied by the ratio of the signal cycle length to the effective green time of the subject movement. The platoon ratio and the arrival type were shown in previous studies to have a significant effect on the frequency of rear-end conflicts at signalized intersections (Essa and Sayed, 2015a, 2015b, 2016). For each cycle, the platoon ratio was measured assuming that the effective green time is the green time plus half of the yellow time.

The last two explanatory variables represent two shock wave characteristics: the shock wave area (**A**) and the backward-moving shock wave speed (**S₁₂**) (as shown in **FIGURE 3.1**). These shock wave characteristics were chosen based on their significant effect on the frequency of rear-end conflicts at signalized intersections. The relationship between shock waves and road safety has been proven in previous studies (Chatterjee and Davis, 2016; Zheng et al., 2010; Machiani and Abbas, 2016).

3.3.2 Model Response

The model response is the number of traffic conflicts per cycle. Only rear-end conflicts at the intersection approaches were considered. Time-to-Collision (TTC) was used as a traffic conflict indicator. TTC is generally recognized as the most frequently used indicator to identify rear-end conflicts. The TTC is defined as "*the time required for two vehicles to collide if they continue at their present speeds and on the same path*" (Hayward, 1972). For each constitutive vehicle trajectories moving in the same lane, the TTC can be continuously estimated over time using the following equation.

$$TTC_t = \frac{X_{L,t} - X_{F,t} - D_L}{V_{F,t} - V_{L,t}} \; ; \; \forall \left(V_{F,t} - V_{L,t} \right) > 0 \qquad \textbf{Eq. (1)}$$

Where:
t: Time interval
L: Leading vehicle
F: Following Vehicle
X: Vehicle position
V: Vehicle speed
D: Vehicle length

Using the minimum TTC of each conflict, the number of rear-end conflicts was determined for each signal cycle. The critical TTC threshold of 1.50 seconds was applied. **FIGURE 3.1** shows an example of the space-time diagram of one signal cycle and illustrates all the extracted traffic parameters.

3.3.3 The Model Structure

The safety models were developed using the generalized linear models (GLM) approach. The GLM approach was widely applied in literature for the development of collision and conflict

prediction models (e.g., Sawalha and Sayed, 2001; El-Basyouny and Sayed, 2013; Persaud et al., 2010). Previous studies showed that the number of potential traffic conflicts related to the number of vehicles arriving within a small time-interval at a road site occurs by a Poisson process (Elvik et al., 2009). Assuming that traffic conflicts are non-negative, discrete, and rare events compared to the circulating traffic volume, mixed-Poisson distribution family might be used in this regard as with crash data (Sacchi and Sayed, 2016). The GLM approach used to model traffic conflict occurrence assumes an error structure that follows Poisson or Negative Binomial (Poisson-Gamma) distribution. Generally, the model must yield logical results. That is, it must predict zero values of conflict frequency for zero values of exposure variable (i.e. traffic volume), as well as it must not lead to a negative number of conflicts. A commonly used model form consists of an exposure measure(s) raised to some power and multiplied by an exponential function incorporating the remaining explanatory variables. Such a model form can be linearized by the logarithm link function (Sawalha and Sayed, 2006b). Thus, the real-time safety models were expressed mathematically as follows:

$$E(Y) = V^{a_1} \, exp \left[a_0 + \sum_j a_j x_j \right]$$
Eq. (2)

Where:

$E(Y)$: The predicted number of rear-end conflicts per cycle;

V: The traffic volume per lane per cycle (exposure);

x_j: Any other explanatory variables (such as A, Q, S12, or P);

a_0, a_1, a_j: The model parameters.

In order to decide whether the error structure follows Poisson or Negative Binomial distribution, the methodology introduced by (Sawalha and Sayed, 2006) was applied. Poisson distribution was first assumed and the model parameters were estimated. Then the dispersion parameter (σ_d) was calculated using the following equation:

$$\sigma_d = \frac{Pearson \; \chi^2}{n - p}$$
Eq. (3)

Where:

n: The number of observations;

p: The number of model parameters.

$Pearson \; \chi^2$ is defined as follows:

$$Pearson \; \chi^2 = \sum_{i=1}^{n} \frac{[y_i - E(Y_i)]^2}{Var(Y_i)}$$
Eq. (4)

Where:

y_i: The observed number of rear-end conflicts at cycle (i);

$E(Y_i)$: The predicted frequency of rear-end conflicts at cycle (i) as obtained from the conflict prediction model;

$Var(Y_i)$: The variance of conflict frequency for the cycle (i).

The dispersion parameter (σ_d) is a useful measure for assessing the amount of variation in the observed data. If the estimated value of (σ_d) is significantly greater than 1.0, this means that the data have a greater dispersion than what can be explained by the Poisson distribution, and then the Negative Binomial distribution provides a better fit to the data (Sawalha and Sayed, 2006).

The scaled deviance (SD) and the Pearson chi-squared (χ^2) were used as statistical measures to assess the goodness of fit of the developed GLM models. Generally, for a well-fitted model with a relatively large number of observations, the expected values of (χ^2) and SD are approximately equal to the number of degrees of freedom (df) (Sawalha and Sayed, 2001). In addition, different developed models were compared using Akiake's Information Criterion (AIC) (Akaike, 1974) which can be estimated as per Eq. (**5**).

$$AIC = 2p - 2(LogLik_{full}) \qquad \textbf{Eq. (5)}$$

Where:

p: The number of model parameters;

$LogLik_{full}$: Log-likelihood for the full model.

3.4   Results and Discussion

3.4.1   *Real-time Safety Models*

Various models were developed in this research using different combinations of the covariates (**V**, **A**, **Q**, **S12**, and **P**). The reason behind developing various models was to investigate the impact of adding different explanatory variables, and to make the proposed approach applicable in different situations where the availability of measuring or estimating some explanatory variables is limited. For all models, the response (**Y**) denotes the number of rear-end conflicts per cycle that have TTC values equal or less than 1.50 seconds. The TTC threshold of 1.50 seconds is commonly used by researchers to define rear-end conflicts (van der Horst and Hogema 1993). The results of the developed models are provided in **TABLE 3.3**. The first model represents the exposure only. In addition to the first model, the table shows four models that consider the exposure and one additional variable. Furthermore, the last model in the table considers the exposure and a combination of three additional explanatory variables. The significance of the explanatory variables, the goodness-of-fit statistics, and the error structure for all models are provided in the table.

TABLE 3.3: Real-time Safety Models

Base models developed from the base jurisdiction dataset (Canada)							
Model# * $E(Y) =$	Variables	Error Structure	K	SD	df	χ^2	AIC
One Variable (Exposure only): **Model 1:** $V^{1.563} exp(-3.231)$	V	NB	3.05	249	220	356	775
(Exposure + One Variable): **Model 2:** $V^{0.706} exp(-1.797 + 0.501\ A)$	V, A	NB	14.9	244	219	241	702
Model 3: $V^{0.65} exp(-2.046 + 0.0122\ Q)$	V, Q	NB	8.73	243	219	253	716
Model 4: $V^{1.637} exp(-3.316 + 0.05\ S_{12})$	V, S_{12}**	NB	3.10	248	219	347	775
Model 5: $V^{1.571} exp(-1.768 - 1.266\ P)$	V, P	Poisson	---	276	219	281	706
Combined Model: **Model** **6:** $V^{1.239} exp(-1.624 + 0.294\ A - 0.828\ P + 0.119\ S_{12})$	V, A, P, S_{12}	Poisson	---	240	217	215	674

K: Shape parameter for Negative Binomial family
All variables are significantly different from zero at 95% confidence level
*Y: Number of rear-end conflicts per cycle with TTC equal or less than 1.50 seconds
**Significantly different from zero at 90% confidence level

Generally, the developed models show good fit and almost all the explanatory variables are statistically significant at the 95% confidence level. Based on the estimated value of the dispersion parameter (σ_d), the error structure was assumed to follow Negative Binomial distribution for four models, and Poisson distribution for two models. All the covariates' coefficients have logical signs. In other words, higher conflict occurrence is expected during the signal cycles that have long queues and bigger shock waves. On the other hand, the higher platoon ratio means that more vehicles arrive during the green time, and subsequently, a better arrival type and lower chances of conflict occurrence during the cycle.

For the exposure-only model (**model 1**), the coefficient of V is statistically significant at 95% confidence level. This model shows a good fit in terms of the (SD) value which is close to the degree of freedom (df). However, the model has a large value of the Pearson chi-squared (χ^2) compared to the (df). Also, the model has the largest value of AIC comparing to the other models. Thus, despite of the significance of the exposure variable V, more explanatory variables are still needed to provide a better prediction of the conflict occurrence beyond what can be expected from the exposure only.

For the models that consider the exposure and one additional variable (**models 2, 3, 4, and 5**), all models are noted to have a better statistical fit comparing to **model 1**. Also, the additional explanatory variable is significant at 95% confidence level. One exception of that is **model 4** (volume and shock wave speed) whose additional variable (S12) is statistically significant at 90% confidence level. **Model 2** (volume and shock wave area) represents the best model in this group in terms of AIC, (χ^2), and (SD) values. **Model 3** (volume and maximum queue length) shows a good fit in terms of the (χ^2) and (SD) values. This model shows a value of AIC significantly lower than **model 1** and slightly higher than **model 2**. **Model 4** has a value of AIC similar to **model 1**; however, the value of (χ^2) is better than **model 1**. **Model 5** has a value of AIC very close to **model**

2 and significantly better than **model 1**. Thus, the shock wave area, the maximum queue length, the shock wave speed, and the platoon ratio are shown to be important characteristics that affect the number of rear-end conflicts at the signal cycle. Incorporating one of these characteristics (A, Q, S12, or P), along with the traffic volume, in the safety model of signalized intersections is recommended to improve the model fit.

Finally, the last model in the table (**model 6**) combines the exposure measure (V) with three additional explanatory variables (A, P, S12). The maximum queue length (Q) was excluded from this model due to the strong correlation between A and Q, or in other words, the multicollinearity effect. **Model 6** shows the best fit comparing to all previous models. The model presents the minimum values of SD, (χ^2), and AIC. As well, all variables' coefficients are statistically significant in this model at 95% confidence level. However, the main disadvantage of this model is the inclusion of many explanatory variables which may be difficult to obtain in some cases.

3.4.2   *Space-time Distribution of Traffic Conflicts*

In addition to the developed model, a space-time conflict heat map diagram was developed from all observed signal cycles to investigate the distribution of traffic conflicts. To plot the conflict space-time distribution, two measurements were considered for each conflict. The first measurement is the time of the conflict with regard to the signal timing and represented as a percentage. The second measurement is the position of the conflict location ascribed to the stop line location and represented as a distance. **FIGURES 3.2** and **3.3** show heat maps that represent the space-time distribution of the rear-end conflicts at TTC thresholds of 1.5 seconds, and 3 seconds, respectively.
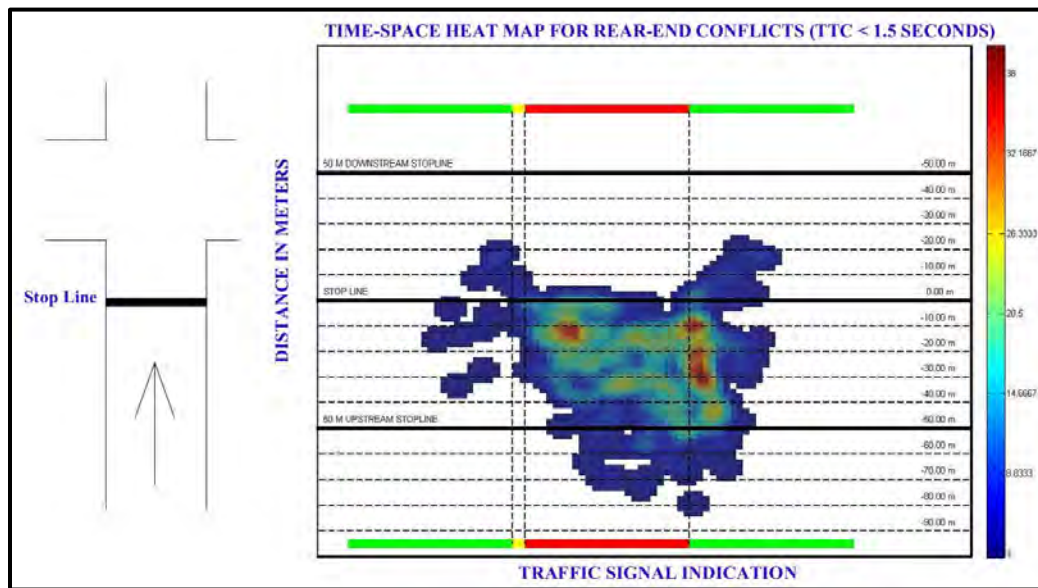
FIGURE 3.2: Space-time Heat Map for Rear-end Conflicts (TTC < 1.5 Seconds) for All Studied Locations (6 Intersections)
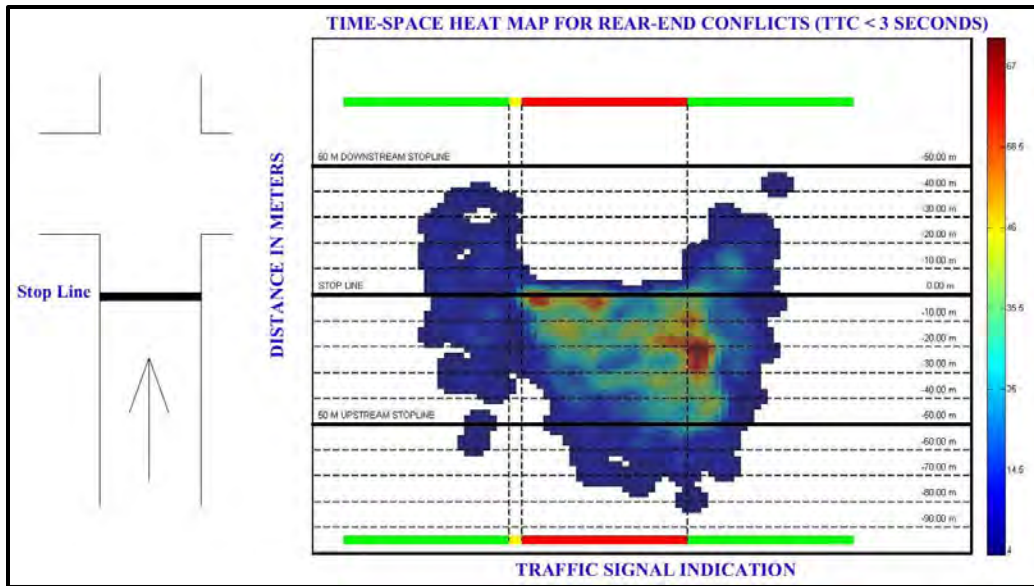
FIGURE 3.3: Space-time Heat Map for Rear-end Conflicts (TTC < 3 Seconds) for All Studied Locations (6 Intersections)

As shown in **FIGURES 3.2** and **3.3**, during the red light, all conflicts occur upstream the stop line. At the beginning of the red light, when the queue length is very short, most of conflicts occur just behind the stop line. After that, the queue length increased gradually, and the most intensive location of conflicts moves backward away from the stop line. By the start of the green light, the cumulative queue starts to discharge and the hot spot of conflicts disappeared gradually with the progression of the green time. It can also be noted that conflicts are distributed with time upstream and downstream the stop line during the green and yellow times. This is reasonable because, during these times, both of the conflicting vehicles are moving with a speed larger than zero which causes some conflicts to have a potential location downstream the stop line.

The heat maps illustrate graphically the association between the rear-end conflicts and the shock wave area. It can be noted that the intensive conflict area in the heat map (red, yellow, and green spots) forms, approximately, a polygon that is similar to the shock wave area shown in **FIGURE 3.1**.

It is also noteworthy that the heat maps show two areas with red spots (most intensive conflict areas). The first one occurs at the beginning of the red light, which most probably represents the dilemma zone where the traffic signal indication changes from green to yellow to red. The second one occurs during the start of the green time where the stopped flow starts to discharge gradually at low speed while other vehicles are arriving at higher speeds to the end of the queue. The heat maps show a relationship between the rear-end conflicts and the queue length. For example, the most intensive conflict area in the heat map is located upstream the stop line within a distance that approximately represents the 50th percentile of the maximum queue length. As well, most of the conflicts occur within a distance that approximately represents the 85th percentile of the maximum queue length.

3.5 Potential Applications

Several potential implementations of the developed models can be summarized as follows:

- **Safety evaluation using field-observed data:**
  The traffic parameters at each signal cycle can be observed in the field or by video camera and used in the models to estimate the predicted number of rear-end conflicts that is necessary for safety evaluation.

- **The calibration of the microsimulation models for safety evaluation:**
  Generally, the use of microsimulation models in safety analysis has been criticized for two main reasons. First, vehicles in the simulation models follow specific rules which are aimed at avoiding collisions. Therefore, it is very difficult to represent unsafe vehicle interactions and near misses. Second, there are many parameters and several ways to model traffic in simulation models in microsimulation models. Therefore, the results can vary significantly depending on the input values of the model parameters and the approach used in modeling (Essa and Sayed, 2016). Furthermore, a rigorous calibration process is essential to avoid inaccurate results. Researchers have advocated the use of field measured conflicts in the calibration process, but this data can be difficult to obtain (Essa and Sayed, 2016). The developed models in this study can be used to facilitate the calibration process of the simulation models. The target of calibration process can be matching the actual and the simulated traffic parameters used in the developed SPFs (such as the queue length and the shock wave characteristics) instead of matching the actual and the simulated traffic conflicts.

- **The real-time safety optimization of signalized intersections:**
  Real-time safety monitoring and evaluation gained interest among researchers as a proactive strategy to improve safety (Shi and Abdel-Aty, 2015; Oh et al., 2005; Hossain and Muromachi, 2012; among others). Real-time data of the approaching vehicles will be available in the connected-vehicles environment via vehicle-to-vehicle (V2V) and vehicle-to-infrastructure (V2I) communications (Harding et al., 2014). The connected-vehicles data can be used in obtaining various traffic parameters and performing a real-time adaption of signal design by minimizing the total delays and the queue length (Feng et al., 2015). Typically, enhancing capacity is the main criterion employed by traffic operator agencies; however, the models, developed in this study, can be further used to predict the number of rear-end conflicts using the obtained traffic parameters in real-time. This can be useful in giving insight about how changes in the signal cycle design affects the safety of the signalized intersection. Thus, the real-time adaption of the signal design can consider both mobility and safety. This can be obtained by solving a multi-objective optimization process that seeks minimizing both the total delays and the total number of traffic conflicts for all the intersection approaches.

CHAPTER 4: TRANSFERABILITY OF REAL-TIME SAFETY MODELS

The objective of this chapter is to investigate the transferability of the real-time safety models presented in **Chapter 3**. The models are conflict-based safety models that relate rear-end conflicts occurring in each signal cycle to dynamic variables such as traffic volume, maximum queue length, shock wave characteristics, and platoon ratio. The models were developed based on actual traffic data extracted from video scenes recorded at six signalized intersections in Canada. The Time-to-Collision (TTC) (Hayward, 1972) was used as a traffic conflict indicator. The regression results showed that the models have good fit with all explanatory variables being statistically significant.

The transferability analysis includes evaluating the performance of the real-time safety models at two new jurisdictions. Several conventional measures of transferability and goodness-of-fit were estimated. Moreover, the models were locally calibrated at the new jurisdictions and their transferability was re-evaluated after the calibration process. The overall goal was to test the validity of using those models for real-time safety evaluation at signalized intersections.

4.1   Background

Many previous studies have examined transferring and calibrating collision-based safety performance functions (SPFs) from one jurisdiction to another. Several approaches were proposed in the literature to calibrate the transferred safety models locally at the destination jurisdiction. For example, the HSM (AASHTO, 2010) presents a calibration procedure to adjust the predictive SPFs which was developed with data from one jurisdiction for application in another jurisdiction. The procedure aims to account for differences between jurisdictions in factors such as climate, driver populations, etc. In this procedure, the baseline SPFs should be first modified by collision modification factors (CMFs) to account for differences in features from the baseline conditions, such as the lane width for two-lane roads or the existence of left-turn lane at signalized intersections. Afterwards, a calibration factor (C) should be applied to adjust the number of the predicted collisions at the new jurisdiction. As shown in **Eq. (1)**, the calibration factor (C) is the ratio of the total observed crash frequencies for a selected set of sites at the new jurisdiction to the total predicted crash frequencies for the same sites, during the same time period (AASHTO, 2010).

$$C = \frac{\sum Observed\ Crashes}{\sum Predicted\ Crashes} \qquad \textbf{Eq. (6)}$$

The HSM calibration procedure has been applied in many previous studies in different jurisdictions for different types of road facilities. **TABLE 4.1** provides a sample of these studies with their description.

TABLE 4.1: Sample of Previous Studies that Adopted the HSM's Calibration Procedure

Study	Country	Road Facility	C
(Srinivasan and Carter, 2011)	USA, NC	Rural 2-Lane, Signalized Intersections 4-Leg	1.04
		Rural 4-Lane, Signalized Intersections 4-Leg	0.49
		Urban 2-Lane, Signalized Intersections 3-Leg	2.47
		Urban 2-Lane, Signalized Intersections 4-Leg	2.79
(Xie et al., 2011)	USA, OR	Rural 2-Lane Undivided, Road segments	0.74
		Rural Multi-Lane Undivided, Road segments	0.36
		Rural Multi-Lane Divided, Road segments	0.78
		Urban 2-Lane Undivided, Road segments	0.63
		Rural 4-Leg Signalized Intersections	0.15
		Urban 3-Leg Signalized Intersections	0.75
		Urban 4-Leg Signalized Intersections	1.10
(Brimley et al., 2012)	USA, UT	Rural 2-way 2-Lane, Road segments	1.16
(Young et al., 2012)	Canada, SK	Urban 3-Leg Unsignalized Intersections	1.47
		Urban 4-Leg Unsignalized Intersections	1.63
		Urban 3&4-Leg Signalized Intersections	2.25
(Mehta and Lou, 2013)	USA, AL	Rural 2-way 2-Lane, Road segments	1.392
		Rural 4-Lane Divided, Road segments	1.103
(Sun et al., 2014)	USA, MO	Rural Multi-Lane Divided, Road segments	0.98
		Urban 2-Lane Undivided, Road segments	0.84
		Urban 4-Lane Divided, Road segments	0.98
		Urban 5-Lane Undivided, Road segments	0.73
		Urban 3-Leg Signalized Intersections	3.03
		Urban 4-Leg Signalized Intersections	4.91
(Cafiso et al., 2012) & (D'agostino, 2014)	Italy	Rural Multi-Lane Divided, Road segments	1.26
(Cunto et al., 2014)	Brazil	Urban Signalized Intersections	0.98
		Urban Unsignalized Intersections	2.15

Although it was applied widely in the literature, the HSM's calibration procedure was criticized by some researchers for several reasons. First, the procedure does not provide a method for testing the model transferability. Moreover, there is no evidence to show that the calibration procedure accounts for the safety differences between various regions. Thus, the procedure may lead to inaccurate estimations and predictions when applied to some jurisdictions, especially outside the United States, due to the large variation in the general level of crash frequencies and the risk factors that vary between jurisdictions. Lastly, the HSM's calibration procedure is an aggregate method that does not correct for the errors in the predicted crashes of individual locations (Sawalha and Sayed, 2006a; Persaud et al., 2002; Chen et al., 2012; Cunto et al., 2014; Farid et al., 2018).

To overcome the limitations of the HSM's procedure, several approaches have been proposed in previous research for calibrating the transferred SPFs locally at the new jurisdiction. This includes the intercept and over-dispersion parameter calibration (Sawalha and Sayed, 2006a), the Bayesian Modelling Averaging (Chen et al., 2012), the calibration function for the Negative Binomial distribution of collisions (Srinivasan et al., 2016), the Modified Empirical Bayes (Farid et al., 2016), the informative priors (Farid et al., 2017), and the local regression (Farid et al., 2018), among others.

To assess the goodness-of-fit of the transferred models, various statistical measures have been applied in the literature. This includes cumulative residual (CURE) plots (Persaud et al., 2002; Chen et al., 2012; Sacchi et al., 2012; Cunto et al., 2014); the transfer index (Hadayeghi et al., 2006; Farid et al., 2016, 2018); the Pearson chi-squared and Z-score (Sawalha and Sayed, 2006a; Cunto et al., 2014); the mean prediction bias, the mean absolute deviation, and the mean absolute percentage error (Chen et al., 2012; Sacchi et al., 2012; Cunto, et al., 2014; Farid et al., 2016, 2018).

In this chapter, the transferability of the real-time safety models (or SPFs) presented in **Chapter 3** is investigated. The calibration procedure proposed by (Sawalha and Sayed, 2006a) was applied to transfer the SPFs to new jurisdictions. The procedure comprises a local calibration at the destination jurisdiction for both the model's intercept and the over-dispersion parameter (the shape parameter of the Negative Binomial model). To test the model transferability, the transfer index (Koppelman and Wilmot, 1982) was applied. Furthermore, several goodness-of-fit measures were used to assess the model fit at the new jurisdictions. This includes: 1) the Pearson's product moment correlation coefficient; 2) the mean prediction bias; 3) the mean absolute deviation; 4) the mean absolute percentage error; 5) the Pearson chi-squared (Pearson, 1900); and 6) the Z-score (Vogt and Bared, 1998).

4.2   Destination Jurisdiction Datasets

Two different datasets, from two corridors of signalized intersections in California and Atlanta in USA, were used as destination jurisdictions for the transferability analysis. For each corridor, detailed traffic data was obtained from the NGSIM vehicle trajectories and supporting data provided online by the United States Department of Transportation (US DOT, 2018). The first corridor is Lankershim Boulevard, an arterial in Los Angeles, California, USA. Vehicle trajectories for three main intersections along this corridor were analyzed. The second corridor is Peachtree Street, an arterial in Atlanta, Georgia, USA. Vehicle trajectories for four main intersections along this corridor were analyzed. **FIGURE 4.1** shows the location and the selected intersections of both corridors. Details on the selected intersections along each corridor are provided in **TABLE 4.2**. This includes: the intersected roads, the date and time of data collection, the selected approaches, the number of lanes per approach, and the signal timing.
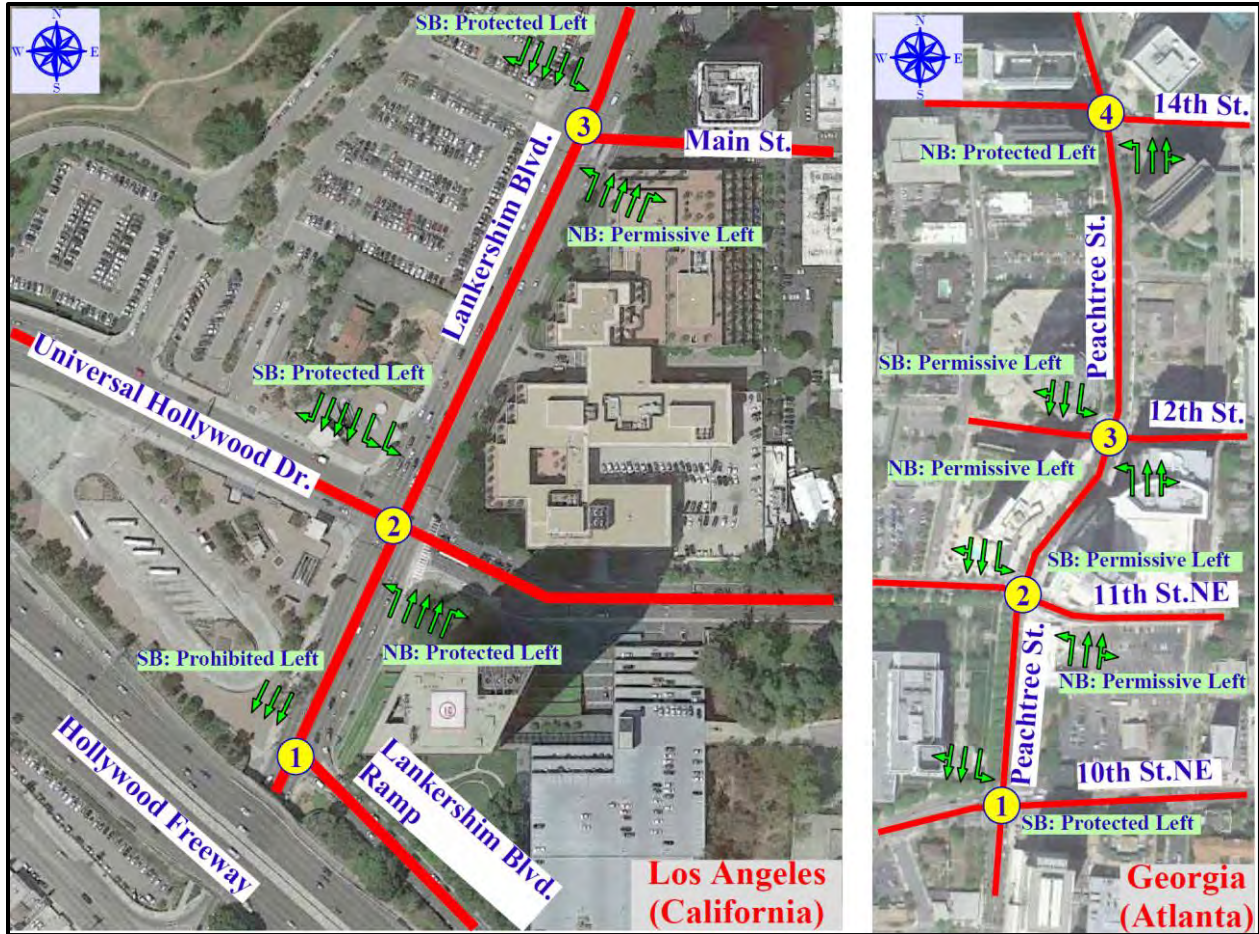
- The left image shows the first destination Jurisdiction (Lankershim Blvd., Los Angeles, California, USA)
- The right image shows the second destination jurisdiction (Peachtree St., Georgia, Atlanta, USA)

FIGURE 4.1: Destination Jurisdictions

TABLE 4.2: Location of the Two Destination Jurisdictions

First Destination Jurisdiction Dataset (California, USA)						
Site #	City (State)	Intersected roads	Video-data was recorded in	Selected approaches	Number of lanes per approach	Traffic signal timing (s)
1	Los Angeles (California)	Lankershim Blvd. & Lankershim Blvd. Ramp	June 16th, 2005 (8:28 – 9:00 am)	Lankershim Blvd. (Southbound)	3 (Through)	🔴 15 to 30 🟡 3 🟢 65 to 85
2	Los Angeles (California)	Lankershim Blvd. & Universal Hollywood Dr.	June 16th, 2005 (8:28 – 9:00 am)	Lankershim Blvd. (Northbound & Southbound)	1 NB or 2 SB (Left) 3 (Through) 1 (Right)	🔴 32 to 77 🟡 3 🟢 30 to 70
3	Los Angeles (California)	Lankershim Blvd. & Main St.	June 16th, 2005 (8:28 – 9:00 am)	Lankershim Blvd. (Northbound & Southbound)	1 (Left) 3 (Through) 1 (Right)	🔴 17 to 33 🟡 3 🟢 59 to 120
Second Destination Jurisdiction Dataset (Atlanta, USA)						
Site #	City (State)	Intersected roads	Video-data was recorded in	Selected approaches	Number of lanes per approach	Traffic signal timing (s)
1	Atlanta (Georgia)	Peachtree St. & 10th St. NE	November 8th, 2006 (12:45 – 1:00 pm) (4:15 – 4:30 pm)	Peachtree St. (Southbound)	1 (Left) 1 (Through) 1 (Through + Right)	🔴 45 to 63 🟡 4 🟢 30 to 44
2	Atlanta (Georgia)	Peachtree St. & 11th St. NE	November 8th, 2006 (12:45 – 1:00 pm) (4:15 – 4:30 pm)	Peachtree St. (Northbound & Southbound)	1 (Left) 1 (Through) 1 (Through + Right)	🔴 15 to 52 🟡 4 🟢 40 to 88
3	Atlanta (Georgia)	Peachtree St. & 12th St. NE	November 8th, 2006 (12:45 – 1:00 pm) (4:15 – 4:30 pm)	Peachtree St. (Northbound & Southbound)	1 (Left) 1 (Through) 1 (Through + Right)	🔴 16 to 33 🟡 4 🟢 60 to 89
4	Atlanta (Georgia)	Peachtree St. & 14th St. NE	November 8th, 2006 (12:45 – 1:00 pm) (4:15 – 4:30 pm)	Peachtree St. (Northbound)	1 (Left) 1 (Through) 1 (Through + Right)	🔴 14 to 59 🟡 4 🟢 31 to 84

The NGSIM data was originally collected by researchers for the NGSIM program through a network of synchronized digital video cameras. NGVIDEO, a customized software application developed for the NGSIM program, transcribed the vehicle trajectory data from the video (US DOT, 2018). For the analysis of this study, the trajectory data for each of the selected corridors was downloaded from (US DOT, 2018) as a spreadsheet. The spreadsheet includes vehicles' identification number, position, length, occupied lane number, speed, direction, and acceleration at each 0.1 second for 30-minutes period. A MATLAB code was developed to filter the NGSIM

data for each intersection approach and divide it into cycles. For each cycle, the code plots the space-time diagram to determine different traffic characteristics and the number of rear-end conflicts. Detailed trajectories of more than 2100 vehicles were extracted and analyzed. **TABLE 4.3** provides a summary of statistics of the first and the second destination jurisdiction datasets.

TABLE 4.3: Summary of Statistics - Destination Jurisdiction Datasets

First Destination Jurisdiction Dataset (California, USA)						
Variable	**Description**	**Unit**	**Mean**	**SD**	**Min**	**Max**
V	Traffic Volume per lane per cycle	---	12.70	4.04	3	26
A	Shock wave area	km. seconds	1.45	1.16	0	4.41
Q	Maximum queue length	meter	44.26	26.75	0	113.63
S12	Backward-moving shock wave speed	meter/second	-1.54	1.22	-7.60	0
P	Platoon ratio	---	1.11	0.38	0.31	2.83
TTC1.5	Number of rear-end conflicts (TTC≤ 1.5sec)	---	2.95	2.51	0	12
Second Destination Jurisdiction Dataset (Atlanta, USA)						
Variable	**Description**	**Unit**	**Mean**	**SD**	**Min**	**Max**
V	Traffic Volume per lane per cycle	---	8.55	3.33	1	19
A	Shock wave area	km. seconds	1.02	0.89	0	3.79
Q	Maximum queue length	meter	33.34	21.48	0	88.61
S12	Backward-moving shock wave speed	meter/second	-1.89	1.59	-6.61	0
P	Platoon ratio	---	1.37	0.60	0.20	3.68
TTC1.5	Number of rear-end conflicts (TTC≤ 1.5sec)	---	2.39	1.89	0	8

4.3   Transferability Analysis

4.3.1   Statistical Measures to Test Transferability

The transferability of the base models was investigated using the data obtained from the destination jurisdictions. To assess the transferability of each model, the transfer index (TI) measure (Koppelman and Wilmot, 1982) was estimated. The Transfer Index (TI) is a relative measure that indicates how well a transferred model performs in predicting the application dataset relative to a model locally-estimated at the application context (Koppelman and Wilmot, 1982). The index has been applied in several studies to perform transferability analysis (Hadayeghi et al., 2006; Sikder et al., 2014; Farid et al., 2016; Farid et al., 2018). The upper bound of TI is 1, which means the transferred model performs on the new jurisdiction dataset (the application dataset) as good as the locally-estimated model. Negative values of TI indicate that the transferred model is worse than the local constant model. The TI can be expressed as follows (Koppelman and Wilmot, 1982; Hadayeghi et al., 2006):

$$TI = \frac{L_j(\widehat{\theta_\iota}) - L_j(\hat{c})}{L_j(\widehat{\theta_j}) - L_j(\hat{c})} \qquad \textbf{Eq. (7)}$$

Where:
TI: $Transfer\ Index$
$L_j(\widehat{\theta_\iota})$: Log-likelihood in application context j using model from context i

$L_j(\hat{\theta}_j)$: Log-likelihood given by application context model j
$L_j(\hat{c})$: Log-likelihood given by constant model estimated in application context j

In addition to TI, several goodness-of-fit (GOF) measures were calculated to assess the ability of the transferred models to predict traffic conflicts at the new jurisdictions (the application jurisdictions). This includes: 1) Akiake's Information Criterion (AIC) (Akaike, 1974); 2) Pearson's product moment correlation coefficient (r); 3) Mean prediction bias (MPB); 4) Mean absolute deviation (MAD); 5) Mean absolute percentage error (MAPD); 6) Pearson chi-squared (χ^2) (Pearson, 1900); and 7) Z-score (Vogt and Bared, 1998). All of these measures compare the predicted conflicts obtained from the model with the observed ones at the new jurisdictions. The AIC of the transferred model can be estimated using equation 6 by getting the log-likelihood in the application context (the new jurisdiction dataset) using the model from the base context. The AIC measure is used to compare models that have the same dependent variable (the same response). For a certain dataset, the model that has the lowest AIC value is the best (Akaike, 1974). The Pearson's product moment correlation coefficient (r) between the observed and the predicted conflicts provides an indication on how well the model predicts the observed conflicts. The r values can range from -1 to +1. The ideal model gives r value of 1 which indicates a perfect fit.

The mean prediction bias (MPB) describes the magnitude and direction of the average bias in the subject model. The closer to zero the value of the MPB is, the better the model predicts the observed data. Positive values of MPB indicate that the model under-predicts the observed conflicts, and vice versa. The MPB can be expressed mathematically as follows:

$$MPB = \sum_{i=1}^{n} \frac{y_i - E(Y_i)}{n} \qquad \textbf{Eq. (8)}$$

Where:
y_i: The observed number of rear-end conflicts at cycle (i) in the new jurisdiction dataset;
$E(Y_i)$: The predicted frequency of rear-end conflicts at cycle (i) in the new jurisdiction dataset as obtained from the conflict prediction model;
n: The sample size of the new jurisdiction dataset.

The mean absolute deviation (MAD) describes the average prediction error of the model. MAD values close to zero indicate that the model on average predicts the observed data well. The MAD can be defined as follows:

$$MAD = \sum_{i=1}^{n} \frac{|y_i - E(Y_i)|}{n} \qquad \textbf{Eq. (9)}$$

The mean absolute percentage error (MAPD) describes the absolute prediction error of the model as a percentage of the total number of the observed conflict. The MAPD value close to zero indicates a good prediction of the subject model. The MAPD can be defined as follows:

$$MAPD = \frac{\sum_{i=1}^{n} |y_i - E(Y_i)|}{\sum_{i=1}^{n} y_i}$$ **Eq. (10)**

The Pearson chi-squared statistic (χ^2), given in equation 5, is a measure of the goodness of fit of a model to any dataset. Therefore, it can be used to test whether a certain model, developed at the base jurisdiction, can provide reliable predictions at a new jurisdiction (Sawalha and Sayed, 2006a; Vogt and Bared, 1998). The Z-score measures how far the calculated χ^2 statistic is from its expected value. Z-score values close to zero indicate that the transferred model predicts the new observed data well. The Z-score can be defined as follows (Sawalha and Sayed, 2006a; Vogt and Bared, 1998):

$$Z\_Score = \frac{\chi^2 - E(\chi^2)}{\sigma(\chi^2)}$$ **Eq. (11)**

Where:
$E(\chi^2)$: The expected value of χ^2 (the number of observations in the new dataset (*n*));
$\sigma(\chi^2)$: The standard deviation of χ^2.

In addition to the previous GOF measures, the HSM calibration factor (C), which is defined in equation 1, was estimated for each model to compare the total number of the predicted conflicts with the total number of the observed conflicts. C values higher than 1 indicate that the model generally underestimate the number of conflicts, and vice versa. However, this factor was used in this study as a GOF measure not as a calibration factor to calibrate the SPFs.

4.3.2   *Transferability Analysis Approaches*

Generally, there are two approaches for analyzing the transferability of a specific model: 1) the application-based approach, and 2) the estimation-based approach. In the application-based approach, the base model developed from the base jurisdiction is applied with no change (without calibration) to the destination jurisdiction (the application context) to assess how well the model predicts at the new region. In the estimation-based approach, the base model parameters estimated from the base jurisdiction data are recalibrated using the destination jurisdiction data to test whether each parameter in the model is transferable (Sawalha and Sayed, 2006a; Sikder et al., 2014). In this research, both approaches were applied to investigate the transferability of the base SPFs.

4.3.2.1   *Application-based approach*

In this approach, the six base SPFs, developed at the base jurisdiction (Canada), were transferred as they are with no change to the new jurisdictions (California and Atlanta). The transfer index and the GOF measures were estimated for each model. **TABLE 4.4** provides the results obtained from the transferred models at each destination jurisdiction.

TABLE 4.4: Transferring the Base SPFs to the Destination Jurisdictions without Calibration

Base Models (Canada's Models) Transferred without Calibration to the First Destination Jurisdiction (California – USA)								
Model #	TI	AIC	r	MPB	MAD	MAPD	χ^2	Z Score	C
Model 1	0.984	517	0.34	0.75	1.91	0.65	175	2.72	1.344
Model 2	0.986	503	0.48	0.34	1.71	0.58	215	5.48	1.130
Model 3	0.909	490	0.77	0.65	1.36	0.46	133	0.97	1.284
Model 4	0.987	516	0.36	0.70	1.88	0.64	165	2.26	1.310
Model 5	0.956	523	0.47	0.26	1.77	0.60	305	10.7	1.097
Model 6	0.980	509	0.50	-0.01	1.79	0.61	235	6.98	0.997
Base Models (Canada's Models) Transferred without Calibration to the Second Destination Jurisdiction (Atlanta – USA)								
Model #	TI	AIC	r	MPB	MAD	MAPD	χ^2	Z Score	C
Model 1	0.916	328	0.44	1.19	1.53	0.64	189	5.8	1.982
Model 2	0.953	312	0.52	0.95	1.31	0.55	158	5.32	1.654
Model 3	0.920	310	0.74	1.10	1.31	0.55	138	3.8	1.858
Model 4	0.892	336	0.37	1.20	1.57	0.66	214	7.07	2.011
Model 5	0.733	378	0.54	1.12	1.38	0.58	1379	57.59	1.877
Model 6	0.857	352	0.47	1.16	1.49	0.62	577	28.29	1.944

The results in **TABLE 4.4** show that the transferred models have high values of TI that range from 0.73 to 0.987. This reveals that the base SPFs developed at the cycle level are fairly transferable to other jurisdictions. The MPB and C results indicate that all models generally underestimate the observed conflicts. One exception of that is model 6, which slightly overestimates the number of conflicts at the first destination jurisdiction. The results also show medium to high correlation (r) between predicted and observed conflicts. In addition, Pearson chi-squared and Z-score values support the transferred models, except for models 5 and 6 at the second destination jurisdiction. In fact, it is very difficult to determine the best model of the six base SPFs when all the GOF measures provided in **TABLE 4.4** are considered. However, it can be noticed that models 2, 3, and 6 have the best performance at the first destination jurisdiction. At the second destination jurisdiction, models 2 and 3 provide the best data fitting.

4.3.2.2 *Estimation-based approach*

In this approach, the base model parameters estimated from the base jurisdiction data are recalibrated using the destination jurisdiction data. Two methods of calibration were considered herein. The first method comprises the calibration of the model intercept and the shape parameter only, while the second method considers the calibration of all the model parameters.

Intercept and shape parameter calibration
In this section, the base SPFs, developed at the base jurisdiction (Canada), were transferred to the new jurisdictions (California and Atlanta) after calibrating both the model intercept and the shape parameter, following the calibration procedure proposed in (Sawalha and Sayed, 2006a). For each model, a new intercept and shape parameter for each model were determined using the method of maximum likelihood. The statistical analysis software "R" was used to perform the GLM regression and the maximum likelihood calculations. The coefficients of all the explanatory

variables were forced to their original values obtained from the base jurisdiction. The "offset" command within the GLM regression functions in "R" was applied to perform this process. Afterwards, the transfer index and the GOF measures were estimated for each model. **TABLE 4.5** provides the results obtained from the transferred models at each destination jurisdiction after the calibration process.

TABLE 4.5: Transferring the Base SPFs to the Destination Jurisdictions with Calibration of the Model Intercept and the Shape Parameter

Base Models (Canada's Models) Transferred with Calibrated Intercept and Shape Parameter to the First Destination Jurisdiction (California – USA)											
Model #	a_0^{c} *	K^{c} **	TI	AIC	r	MPB	MAD	MAPD	χ^2	Z Score	C
Model 1	-2.899	3.13	0.998	486	0.34	-0.11	1.95	0.66	97	-0.79	0.964
Model 2	-1.58	3.98	0.996	471	0.48	-0.29	1.86	0.63	112	-0.08	0.910
Model 3	-1.796	Poisson	0.968	417	0.77	0.00	1.30	0.44	110	-0.22	1.000
Model 4	-3.013	3.27	0.997	486	0.36	-0.10	1.92	0.65	98	-0.75	0.968
Model 5	-1.599	2.96	0.967	501	0.47	-0.29	1.91	0.65	156	1.85	0.910
Model 6	-1.522	3.74	0.983	482	0.50	-0.33	1.90	0.64	125	0.53	0.900
Base Models (Canada's Models) Transferred with Calibrated Intercept and Shape Parameter to the Second Destination Jurisdiction (Atlanta – USA)											
Model #	a_0^{c} *	K^{c} **	TI	AIC	r	MPB	MAD	MAPD	χ^2	Z Score	C
Model 1	-2.525	10.59	0.998	271	0.44	-0.05	1.26	0.53	69	-0.33	0.979
Model 2	-1.273	16.92	0.999	261	0.52	-0.05	1.25	0.52	65	-0.62	0.979
Model 3	-1.427	Poisson	0.999	236	0.74	0.00	0.95	0.40	48	-1.84	1.000
Model 4	-2.576	6.80	0.982	280	0.37	-0.10	1.36	0.57	69	-0.3	0.960
Model 5	-1.008	3.85	0.874	324	0.54	-0.38	1.50	0.63	557	23.67	0.863
Model 6	-0.894	7.16	0.948	294	0.47	-0.16	1.28	0.54	213	8.27	0.937

*a_0^{c}: Model intercept calibrated at the new jurisdiction
**K^{c}: Model shape parameter calibrated at the new jurisdiction

The results in **TABLE 4.5** show that there is a notable improvement in the GOF measures for all models in general after calibrating the intercept and the shape parameter. Specifically, the measures TI, AIC, χ^2 and Z-Score were significantly improved. This is expected as the local calibration of the intercept and the shape parameter allows the transferred models to better suit local conditions at the destination jurisdictions. The intercept usually accounts for most factors outside the explanatory variables. On the other hand, for negative binomial models, the shape parameter (k) of the model determines the variability of the data around the model regression hyper-surface. This variability for the new jurisdiction dataset might be different than that for the original dataset. Furthermore, χ^2 and Z-Score values are dependent upon the shape parameter. Therefore, the shape parameter calibration is necessary and expected to improve the fit of the transferred models (Sawalha and Sayed, 2006a).

As shown in **TABLE 4.5**, the TI values of the transferred models are much closer to 1. The TI values range from 0.874 to 0.999. This confirms that the base SPFs are considerably transferable to other jurisdictions if the intercept and the shape parameter are locally-calibrated. The MPB and C values became much closer to zero and one, respectively. The correlation (r) values are the same

as **TABLE 4.4**. This is because the coefficients of all the explanatory variables were forced to their original values during the calibration process. Pearson chi-squared and Z-score values support the transferred models, except for models 5 and 6 at the second destination jurisdiction. It is still difficult to determine the best model of the six base SPFs when all the GOF measures provided in **TABLE 4.5** are considered. However, it can be noticed again that models 2, 3, and 6 have the best performance at the first destination jurisdiction. At the second destination jurisdiction, models 2 and 3 provide the best data fitting.

Full model calibration

In this section, the six SPFs (shown in **TABLE 3.3**) were redeveloped at the two new jurisdictions: California and Atlanta, using the same procedure described earlier. The main goal is to confirm that the selected explanatory variables (**V, A, Q, P, S₁₂**) are important characteristics that affect the number of rear-end conflicts at the signal cycle and can provide a better prediction of the conflict occurrence beyond what can be expected from the traffic volume only. In addition, developing these models using different datasets can help in recommending the best one of them to be used for real-time safety evaluation. **TABLE 4.6 (a, b)** provides a summary of the SPFs redeveloped using the two destination jurisdiction datasets.

TABLE 4.6: SPFs at the Cycle Level Developed at the Destination Jurisdictions

a) Models redeveloped at the first destination jurisdiction (California - USA)							
Model# * $E(Y) =$	**Variables**	**Error Structure**	**K**	**SD**	**df**	χ^2	**AIC**
One Variable (Exposure only): **Model 1a:** $V^{1.067}exp(-1.633)$	V	NB	3.46	129	112	99	482
(Exposure + One Variable): **Model 2a:** $V^{0.625}exp(-1.049 + 0.316\,A)$	V, A	NB	6.21	128	111	113	459
Model 3a: This model was excluded	V, Q	---	---	---	---	---	---
Model 4a: $V^{1.232}exp(-1.853 + 0.13\,S_{12})$	V, S_{12}	NB	3.70	129	111	99	481
Model 5a: $V^{0.987}exp(-0.937 - 0.461\,P)$	V, P	NB	4.14	132	111	106	478
Combined Model**: **Model 6a:** $V^{0.805}exp(-1.295 + 0.32\,A + 0.143\,S_{12})$	V, A, S_{12}	NB	7.01	127	110	110	456
b) Models redeveloped at the second destination jurisdiction (Atlanta - USA)							
Model# * $E(Y) =$	**Variables**	**Error Structure**	**K**	**SD**	**df**	χ^2	**AIC**
One Variable (Exposure only): **Model 1b:** $V^{1.116}exp(-1.531)$	V	NB	19.8	80	72	69	268
(Exposure + One Variable): **Model 2b:** $V^{0.924}exp(-1.49 + 0.307\,A)$	V, A	Poisson	---	74	71	65	255
Model 3b: $V^{0.483}exp(-1.078 + 0.023\,Q)$	V, Q	Poisson	---	55	71	47	236
Model 4b: This model was excluded	V, S_{12}	---	---	---	---	---	---
Model 5b: This model was excluded	V, P	---	---	---	---	---	---
Combined Model: **Model 6b:** This model was excluded	V, A, P, S_{12}	---	---	---	---	---	---

K: Shape parameter for Negative Binomial family
All variables are significantly different from zero at 95% confidence level
*Y: Number of rear-end conflicts per cycle with TTC equal or less than 1.50 seconds
**The platoon ratio (P) was removed from this model as it was not statistically significant at 95% confidence level

Overall, the redeveloped models at the two new jurisdictions, shown in **TABLE 4.6**, show good fit with almost all the explanatory variables are statistically significant. Based on the estimated value of the dispersion parameter (σ_d), the error structure was assumed to follow Negative Binomial distribution for all models except two models whose error structure follows Poisson distribution. The redeveloped models emphasize that the shock wave area, the maximum queue length, the shock wave speed, and the platoon ratio are important covariates that affect the number of rear-end conflicts. Incorporating one of these covariates or a combination of them, along with the traffic volume, in the SPFs improves the model fit and provides a better conflict prediction. This can be noticed from the improvement in the AIC value when adding one of these covariates to the traffic volume in the developed SPFs. Moreover, all the covariate coefficients have logical signs that conform to those of the base models provided in **TABLE 3.3**. In other words, the number of conflicts is expected to increase during signal cycles that have higher volumes, longer queues, and bigger shock waves. On the other side, it is intuitive that more vehicle-arrivals on green time lead to higher platoon ratios and less conflict probability.

It should be noted that some models were excluded from **TABLE 4.6**, such as models **3a**, and **4b-6b**. Basically, a model is excluded either because the model does not show an AIC value better than that obtained from another model with a smaller number of covariates, or because some covariates in the model are not statistically significant at 95% confidence level. This insignificance is usually due to the correlation between the model covariates (the multicollinearity effect). One factor that may contribute to the multicollinearity effect in the excluded models is the existing signal coordination along the selected corridors (Lankershim Boulevard and Peachtree Street). Future research is recommended to incorporate the effect of the signal coordination into real-time SPFs.

After redeveloping the SPFs at the new jurisdictions, the GOF measures were estimated for each model. **TABLE 4.7** provides the GOF results for each model at each destination jurisdiction.

TABLE 4.7: Goodness-of-Fit Measures of SPFs Developed at the Destination Jurisdictions

Model #	AIC	r	MPB	MAD	MAPD	χ^2	Z Score	C
Full Model Calibration at the First Destination Jurisdiction (California – USA)								
Model 1a	482	0.35	-0.01	1.87	0.63	99	-0.72	0.997
Model 2a	459	0.52	-0.02	1.61	0.55	113	-0.05	0.992
Model 3a	---	---	---	---	---	---	---	---
Model 4a	481	0.38	-0.01	1.8	0.61	99	-0.72	0.997
Model 5a	478	0.45	0.00	1.78	0.60	106	-0.41	1.001
Model 6a	456	0.54	-0.02	1.58	0.54	110	-0.19	0.993
Full Model Calibration at the Second Destination Jurisdiction (Atlanta – USA)								
Model 1b	268	0.47	0.00	1.24	0.52	69	-0.36	0.998
Model 2b	255	0.59	0.00	1.13	0.47	65	-0.61	1.000
Model 3b	236	0.74	0.00	0.94	0.39	47	-1.92	1.000
Model 4b	---	---	---	---	---	---	---	---
Model 5b	---	---	---	---	---	---	---	---
Model 6b	---	---	---	---	---	---	---	---

The results in **TABLE 4.7** indicate that the GOF measures, especially AIC, r, and Z-Score, were improved after redeveloping the SPFs. Since the new models are locally developed by maximizing the likelihood function at the new jurisdictions, they are expected to provide a better fit to the new data. However, comparing to **TABLE 4.5**, the improvement in the GOF measures in **TABLE 4.7** is slight. This means that the prediction performance of the models in **TABLE 4.5** at the new jurisdictions is still good. Therefore, calibrating only the intercept and the shape parameter seems sufficient to transfer the base SPFs to new jurisdictions.

With regard to the models shown in **TABLES 4.6** and **4.7**, it can be noticed that models 2 and 6 have the best performance at the first destination jurisdiction; while models 2 and 3 provide the best data fitting at the second destination jurisdiction.

4.4   Recommended Real-time Safety Evaluation Model

Although all the developed SPFs show a good fit with statistically significant explanatory variables and high transfer indices, it is useful to recommend a specific model for real-time safety evaluation. Based on the transferability analysis results and considering the base jurisdiction as well as the two destination jurisdictions, **model 2** is the most recommended model. **Model 2** includes two explanatory variables to predict rear-end conflicts: the traffic volume (**V**), and the shock wave area (**A**). The model is recommended due to several reasons. First, the inclusion of the shock wave area as an explanatory variable in the SPF is logical. Considering the shock wave area enables the SPF to discriminate between different cycles even if the traffic volume is the same. Basically, at a specific traffic volume, cycles with bigger shock waves most likely are expected to cause more conflicts. In addition, the shock wave area can describe, indirectly, the maximum queue length and the vehicle arrival pattern. Most importantly, the shock wave area is affected by the signal timing. Therefore, the effects of real-time signal changes on traffic conflicts can be captured in the real-time SPF through the shock wave area.

Second, **model 2** shows a good fit at the three studied jurisdictions. The explanatory variables of the model (**V** and **A**) are statistically significant at 95% confidence level. The model has AIC value that is significantly lower than that of the exposure-only model (**model 1**). This means that the model provides a better prediction of the conflict occurrence beyond what can be expected from the traffic volume only.

Third, **model 2** shows high transfer indices, 0.986 and 0.953, at the two new jurisdictions. These indices have further improved to 0.996 and 0.999 after calibrating the intercept and the shape parameter. The high values of the TI confirm the transferability of the model among different contexts. Furthermore, the other GOF measures of **model 2** at the new jurisdictions affirm the model transferability. As shown in **TABLES 4.4-4.7**, the model shows r values range from 0.48 to 0.59, Z scores range from -0.62 to 5.48, C values close to 1, scaled deviance and χ^2 values close to the degree of freedom, and MPB and MAD values close to zero. However, it should be noted that calibrating the intercept and the shape parameter is important to improve the model fit when transferring to new jurisdictions.

Finally, the regression results of **model 2** are consistent at the three jurisdictions (**TABLE 3.3** and **TABLE 4.6a, b**) in terms of the sign and the value of the model parameters. As logically-expected, the signs of the traffic volume (**V**) and the shock wave area (**A**) coefficients are positive when **model 2** is developed at any of the three jurisdictions. The coefficient of the traffic volume (a_1) is 0.706, 0.625, and 0.924 at the base jurisdiction, the first destination jurisdiction, and the second destination jurisdiction, respectively. All the (a_1) values are consentient to be less than 1, meaning that the projection of the model function in the **Y-V** plane concaves down. The coefficient of the shock wave area (a_2) has consistent positive values that range from 0.307 to 0.501.

CHAPTER 5: SELF-LEARNING ADAPTIVE TRAFFIC SIGNAL CONTROL FOR REAL-TIME SAFETY OPTIMIZATION

5.1   Introduction

Real-time optimization of traffic signals has recently received increasing interest among researchers and practitioners, especially with the availability of real-time traffic data from emerging technologies such as connected-vehicles (CVs) (U.S. Department of Transportation 2015) and innovative video detection techniques. Over the past few decades, adaptive traffic signal control (ATSC) systems have shown considerable advances. Several ATSC algorithms have been developed and implemented (e.g., Sims 1979; Hunt et al. 1981; Gartner 1983; Head et al. 1992; Luyanda et al. 2003), while numerous have been proposed (e.g., Abdulhai et al. 2003; Camponogara and Kraus 2003; Salkham et al. 2008; Balaji et al. 2010; Goodall et al. 2013; El-Tantawy et al. 2013; Guler et al. 2014; Yang et al. 2016; Shabestary and Abdulhai 2018; Gong et al. 2019). The common objective of these algorithms is to accommodate real-time traffic conditions and optimize traffic efficiency by maximizing throughput capacity, minimizing traffic delay, and/or reducing queue lengths. Compared to the traditional fixed-time or actuated signals, ATSC algorithms have shown a significant improvement in traffic efficiency at signalized intersections.

However, despite the aforementioned mobility benefits, the safety impact of the existing ATSC algorithms remains unclear. Some studies showed that mobility-oriented ATSC algorithms can improve safety and significantly reduce traffic collisions (Fink et al. 2016; Ma et al. 2016; Khattak et al. 2018) or traffic conflicts (Stevanovic et al. 2011; Fyfe and Sayed 2017). Meanwhile, other studies indicated that implementing ATSC algorithms either leads to insignificant reduction in traffic collisions (Dutta et al. 2010; Lodes and Benekohal 2013) or increases traffic conflicts significantly and worsens traffic safety (Tageldin et al. 2014). This inconsistency in the safety impact of existing ATSC algorithms maybe related to that these algorithms do not consider optimizing traffic safety as a primary objective. More importantly, optimizing mobility does not necessarily mean optimizing safety (Sabra et al. 2010). For example, an ATSC algorithm might tend to minimize the total delay by generating many stops, each with a short duration. Although this might lead to improved mobility, generating many stops can increase the potential risk of collision and deteriorate safety.

A few studies (Sabra et al. 2013; Stevanovic et al. 2013; 2015) have attempted to optimize safety of signalized intersections using traffic simulation and the Surrogate Safety Assessment Model (SSAM) (Gettman et al. 2008). The safety optimization process comprises tuning various signal timing parameters (e.g., cycle length, offset, and phase change interval) to minimize the number of traffic conflicts. Multiple signal designs were tested offline and their corresponding safety levels were evaluated using SSAM. However, the optimization algorithms in these studies are not as practically effective as self-learning ATSC algorithms, in terms of responding instantaneously to real-time traffic changes and covering all possible traffic conditions. Besides, using SSAM to evaluate traffic safety has generally been criticized due to several concerns. First, vehicles in

simulation models follow specific rules that aim to produce a crash-free environment. Using these safe-moving vehicles to evaluate conflicts and near-misses may lead to inaccurate results. Second, the SSAM results can vary significantly depending on the assumed values of the simulation model parameters and the approach used in modelling. Finally, unrealistic crashes and unusual movements are often recorded in traffic simulations, most likely due to an insufficient minimum gap size, a failure to yield to a priority rule, an abrupt lane change of a vehicle, or an irregular queuing up at left/right turn bay tapers (Gettman and Head 2003; Gettman et al. 2003; 2008; Essa and Sayed 2015a).

Despite the importance of the real-time safety optimization, it has generally been disregarded in existing ATSC algorithms, most likely due to the lack of tools to evaluate safety of signalized intersections in real time. Unlike vehicle delay and travel time, the safety level of signalized intersections cannot be directly estimated from real-time traffic data. However, the safety models that are presented in **chapter 3** (**TABLE 3.3**) can be used to evaluate safety in real time. Subsequently, they can enable developing ATSC strategies for real-time safety optimization.

This chapter presents a novel self-learning adaptive traffic signal control algorithm to optimize traffic safety in real time using CVs data. The algorithm is referred to as RS-ATSC (*Real-time Safety-optimized Adaptive Traffic Signal Control"*. The RS-ATSC algorithm has several advantages. First, the safety evaluation is not based on simulated conflicts which were shown not to well represent actual-field conflicts and crashes (Essa and Sayed 2015a; 2015b; Zheng et al. 2019c). Rather, the optimization is based on real-time safety models that were originally developed and validated using real-world traffic data. Second, the algorithm is developed using the Reinforcement Learning (RL) technique as an efficient approach to solve the ATSC problem considering real-time and stochastic traffic changes (Abdulhai and Kattan 2003; Abdulhai et al. 2003; El-Tantawy et al. 2014). Third, the algorithm is practical since it respects all traffic signal operation standards, including the phasing sequence, the minimum/maximum green time, and the intersection clearance time. Fourth, the algorithm is validated using real-world traffic data obtained from two signalized intersections. Fifth, the presented algorithm is found to be effective and feasible under low market penetration rates of CVs. Lastly, to the best of the authors' knowledge, this is the first self-learning ATSC algorithm that optimizes traffic safety in real time (i.e., safety is evaluated and optimized over a very short time period, a few seconds).

5.2   The Proposed RS-ATSC Algorithm

5.2.1   *Reinforcement Learning*

The Reinforcement Learning (RL) technique was applied to develop the proposed RS-ATSC algorithm. RL is an area of machine learning that has widely been applied in the literature for self-learning ATSC algorithms (e.g., Wiering 2000; Abdulhai et al. 2003; Camponogara and Kraus 2003; Richter et al. 2007; Shoufeng et al. 2008; Salkham et al. 2008; Balaji et al. 2010; Arel et al. 2010; El-Tantawy et al. 2014; Gong et al. 2019; Shabestary and Abdulhai 2018). In RL, the agent or the decision-maker (e.g., the signal controller) dynamically interacts with its surrounding environment (e.g., the traffic network). The agent iteratively observes the state of the environment,

takes an action accordingly (e.g., determining which signal phase will be green), and receives a reward or an evaluative feedback (**Figure 5.1**). Unlike the supervised machine learning paradigm, the RL agent is not told which actions to take. Instead, it learns and discovers which actions yield the maximum reward over time. In other words, RL is a goal-directed learning, in which, the agent learns how to map states and actions to achieve a specific goal (i.e., maximizing the total cumulative reward). This state-action mapping is called the control policy. The agent tries to learn the optimal control policy by iteration (i.e., trial-and-error search). It should also be noted that actions may affect not only the immediate reward but also the next state and subsequently the future rewards. Thus, RL has two main distinguishing characteristics: trial-and-error search and delayed reward (Sutton and Barto 1998).
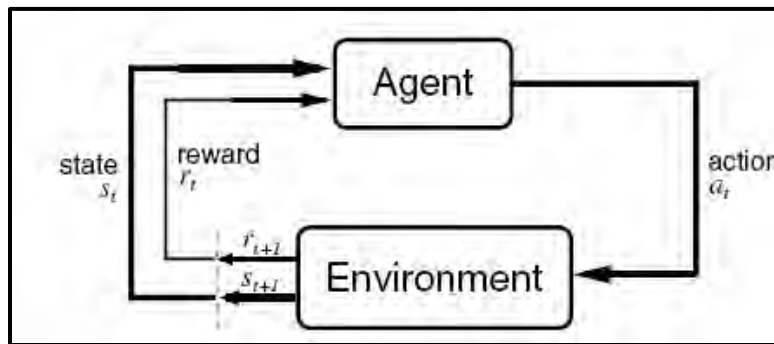

FIGURE 5.1: The Agent–environment Interaction in Reinforcement Learning (Sutton and Barto 1998)

5.2.2   Q-learning

There are numerous methods to solve the RL problem and compute the optimal control policy. Generally, the RL methods can be classified into three main classes: dynamic programming (DP) methods, Monte Carlo (MC) techniques, and temporal difference (TD) learning methods. TD learning methods are recommended as the most relevant to the ATSC problem (El-Tantawy et al. 2014; Abdulhai and Kattan 2003). TD methods have an advantage over DP methods. Unlike DP methods, TD methods do not require a model of the environment dynamics. Instead, the agent learns directly through interaction with the environment. TD methods also have an advantage over MC methods. While MC methods require waiting until the end of an episode to find out the return, TD methods require waiting for only one time-step (Sutton and Barto 1998; Abdulhai and Kattan 2003).

There are several TD methods, such as the SARSA method, the Q-learning method, and the n-step difference learning method. Of the existing TD methods, the Q-learning method (Watkins 1989; Watkins and Dayan 1992) was applied in this research. The Q-learning is an off-policy TD method, in which the algorithm uses the experience of each state transition to update one element of a table called Q-table. Each element in this table represents Q-value of a specific state-action pair $Q(s, a)$ (Sutton and Barto 1998). When the agent performs action a^t at state s^t, leading to a new state s^{t+1} and a reward r^{t+1}, the Q-learning algorithm improves its policy by updating the Q-table according to Bellman's equation as follows:

$$Q^{t+1}(s^t, a^t) = Q^t(s^t, a^t) + \propto^{t+1} \left[r^{t+1} + \gamma \max_{a \in A} Q^t(s^{t+1}, a^{t+1}) - Q^t(s^t, a^t) \right]$$ **Eq. (12)**

Where:

s^t, a^t: the current state and the selected action at the current state;

Q^{t+1}, Q^t: the updated and the old Q-value;

r^{t+1}: the reward of applying action a^t at state s^t;

s^{t+1}, a^{t+1}: the new state and the best action at the new state;

$\propto^{t+1}$: the learning rate;

γ: the discount rate;

A: the action's space.

5.2.3   Modeling the Environment

The traffic microsimulation model VISSIM (v7.00.16) (PTV 2015a) was utilized in this study. VISSIM is a time-step and behavior-based model developed to simulate traffic and depends on a psycho-physical car-following model that is based on Wiedemann's model (Wiedemann 1974; PTV 2015a). The Wiedemann model assumes that the driver can have one of four driving modes: free driving, approaching, following, and braking (PTV 2015a).

An isolated signalized intersection was modeled in VISSIM, representing a connected-vehicle environment for the proposed RS-ATSC algorithm. The modeled intersection has four approaches with two through lanes and a single left-turn lane. The left-turn phasing is operated as protected-permissive at all approaches. The traffic control unit, the agent, receives real-time V2I information from all connected-vehicles that exist within a specific distance from the stop lines. This distance virtually represents the standard V2I DSRC domain. Since the standard V2I DSRC domain roughly ranges from 150 to 300 meters (U.S. Department of Transportation 2015), the distance was assumed to be 225m (i.e., the average). Furthermore, various market penetration rates of CVs were represented in the VISSIM model by creating a new vehicle class called *"connected vehicle"* and varying traffic composition percentages of each traffic input point. In addition to CVs, loop detectors installed at each lane are assumed to provide real-time traffic information to the traffic controller. Two types of loop detectors were considered: traffic counting detectors at through lanes, and left-turn detectors at the beginning and the end of each left-turn bay (**Figure 5.2**).

To simulate the CVs environment and the RS-ATSC algorithm, an external MATLAB code was developed to control the VISSIM model through its COM interface (PTV 2015b). The MATLAB code can run/pause simulation at any time using the *"sim-break-at"* function, record detailed information on traffic signals and vehicles (i.e., vehicle identification number, class, position, and speed), and apply any required real-time changes to traffic signal heads in VISSIM. Thus, this code represents the agent (i.e., the traffic controller) for the Q-learning, since it is able to receive the environment's state and take various actions.
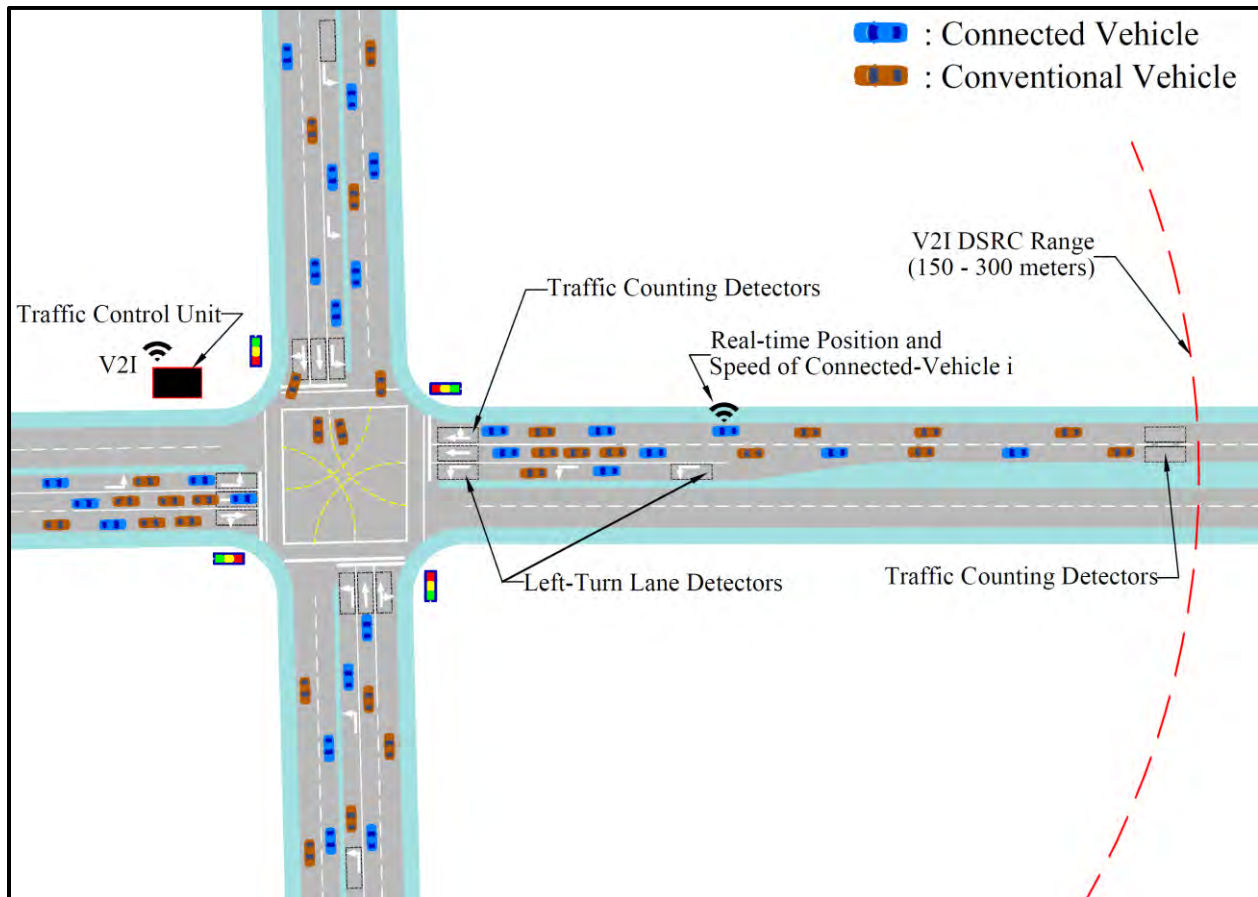
FIGURE 5.2: Modelling an Isolated Signalized Intersection with Connected-vehicles in a Simulation Platform for the Proposed RS-ATSC Algorithm

5.2.4 State Representation

One of the main challenges in the Q-learning method is the use of the tabular form of the Q-matrix to represent realistic environments that have a very large or infinite number of states. Including large number of states in the Q-matrix can result in most states being not experienced by the agent. This issue exists in the ATSC problem, where the continuous and stochastic nature of traffic leads to an infinite number of possible states (i.e., various vehicle positions and speeds). To overcome this issue, there are typically two ways. The first is to enable generalization among states by representing Q-values not as a table but as a trainable parameterized function. Such a generalization is called *"function approximation"* because it takes examples from a desired function and attempts to generalize from them to construct an approximation of the entire function. There are many methods for the function approximation, such as artificial neural networks and statistical curve fitting (Sutton and Barto 1998). However, due to its imperfect value estimations, the function approximation can have many consequences that can affect the quality of the solution, such as the divergence of Q-estimates (Abdulhai and Kattan 2003). Another simpler way, that overcomes the problem of having a very large number of states, is to discretize all possible states

into ranges and define only these ranges in the Q-matrix. Since Q-matrix with discretized ranges of states was successfully applied in previous studies for the ATSC problem (e.g., Wiering 2000; Abdulhai et al. 2003; Camponogara and Kraus 2003; Richter et al. 2007; Shoufeng et al. 2008; Salkham et al. 2008; Balaji et al. 2010; Arel et al. 2010; El-Tantawy et al. 2014), this method was selected for the state representation in our proposed RS-ATSC.

In the proposed RS-ATSC, the state is represented by the current green phase as well as the status of existing vehicles in each approach within the V2I DSRC domain (i.e., 225 meters) upstream the stop line. Specifically, the state vector consists of 5 elements. The first element is the current green phase, while the other four elements represent the current traffic status of each approach. Representing the current traffic status took several forms in the literature. This includes the number of existing vehicles (Camponogara and Kraus 2003; Salkham et al. 2008), the queue length (Abdulhai et al. 2003; El-Tantawy et al. 2014), the number of arriving vehicles to the current green phase and the queue length at the red phase (El-Tantawy et al. 2014), the cumulative delay (El-Tantawy et al. 2014; Shoufeng et al. 2008), the relative delay (Arel et al. 2010), and the detectors status (Richter et al. 2007). In this research, since the overall objective of the RS-ATSC algorithm is to optimize safety, not only traffic counts but also vehicles' positions and speeds need to be considered in the traffic state definition. Therefore, a factor called "*arrival-queue factor*" was developed to represent the real-time traffic status at each approach. The arrival-queue factor of an approach is a weighted sum of the number of vehicles that exist at this approach. This weighted sum considers the position and speed of every vehicle. If the vehicle is stopping or moving at speed less than 5 km/h (i.e., vehicle is in a queue), it is counted as one vehicle. Otherwise, it is counted as a fraction (i.e., between zero and one). The value of this fraction depends on the distance from the vehicle position to the end of the queue or to the stop line, whichever is shorter. The closer this distance, the higher the value of that fraction. For example, if the vehicle exists at the stop line, it will be counted as one (i.e., the highest value). **Figure 5.3** shows the relationship between the arrival-queue factor and the distance from the stop line. The arrival-queue factor for each approach is estimated as follows:

$$f_{arrival-queue(App)} = \sum_{i=1}^{n} f_{arrival-queue(i)} \qquad \text{Eq. (13)}$$

$$f_{arrival-queue(i)} = \begin{cases} 1 & if\ S_i \leq 5\ km/h \\ 1/\exp(a\,.\,D_i) & Else \end{cases} \qquad \text{Eq. (14)}$$

Where:
$f_{arrival-queue(App)}$: the arrival-queue factor for the approach;
$f_{arrival-queue(i)}$: the arrival-queue factor for vehicle i;
n: the number of vehicles exist on the approach;
D_i: the distance from the stop line or the end of the queue to vehicle i;
S_i: the speed of vehicle i;
a: constant (assumed to be 0.005).

The arrival-queue factor values are then discretized into 15 ranges to create a Q-matrix that covers all possible states.
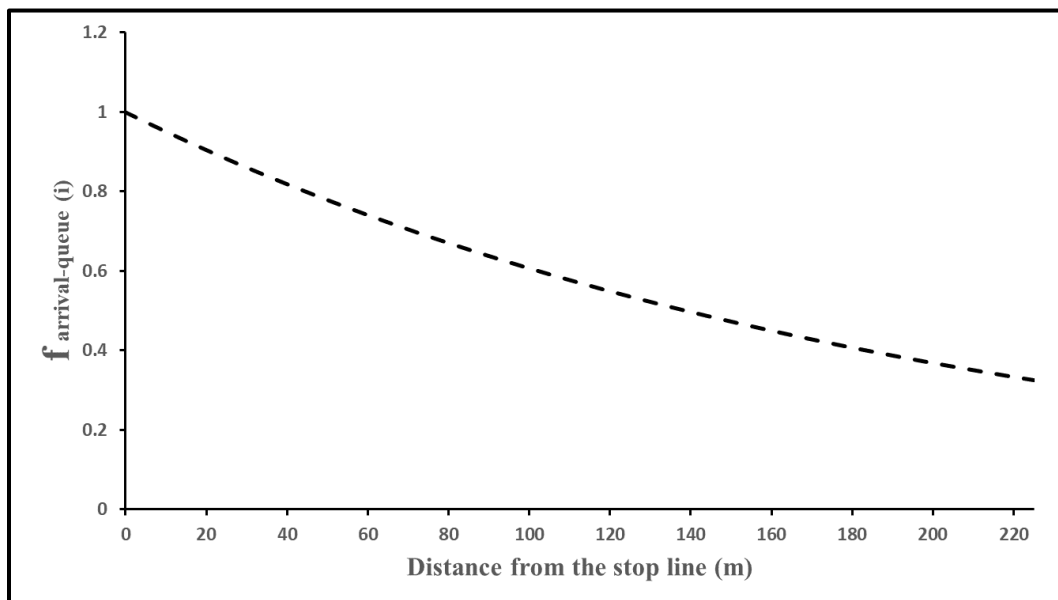

FIGURE 5.3: Queue-arrival Factor at Various Distances from the Stop Line for Vehicle (i) Moving at a Speed Higher than 5 km/h

5.2.5   Action Representation

For signalized intersections that have protected-permissive left turns at all approaches, the green phase can be one of the eight standard National Electric Manufacturers Association (NEMA) phases. In RL-based ATSC algorithms, the action, taken by the agent at each decision point, is to determine the next green phase. The size of the action space (i.e., the number of possible actions) depends on the phasing sequence. If the phasing sequence is variable, the action space typically includes 8 actions: 1) to extend the current green phase, and 2-8) to switch the green light to any of the other 7 NEMA phases. If the phasing sequence is fixed, the action space has only two actions: 1) extending the current green phase, and 2) switching the green light to the following phase. Several previous studies have applied the variable phasing sequence (e.g., Wiering 2000; Richter et al. 2007; Salkham et al. 2008; Arel et al. 2010; El-Tantawy et al. 2014; Gong et al. 2019; Shabestary and Abdulhai 2018), while others have used the fixed phasing sequence (e.g., Abdulhai et al. 2003; Camponogara and Kraus 2003; Shoufeng et al. 2008; Balaji et al. 2010; El-Tantawy et al. 2014).

The variable phasing sequence could theoretically lead to a better performance, since it gives the RL agent more actions to investigate. However, it is generally recommended to prohibit ATSC systems from changing the phase sequence (NCHRP 2015) for several safety and mobility concerns. The variable phasing sequence may confuse road-users, leading to unsafe traffic movements. For example, at 4-leg intersections with protected-permissive left turns, varying the phasing sequence could cause a yellow trap. The yellow trap is defined as a condition that leads

the left-turning user into the intersection believing the opposing user is seeing a yellow (NCHRP 2015). In addition, when the next green phase is not expected, road-users tend not to react quickly to the green indication. This could increase the start-up lost time causing additional delays. The fixed phasing sequence, on the other hand, meets the road-users' expectation, providing a safer traffic environment without unnecessary start-up delays. Furthermore, having only two possible actions in the fixed phasing sequence, instead of eight actions, decreases the Q-matrix size dramatically, which enables faster convergence of the RL algorithm to the optimal policy. Therefore, we adopted the fixed phasing sequence for the proposed RS-ATSC algorithm.

The adopted fixed phasing sequence is the protected-permissive lead-lead left turn phase sequence. This is the most common left-turn phase, which starts opposing left-turn phases prior to the through phases. This sequence has several advantages. First, unlike lag-lag phasing, the lead-lead phasing alleviates the yellow trap. Second, the lead-lead left turn phasing sequence minimizes conflicts between left-turn and through movements on the same approach, especially when the left-turn bay is oversaturated. Third, drivers generally react quickly to the leading green arrow indication. Lastly, the lead-lead sequence gives unused time to the through movements (NCHRP 2015).

Figure 5.4 illustrates the adopted phasing sequence and the possible actions in the proposed RS-ATSC algorithm. The figure shows the standard ring-and-barrier controller (RBC) diagram for protected-permissive lead-lead left-turn phasing. The RBC diagram includes two barriers representing the two intersected roads and two rings representing the compatible phases. As a general rule, any phase in ring 1 can be operated with any phase in ring 2 as long as both phases are between the same barriers. Also, any phase in a ring can be skipped and/or give unused time to a following phase in that ring.
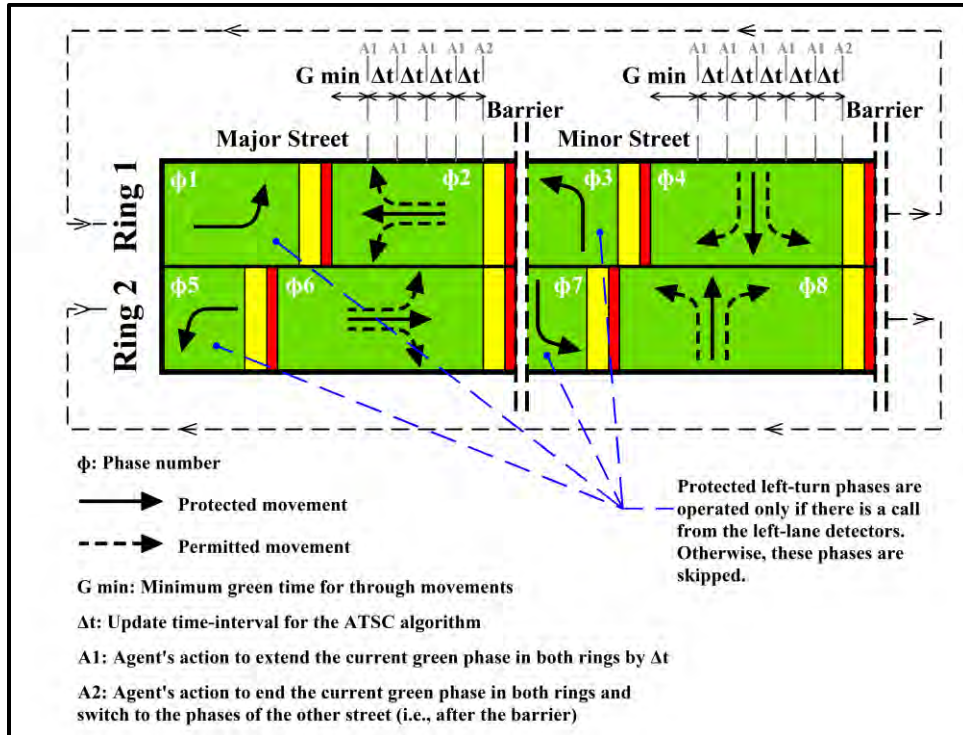
FIGURE 5.4: Phasing Sequence and Possible Actions of the RL Agent in the Proposed RS-ATSC Algorithm for 4-leg Intersections with Protected-permissive Left-turns

As shown in **Figure 5.4**, the RS-ATSC agent performs one of the two following actions: 1) extending the current green phase (A1); and 2) switching the green light to the phases of the other road after the barrier (A2). If action A1 is selected, the current green phase of the through movements (e.g., ϕ2 and ϕ6) will be extended by a specific time interval (assumed to be 5 seconds). On the other hand, if action A2 is selected, the yellow (Y) and the all-red (AR) times will be applied before switching the green light to the through phases of the other road (e.g., ϕ4 and ϕ8) and applying their minimum green time (G_{minTH}). It should also be noted that the protected left-turn phases (ϕ1, ϕ3, ϕ5, and ϕ7) are to be skipped unless vehicles are detected at a left-turn bay either by lane detectors or by V2I communications (**Figure 5.2**). If vehicles are detected at a left-turn bay, the corresponding protected left phase will be called with the minimum green time (G_{minL}) followed by the yellow and the all-red times, prior to the opposing through phase. Thus, the update time interval Δt (i.e., the time between decision points) for the RS-ATSC algorithm can be expressed as follows:

$$\Delta t = \begin{cases} 5 & if\ a^t = A1 \\ k & if\ a^t = A2 \end{cases} \qquad \text{Eq. (15)}$$

$$k = \begin{cases} Y + AR + G_{minTH} & \textit{if protected left turn is not called} \\ Y + AR + G_{minL} + Y + AR + G_{minTH} & \textit{if protected left turn is called} \end{cases} \qquad \textbf{Eq. (16)}$$

Where:

Δt: the update time interval in seconds for the RS-ATSC algorithm;

Y: the yellow time in seconds;

AR: the all-red time in seconds;

G_{minTH}: the minimum green time for through phases in seconds;

G_{minL}: the minimum green time for protected left-turn phases in seconds.

To satisfy driver expectancy, typical values of minimum green, yellow, and all-red times are applied in the RS-ATSC algorithm following the standard signal timing manual (NCHRP 2015). Specifically, the values of Y, AR, and G_{minTH} are assumed to be 4s, 2s, and 10s, respectively. It is worth noting that the aforementioned minimum green value assumes pedestrian detection and indications are existing. If pedestrians are detected (i.e., by pushbutton), the minimum green time must be equal to the minimum pedestrian timing (i.e., walk time and pedestrian clearance). To satisfy the queue clearance at left-turn bays, the minimum green time for protected-left phases is assumed as follows:

$$G_{minL} = 3 + 2n \qquad \textbf{Eq. (17)}$$

Where: n is the number of vehicles detected at the left-turn bay.

The maximum green time is also set as a constraint in the RS-ATSC algorithm. This constraint defines the maximum length of time that a phase can be green in the presence of a conflicting call. If the maximum green is reached, the RS-ATSC agent is prohibited from extending the green time for through phases (i.e., applying action A1). A typical value of 70s is assumed for the maximum green time (NCHRP 2015).

5.2.6   *Reward Representation*

Since the main objective of the proposed RS-ATSC is to optimize traffic safety, a dynamic traffic parameter that is correlated with the safety level of the intersection was needed to represent the RL reward. We selected the shock wave area, illustrated in **Figure 3.1**, to be that reward-representing dynamic traffic parameter. Shock waves commonly occur at signalized intersections due to the repeated stop-and-go situations. Previous research has demonstrated the shock wave's effect on traffic safety by examining its relationship with rear-end crashes (Zheng et al. 2010; Chatterjee and Davis 2016; Zheng et al. 2019a; 2019b) or with rear-end traffic conflicts (Machiani and Abbas 2016). As a general conclusion, safer traffic conditions are associated with smaller shock waves. Thus, the reward for each state-action pair in the RS-ATSC algorithm is defined by the shock wave area (**Figure 3.1**) as a penalty. The shock wave area for each lane at each approach is estimated between every two consecutive actions a^t and a^{t+1}. Then, the reward value r^{t+1} for performing action a^t at state s^t can be defined as follows:

$$r^{t+1} = -\sum_{i=1}^{M}\sum_{j=1}^{N} A_{ij} \qquad \textbf{Eq. (18)}$$

$$A_{ij} = \int_{t}^{t+1} x_{ij} \qquad \textbf{Eq. (19)}$$

Where:
r^{t+1}: the reward value for the state-action pair (a^t, s^t) estimated at state s^{t+1};
N: the number of lanes per approach;
M: the number of approaches at the signalized intersection;
A_{ij}: the shock wave area for lane j at approach i within the interval $[\,t\,,\ t+1]$;
x_{ij}: the backward-moving shock wave polyline for lane j at approach i.

It is worth noting that the shock wave area not only affects the safety level of the signalized intersection, but also is directly affected by real-time signal changes (i.e., actions). Thus, it is an ideal dynamic traffic parameter that can provide the RS-ATSC agent with an evaluative feedback after applying a specific action at a specific state.

5.2.7   *Learning Rate and Discount Rate*

The learning rate $\propto^{t+1}$ in **Eq. (12)** is determined every time-step as the reciprocal of the number of visits by the agent to the state–action pair (s^t, a^t) as follows (Sutton and Barto 1998; El-Tantawy et al. 2014):

$$\propto^{t+1} = \frac{1}{V^{t+1}(s^t, a^t)} \qquad \textbf{Eq. (20)}$$

Where: $V^{t+1}(s^t, a^t)$: the number of visits by the agent to the state–action pair (s^t, a^t).

In addition, the discount rate γ in **Eq. (12)**, which considers the long-run reward, is assumed to be 0.5.

5.2.8 Exploration versus Exploitation

The trade-off between exploration and exploitation is one of the main challenges in RL. While the agent must exploit the most effective experienced actions to obtain a lot of reward, it must also explore new actions in order to make better action selections in the future. To obtain the optimal policy, neither exploitation nor exploration can be followed exclusively. Rather, an action selection strategy should be applied to balance the exploration and exploitation. The typical action selection strategies used in the literature are ∈-greedy and softmax (Sutton and Barto 1998).

In this research, the ∈-greedy method is adopted as the action selection strategy. This means the RS-ATSC agent selects, in each iteration, the greedy action most of the time except for ∈ amount of time, when it selects a random action uniformly. The rate of exploration ∈ is assumed to decrease gradually with the number of iterations (i.e., the age of the agent). The highest exploration occurs at the beginning of the learning, since the agent does not have much experience. At the end of the learning, the lowest exploration occurs, and more exploitation takes place as the agent converges to the optimal policy (Sutton and Barto 1998). The gradual decreasing rate of exploration ∈ can be represented as follows (El-Tantawy et al. 2014):

$$\epsilon = e^{-En} \qquad \qquad \textbf{Eq. (21)}$$

Where: E is a constant and n is the iteration number.

5.2.9 Training the Algorithm

The RS-ATSC algorithm was trained by running the VISSIM simulation model of the isolated intersection depicted in **Figure 3**. The simulation was run for 633 episodes. Each episode included 20,000 simulation seconds divided into 1500s as a warming-up period, 500s as a cooling-down period, and 18000s (i.e., 5 hours) to train the algorithm. During the training period of each episode, the simulation was paused every Δt seconds (as per **Eq. 4**), the state was defined, the next action was selected and applied, the reward was calculated, and lastly, the Q-matrix was updated. To account for the stochastic nature of traffic, two different random seeds were considered in VISSIM. Additionally, to allow the algorithm to visit many states as possible, the traffic volume entering each approach was randomized between 200 vehicle/hour to 1600 vehicle/hour. **Figure 5.5** illustrates the learning progress of the agent represented by the average shock wave area normalized by the traffic volume. As shown in the figure, the RS-ATSC agent converged to the optimal policy after about 550 episodes. The average shock wave area was reduced from approximately 0.11 km. s/vehicle at the beginning of the learning process to 0.02 km. s/vehicle when the convergence was reached.
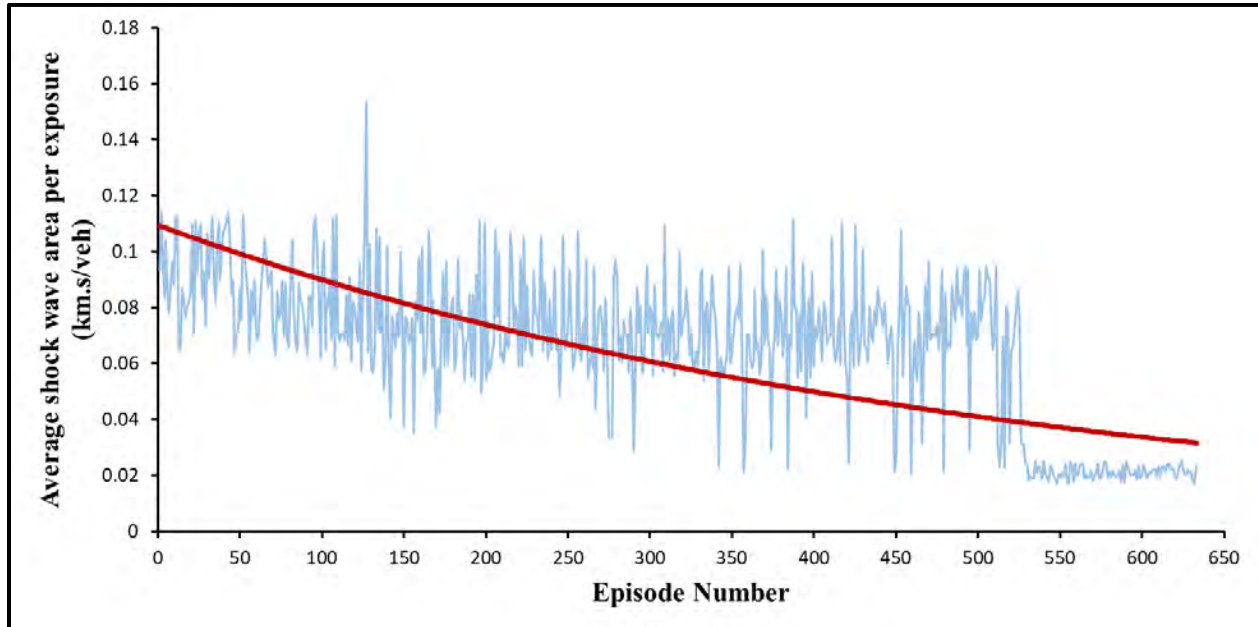
FIGURE 5.5: Learning Progress of the Proposed RS-ATSC Algorithm

5.3   Validation Using Real-world Traffic Data

The proposed RS-ATSC algorithm was validated using real-world traffic data obtained from two signalized intersections in the City of Surrey, British Columbia, Canada. For both intersections, the real-world signal control is a typical NEMA fully-actuated signal control with stop-line and extension detectors. The real-world actuated signal control was set as a benchmark to evaluate the effectiveness of the RS-ATSC. For each intersection, both the trained RS-ATSC and the real-world benchmark actuated signal control (ASC) were implemented in a calibrated VISSIM model. Various measures of performance were then observed and compared. These measures include the average shock wave area, the platoon ratio, and the number of rear-end conflicts.

5.3.1   Real-world Traffic Data

The first selected intersection is 72nd Avenue and 128 Street, while the second selected intersection is 72nd Avenue and 132 Street. Both intersections are urban signalized intersections with 4 protected-permissive left-turns. At each intersection, video data were collected using 8 high-resolution cameras (29.97 frames per second) distributed to cover the four approaches (i.e. two cameras for each approach). The data were collected during a weekday from 9:00 am to 6:00 pm, to cover both peak and off-peak hours. Thus, the total amount of the collected data is 144 video-hours (8 cameras * 9 hours * 2 intersections). **Figure 5.6** shows the location of the selected intersections, the selected approaches, and the recorded video scenes.
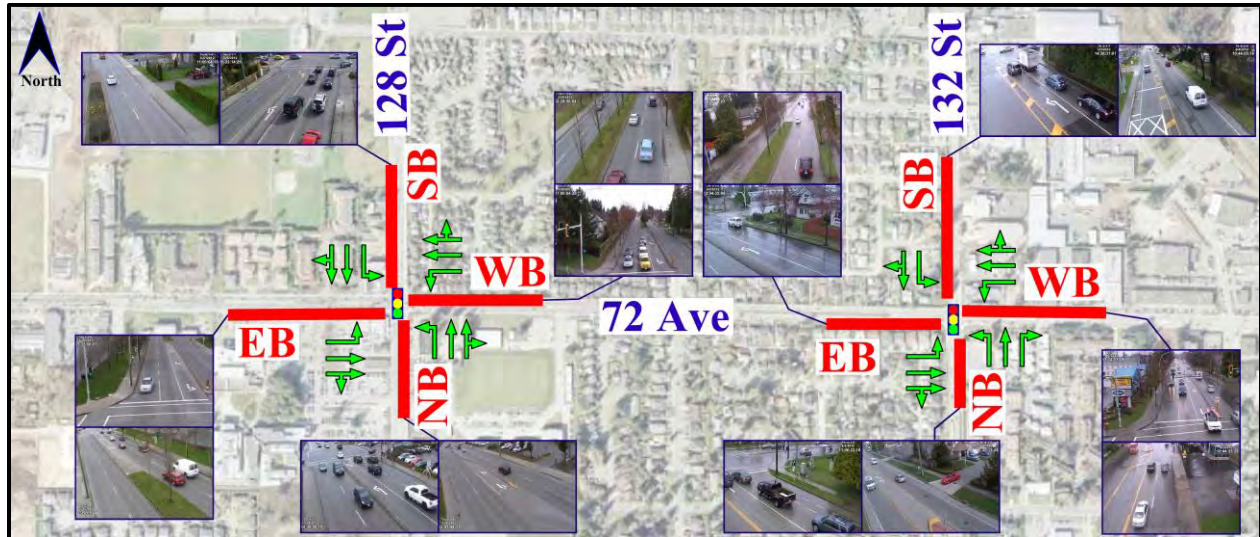
FIGURE 5.6: Study Locations and Video Scenes*
(EB: eastbound, WB: westbound, NB: northbound, SB: southbound)

Detailed real-world traffic data for each approach were extracted from the video recordings. These data include the actual signal program, the traffic volume of all movements, the number of vehicles arriving on green, the average platoon ratio, the average delay time, the traffic composition, and the desired speed distribution.

5.3.2   Calibrated Simulation Models

VISSIM models of the two selected intersections came from previous studies (Essa and Sayed 2015a; 2015b; 2016). The VISSIM models were built accurately to match actual field conditions in terms of intersection geometry, traffic volumes, traffic composition, traffic signal settings. The real-world ASC were defined in VISSIM using the Ring Barrier Controller (RBC) module (PTV 2015a). Visual inspection was also performed to ensure that there are no abnormal movements of the simulated vehicles. In addition, the VISSIM models were precisely calibrated in (Essa and Sayed 2015a; 2015b) using a comprehensive two-step calibration procedure. The first calibration step aimed to match the simulated delay times with the field-observed delay times. This was achieved by matching the arrival pattern and the desired speed to the field conditions. The second calibration step aimed at enhancing the correlation between field-observed and simulated traffic conflicts by calibrating the VISSIM parameters. Firstly, important VISSIM parameters that had the most significant effect on the simulated conflicts were determined through a sensitivity analysis. Subsequently, a Genetic Algorithm was applied to estimate the best values of these parameters with the objective of enhancing correlation between field-observed and simulated conflicts. **TABLE 5.1** shows the selected VISSIM parameters and their calibrated values at each intersection (Essa and Sayed 2015a; 2015b).

TABLE 5.1: Goodness Calibrated VISSIM Parameters (Essa and Sayed 2015a; 2015b)

Parameter	Description	Unit	Default Value	Calibrated Value (128 St &72 Ave)	Calibrated Value (132 St & 72 Ave)
Standstill distance	The desired distance between stopped vehicles	m	1.50	2.50	2.10
Headway time	The time that a driver wants to keep	s	0.90	1.3	1.30
Following thresholds	The thresholds which control the speed differences during the 'Following' state	—	±0.35	±0.25	±1.10
Reduction factor for safety distance closed to stop line	This reduction factor defines the vehicle behavior close to stop line at signalized intersections	—	0.60	0.75	0.60
Start upstream of stop line	Distance upstream of the stop line of signalized intersection	m	100	110	100
Desired deceleration	Desired deceleration is used as the maximum for: the deceleration caused by a desired speed decision; the deceleration in case of Stop & Go traffic, when closing up to a preceding vehicle; the deceleration toward an emergency stop position (route); and for co-operative braking	m/s^2	-2.80	-2.80	-2.80

5.3.3   *Measures of Performance and Safety Evaluation*

To validate the proposed RS-ATSC, its performance where compared to the benchmark ASC. Three measures of performance were considered, including the shock wave area, the platoon ratio, and the number of traffic conflicts. To evaluate these measures, the calibrated VISSIM model for each intersection was run for a 9-hour period (i.e., 9:00 am to 6:00 pm). For each hour, two signal controllers in VISSIM were simulated separately: (1) the RBC module that represents the real-world benchmark ASC, and (2) an external real-time MATLAB code that represents the trained RS-ATSC. For each signal controller, two different random seeds were applied, and the results were then averaged. During each simulation run, detailed simulated traffic data were continuously recorded at a very short time step (e.g., every second of simulation). These data included position and speed of every vehicle, vehicle types, and status of all signal heads. The data recording was obtained using an external program that controls the simulation model via the VISSIM COM interface (PTV 2015b).

After running the simulation and recording detailed traffic data, several steps were applied to estimate the measures of performance (e.g., the shock wave area and the platoon ratio) and evaluate safety. First, signal cycles for each approach of the intersection were determined using the recorded status of the approach signal head. Second, recorded vehicle trajectories were filtered by time and

space to specify vehicle trajectories for each lane per each signal cycle. Third, for each lane, the space-time diagram for each signal cycle (**Figure 3.1**) was obtained using both the filtered trajectories and the cycle timing. This space-time diagram was then used to calculate various traffic parameters at the signal-cycle level, including traffic volume, shock wave area, shock wave speed, and platoon ratio. Lastly, the estimated cycle-related parameters were inputted into the real-time safety models, presented in **TABLE 3.3**, to predict the number of rear-end conflicts at the cycle level. Specifically, **model 2** in **TABLE 3.3** was used, as recommended in a recent study (Essa et al. 2019). The model predicts the number of conflicts per a signal cycle using the traffic volume and the shock wave area of this cycle.

5.3.4   Validation Results

The aforementioned measures of performance were extracted from simulation for the selected intersections for the 9-hour analysis period (9:00 am to 6:00 pm). The performance of the trained RS-ATSC was compared with that of the real-world benchmark ASC. Overall, the RS-ATSC led to positive safety impacts in terms of alleviating shock waves and reducing rear-end conflicts. **Figures 5.7** shows the average shock wave area and the conflict rate for each hour at the two selected intersections with both ASC and RS-ATSC. As shown in the figure, when the RS-ATSC was implemented instead of the ASC, the average shock wave area was reduced from 0.05 to 0.01 km. s at the first intersection, and from 0.09 to 0.03 km. s at the second intersection. The average conflict rate was also decreased from 0.11 to 0.08 conflict/vehicle/hour at the first intersection and from 0.16 to 0.10 conflict/vehicle/hour at the second intersection.
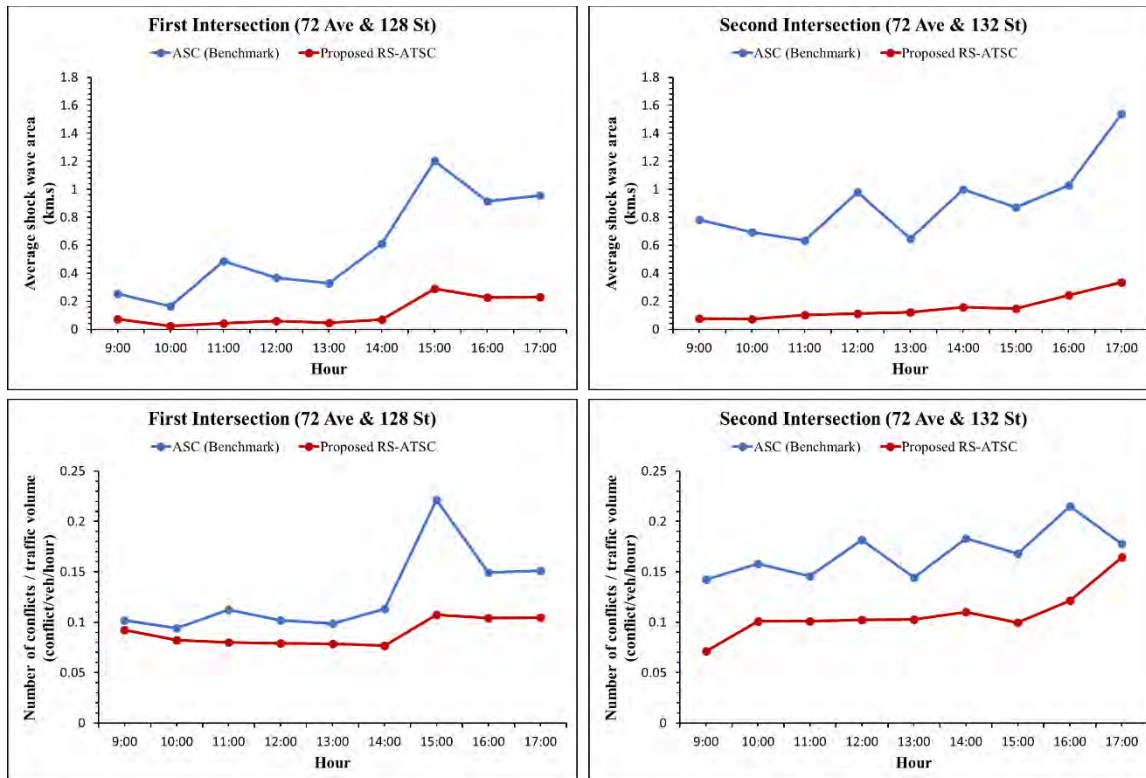
FIGURE 5.7: Average shock wave area and the number of conflicts at the selected intersections before and after implementing the proposed RS-ATSC

The real-time variation of the shock wave area was investigated at each approach of both intersections. **Figures 5.8 and 5.9** illustrate the shock wave area, measured cycle by cycle, for the first and the second intersection, respectively. The shock wave area of each approach varies with time due to the traffic volume fluctuation. Compared to the ASC, the RS-ATSC resulted in smaller shock wave areas at all approaches. However, the reduction in the shock wave area is not the same for all approaches. Some approaches showed a considerable reduction in the shock wave area, such as the eastbound approach at the first intersection (**Figures 5.8**) and the southbound approach at the second intersection (**Figures 5.9**). Whereas, other approaches showed a slight reduction in the shock wave area, such as the northbound approach at the first intersection (**Figures 5.8**) and the eastbound approach at the second intersection (**Figures 5.9**). This is reasonable since the objective of the RS-ATSC is to minimize the total shock wave area for the whole intersection. Therefore, approaches with higher shock wave areas are expected to have higher reduction.
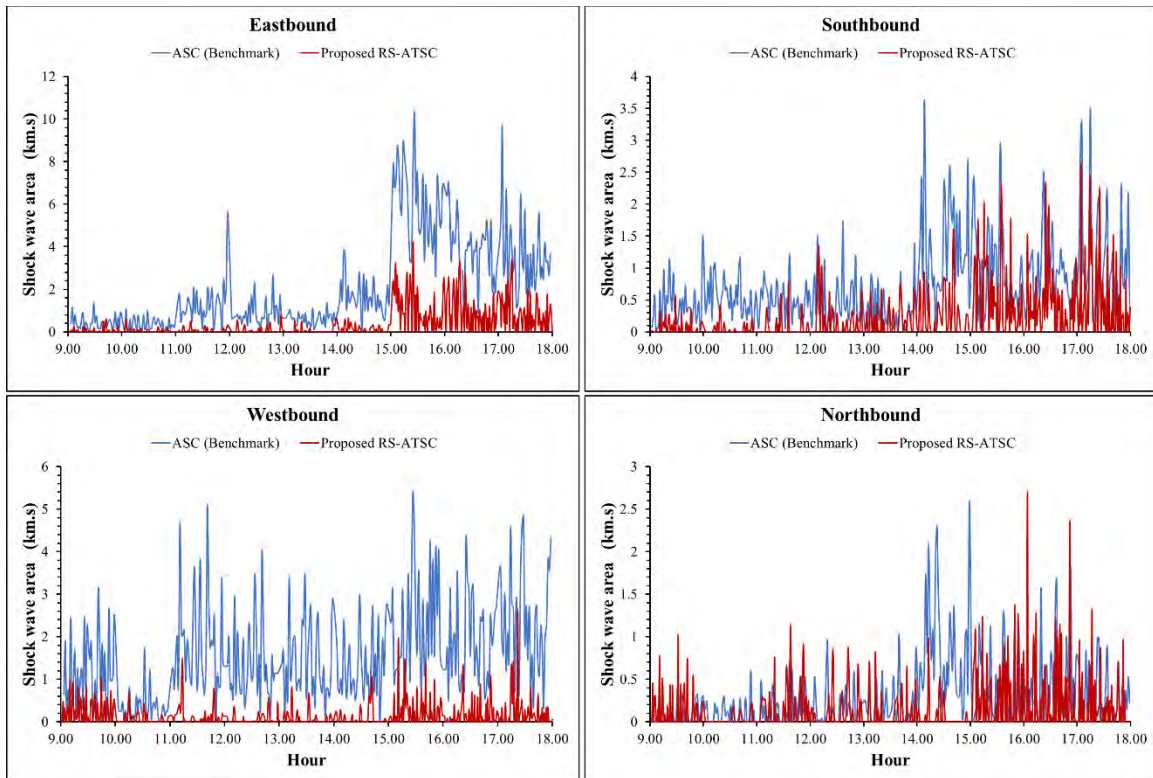
FIGURE 5.8: Real-time variation of the shock wave area at each approach of the first intersection (72 Ave and 128 St) before and after implementing the proposed RS-ATSC
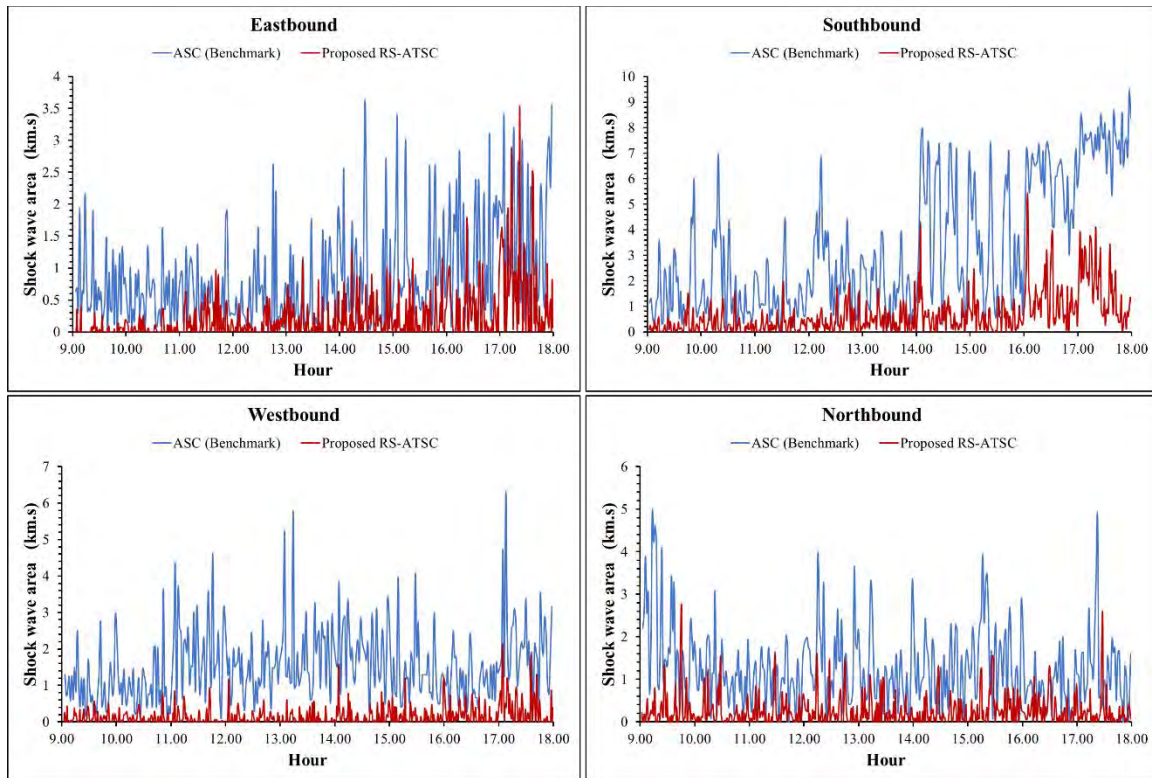
FIGURE 5.9: Real-time variation of the shock wave area at each approach of the second intersection (72 Ave and 132 St) before and after implementing the proposed RS-ATSC

In addition to the shock wave area, the real-time variation of the platoon ratio was investigated at each approach of both intersections. The platoon ratio is an important dynamic traffic parameter for signalized intersections. It depends on the proportion of all vehicles arriving during green and the ratio of effective green time to the cycle length (AASHTO 2000). The more vehicle arrivals during green, the higher the platoon ratio. The platoon ratio also represents the safety of the intersection. Previous studies have showed that the platoon ratio is inversely correlated with the number of rear-end conflicts (Zheng et al. 2019a; 2019b). **Figures 5.10 and 5.11** illustrate the platoon ratio, estimated cycle by cycle, for the first and the second intersection, respectively. As shown in the figures, implementing the proposed RS-ATSC resulted in higher platoon ratios at all approaches. This means more vehicles arrived during green time, leading to a smaller number of stops and less traffic conflicts.
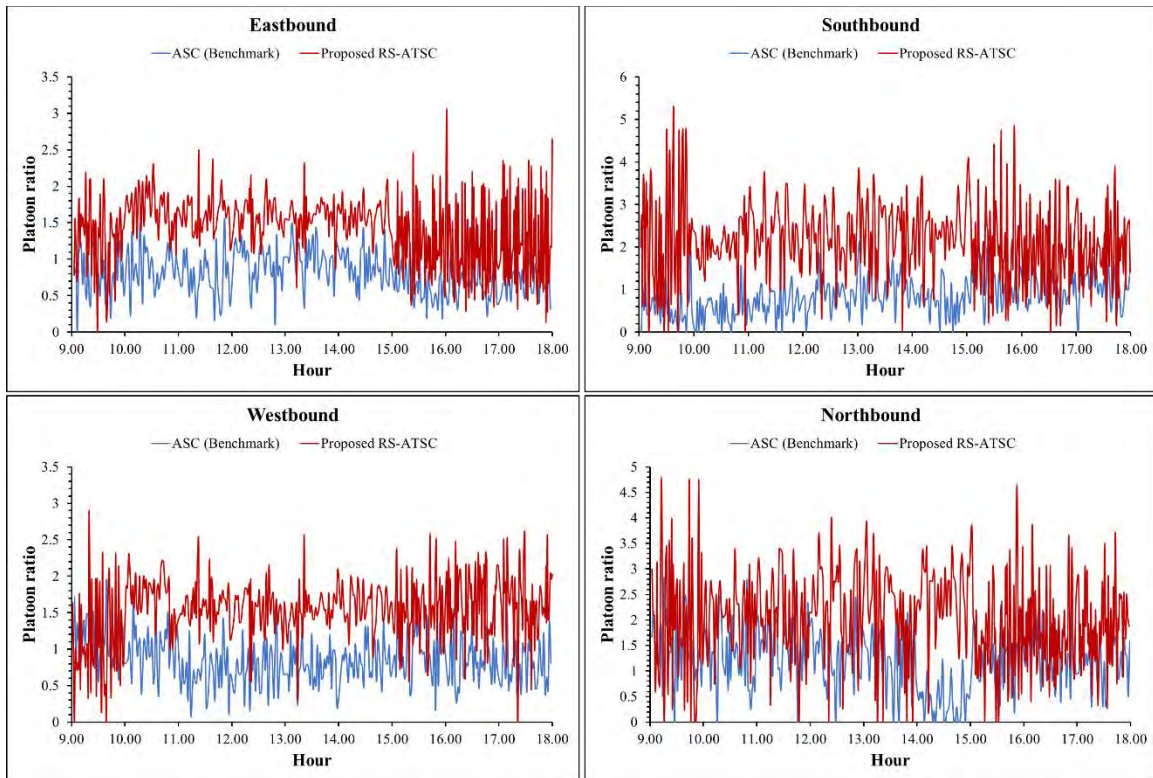
FIGURE 5.10: Real-time variation of the platoon ratio at each approach of the first intersection (72 Ave and 128 St) before and after implementing the proposed RS-ATSC
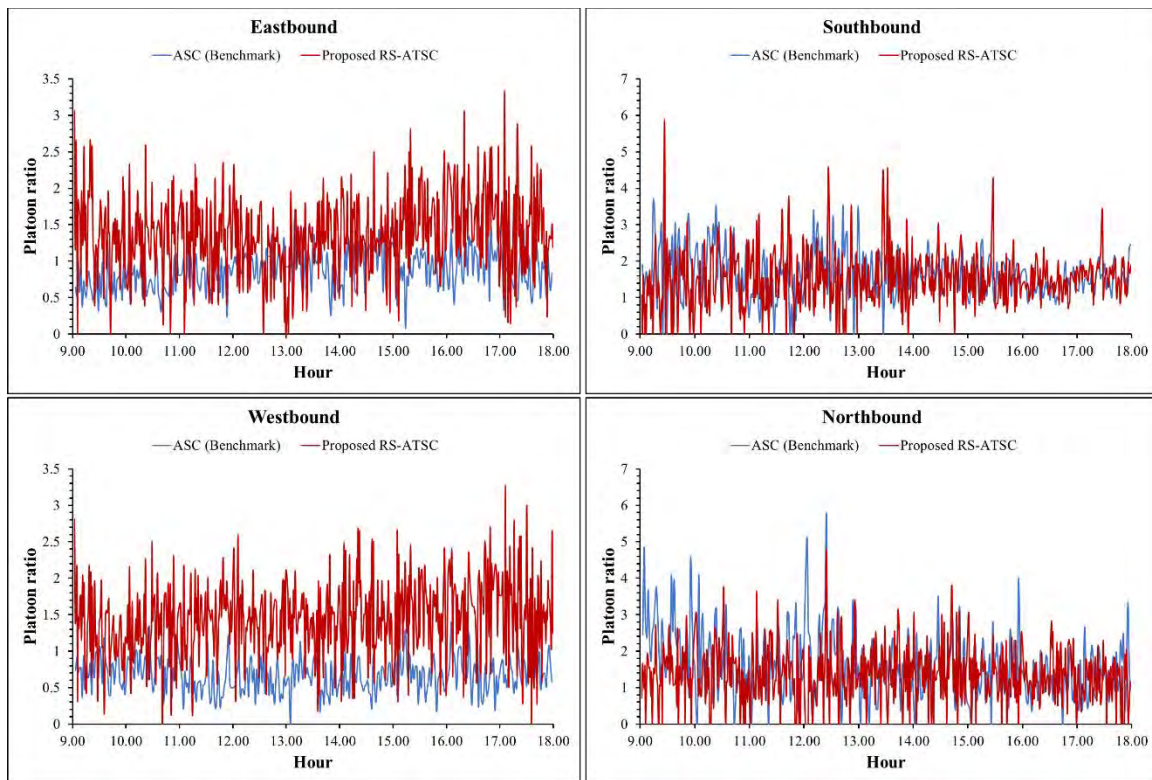
FIGURE 5.11: Real-time variation of the platoon ratio at each approach of the second intersection (72 Ave and 132 St) before and after implementing the proposed RS-ATSC

In addition, the real-time variation of traffic conflicts was investigated at each approach of both intersections. The number of rear-end conflicts were estimated for each lane per each signal cycle from **model 2** in **TABLE 3.3**. The conflict rate (conflict/second) was then estimated by dividing the number of conflicts at each cycle by the cycle length. **Figures 5.12 and 5.13** show the real-time variation of the conflict rate for each approach at the first and the second intersection, respectively. Moreover, the cumulative numbers of rear-end conflicts throughout the 9-hour analysis period for both intersections are shown in **Figures 5.14 and 5.15**. Compared to the benchmark ASC, the proposed RS-ATSC reduced the number of rear-end conflicts significantly at both intersections. Like the shock wave area, the reduction in the rear-end conflicts was not the same for all approaches. Some approaches experienced a significant reduction in the number of conflicts, such as the eastbound approach at the first intersection (**Figures 5.12 and 5.14**) and the southbound approach at the second intersection (**Figures 5.13 and 5.15**). At the same time, some approaches showed a little reduction in the number of conflicts, such as the northbound approach at the first intersection (**Figures 5.12 and 5.14**) and the eastbound approach at the second intersection (**Figures 5.13 and 5.15**). More importantly, the results do not indicate any increase in the cumulative number of conflicts at any approach. This means that the RS-ATSC not only improved the overall safety level of each intersection, but also it did not deteriorate the safety level of any individual approach.
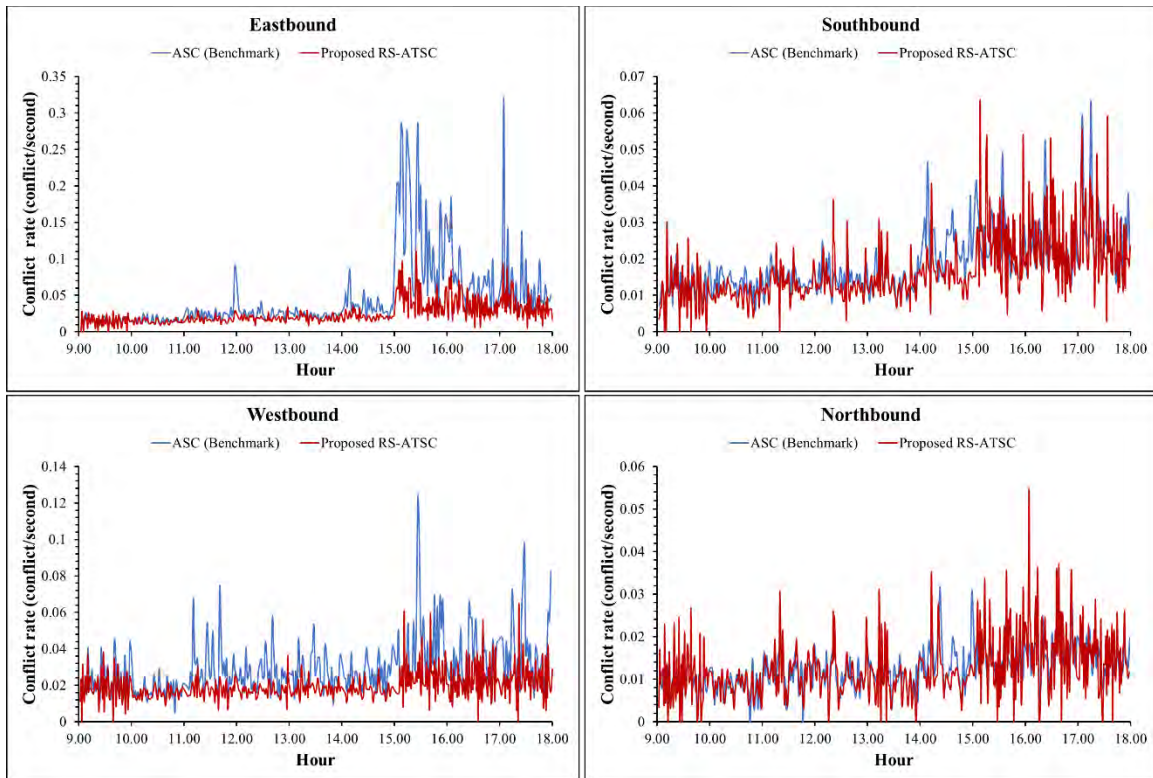
FIGURE 5.12: Real-time variation of the conflict rate at each approach of the first intersection (72 Ave and 128 St) before and after implementing the proposed RS-ATSC
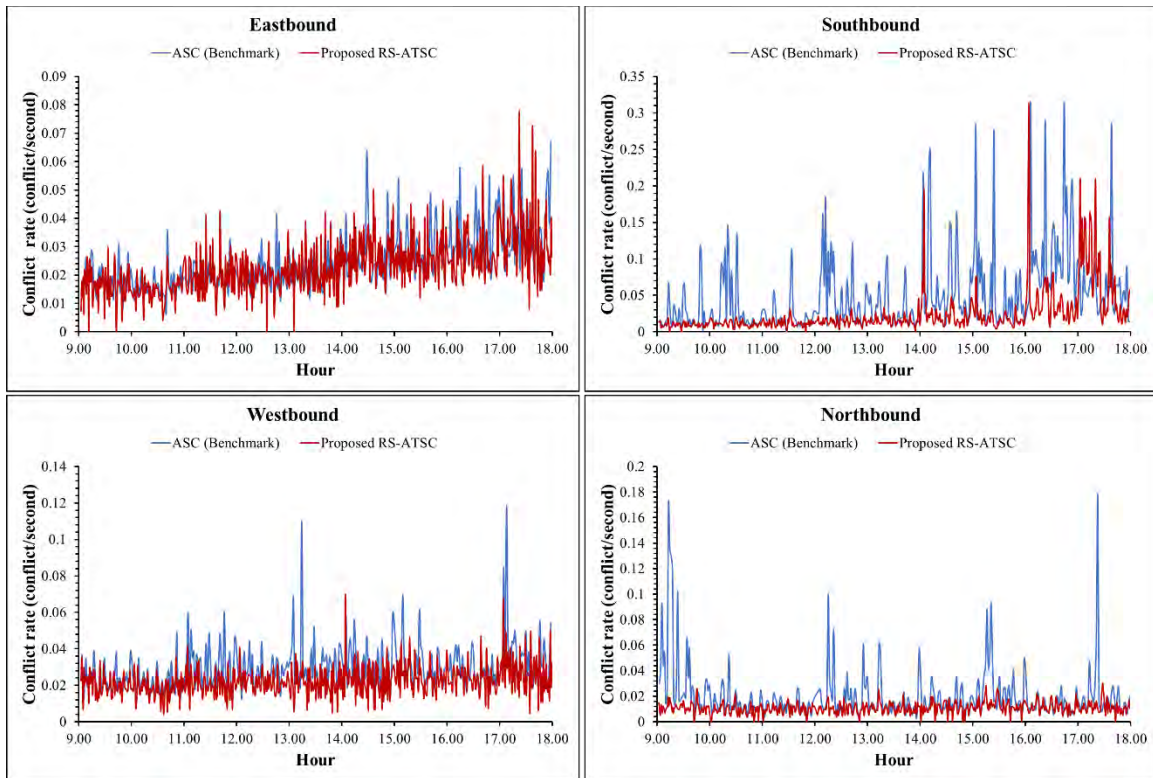
FIGURE 5.13: Real-time variation of the conflict rate at each approach of the second intersection (72 Ave and 132 St) before and after implementing the proposed RS-ATSC
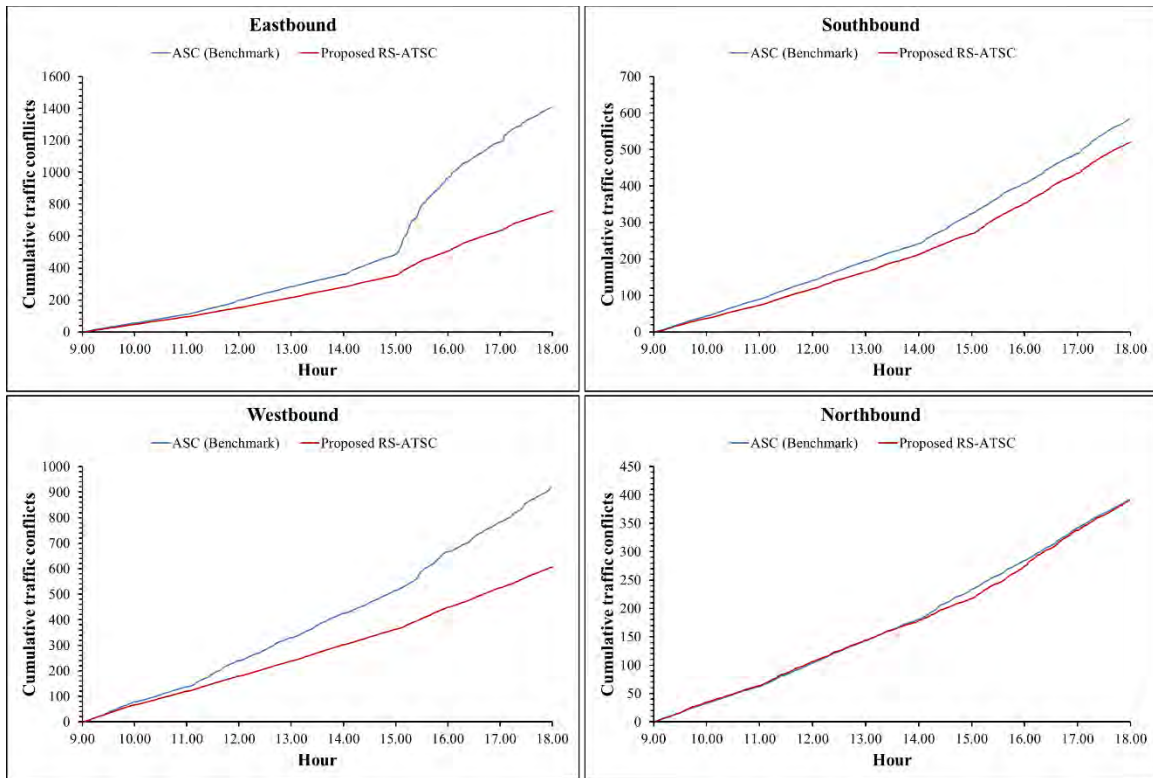
FIGURE 5.14: Cumulative traffic conflicts each approach of the first intersection (72 Ave and 128 St) before and after implementing the proposed RS-ATSC
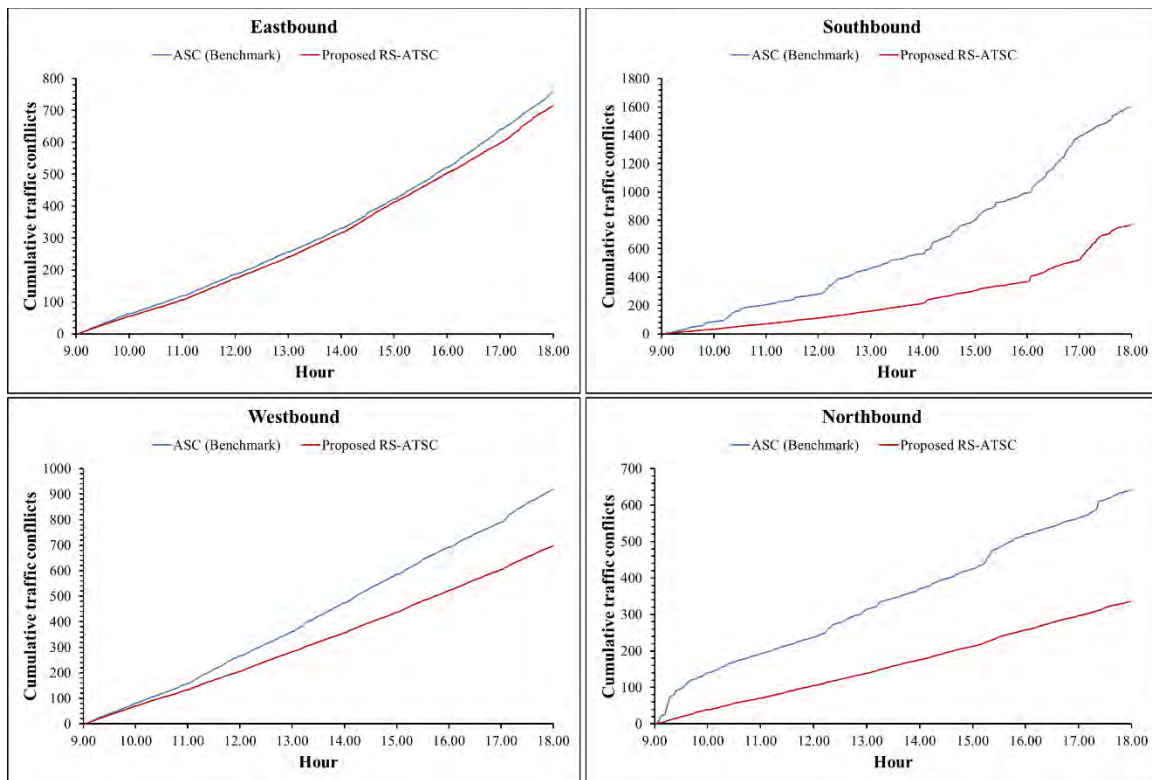
FIGURE 5.15: Cumulative traffic conflicts each approach of the second intersection (72 Ave and 132 St) before and after implementing the proposed RS-ATSC

The overall comparative performance of the proposed RS-ATSC as opposed to the benchmark ASC is reported in **TABLE 5.2**. For the 9-hour analysis period, the RS-ATSC led to a significant improvement in the safety level of both analyzed intersections. The total shock wave area was reduced by 71% at each intersection. The overall platoon ratio was increased by 86% and 17% at the first intersection and the second intersection, respectively. Most importantly, the overall rate of rear-end conflicts (i.e., the total number of conflicts normalized by the exposure) was reduced by 31% and 36% at the first intersection and the second intersection, respectively. At the first intersection, the most reduction in the conflict rate is 46% at the eastbound approach, while the least reduction is 1 % at the northbound approach. At the second intersection, the southbound approach had the highest reduction in the conflict rate (52%), while the eastbound approach had the lowest reduction (6%).

It is noteworthy that the performance results provided in **TABLE 5.2** were derived based on the geometric and traffic characteristics of the selected intersections. These results can vary if the algorithm is implemented to other intersections with different characteristics. It should also be noted that the V2I DSRC domain was assumed to be 225 meters. Using a higher value of this domain can potentially improve the algorithm's performance.

TABLE 5.2: Goodness Safety Optimization Results of the Proposed RS- ATSC Algorithm Compared to the ASC

First intersection (128 St & 72 Ave) Analysis period of 9 hours in total (9:00 am to 6:00 pm)		EB	SB	WB	NB	Overall
Approach*		EB	SB	WB	NB	Overall
Traffic Volume		9435	6720	8025	5430	29610
Benchmark ASC	Total shock wave area (km.s)	674.3	246.4	501.0	98.9	1520.7
	Average shock wave area per exposure (km.s/veh)	0.07	0.04	0.06	0.02	0.05
	Average platoon ratio	0.81	0.85	0.86	1.21	0.93
	Rear-end conflicts per exposure (conflict/veh)	0.15	0.09	0.11	0.07	0.11
Proposed RS-ATSC	Total shock wave area (km.s)	170.0	117.2	71.8	79.1	438.2
	Average shock wave area per exposure (km.s/veh)	0.02	0.02	0.01	0.01	0.01
	Average platoon ratio	1.41	2.06	1.52	1.95	1.74
	Rear-end conflicts per exposure (conflict/veh)	0.08	0.08	0.08	0.07	0.08
Percentage of reduction/increase**	Total shock wave area (km.s)	-75%	-52%	-86%	-20%	-71%
	Average shock wave area per exposure (km.s/veh)	-75%	-52%	-86%	-20%	-71%
	Average platoon ratio	75%	143%	77%	60%	86%
	Rear-end conflicts per exposure (conflict/veh)	-46%	-11%	-34%	-1%	-31%
Second intersection (132 St & 72 Ave) Analysis period of 9 hours in total (9:00 am to 6:00 pm)		EB	SB	WB	NB	Overall
Approach*		EB	SB	WB	NB	Overall
Traffic Volume		8666	4584	8395	3552	25197
Benchmark ASC	Total shock wave area (km.s)	283.1	1114.7	506.4	423.5	2327.6
	Average shock wave area per exposure (km.s/veh)	0.03	0.24	0.06	0.12	0.09
	Average platoon ratio	0.87	1.64	0.67	1.62	1.20
	Rear-end conflicts per exposure (conflict/veh)	0.09	0.35	0.11	0.18	0.16
Proposed RS-ATSC	Total shock wave area (km.s)	122.7	340.1	81.3	126.8	670.9
	Average shock wave area per exposure (km.s/veh)	0.01	0.07	0.01	0.04	0.03
	Average platoon ratio	1.37	1.50	1.43	1.33	1.41
	Rear-end conflicts per exposure (conflict/veh)	0.08	0.17	0.08	0.09	0.10
Percentage of reduction/increase**	Total shock wave area (km.s)	-57%	-69%	-84%	-70%	-71%
	Average shock wave area per exposure (km.s/veh)	-57%	-69%	-84%	-70%	-71%
	Average platoon ratio	57%	-9%	113%	-18%	17%
	Rear-end conflicts per exposure (conflict/veh)	-6%	-52%	-24%	-48%	-36%

*EB: eastbound, WB: westbound, NB: northbound, SB: southbound
** Positive values indicate increase and negative values indicate reduction

Overall, the reductions in the shock wave area and the conflict rate confirm the positive safety impact of the proposed RS-ATSC algorithm. In addition, the proposed algorithm has positive mobility impacts. This is reasonable because reducing shock waves most likely decreases vehicle delays and improves mobility. The average delay time was estimated for both intersections with and without the RS-ATSC. Compared to the benchmark ASC, the RS-ATSC reduced the average delay time by 44% and 61% for the first intersection and the second intersection, respectively. However, this cannot be considered the optimum mobility performance, since the RS-ATSC is a safety-oriented algorithm whose optimal policy is based on minimizing shock waves to optimize safety. Other ATSC algorithms that consider minimizing delay times as a primary objective can lead to a better mobility performance. Moreover, considering both mobility and safety in a multi-objective real-time ATSC algorithm is an interesting area for future research. Based on this study, safety and mobility of signalized intersections seem to be non-conflicting objectives, although their optimum designs may not be the same.

Given the validation results that demonstrate the positive safety and mobility impacts of the RS-ATSC, the proposed algorithm can be implemented in real-world to optimize the safety of signalized intersections using CVs real-time data. Moreover, when implemented to a specific intersection, the RS-ATSC algorithm can be designed to continue learning itself using real-world traffic and geometric data of this intersection. Considering these site-specific data can potentially lead to better safety and mobility performances.

5.3.5 *Effect of CVs Market Penetration Rate*

The CVs technology is supposed to be deployed gradually. A mix of CVs and conventional vehicles is expected to exist in road networks during the transition period that predates the full deployment of CVs technology. Subsequently, it is not feasible to validate any ATSC algorithm assuming that all vehicles are CVs. Rather, various market penetration rates (MPRs) of CVs should be considered. Therefore, in this study, we investigated the performance of the proposed RS-ATSC at the two selected intersections under various MPRs of CVs, ranging from 10% to 100%. The results were compared to the benchmark ASC. When implementing the RS-ATSC algorithm with a specific MPR value, the estimated queue-arrival factor for each approach was estimated from CVs only as per **Eq. (13)** and **Eq. (14)**, and then it was multiplied by a magnification factor that equals the reciprocal of the MPR value. The exact MPR value can be estimated in real time, given the number of CVs from the V2I communications and the total traffic counts from the counting detectors upstream each approach of the intersection.

Figure 5.16 shows the average conflict rate of the analyzed intersections when the RS-ATSC is applied under various MPRs. The benchmark ASC is also illustrated for comparison. As shown in the figure, the maximum safety benefit of the RS-ATSC is corresponding to the MPR of 100% (i.e., all vehicles are connected). At this MPR, the conflict rate was reduced from 0.112 to 0.076 at the first intersection and from 0.152 to 0.098 at the second intersection. However, it should be noted that 98% of these benefits can be achieved when the MPR value is 50%. Moreover, the MPR of 20% seems sufficient to achieve more than 60% of the maximum safety benefit.
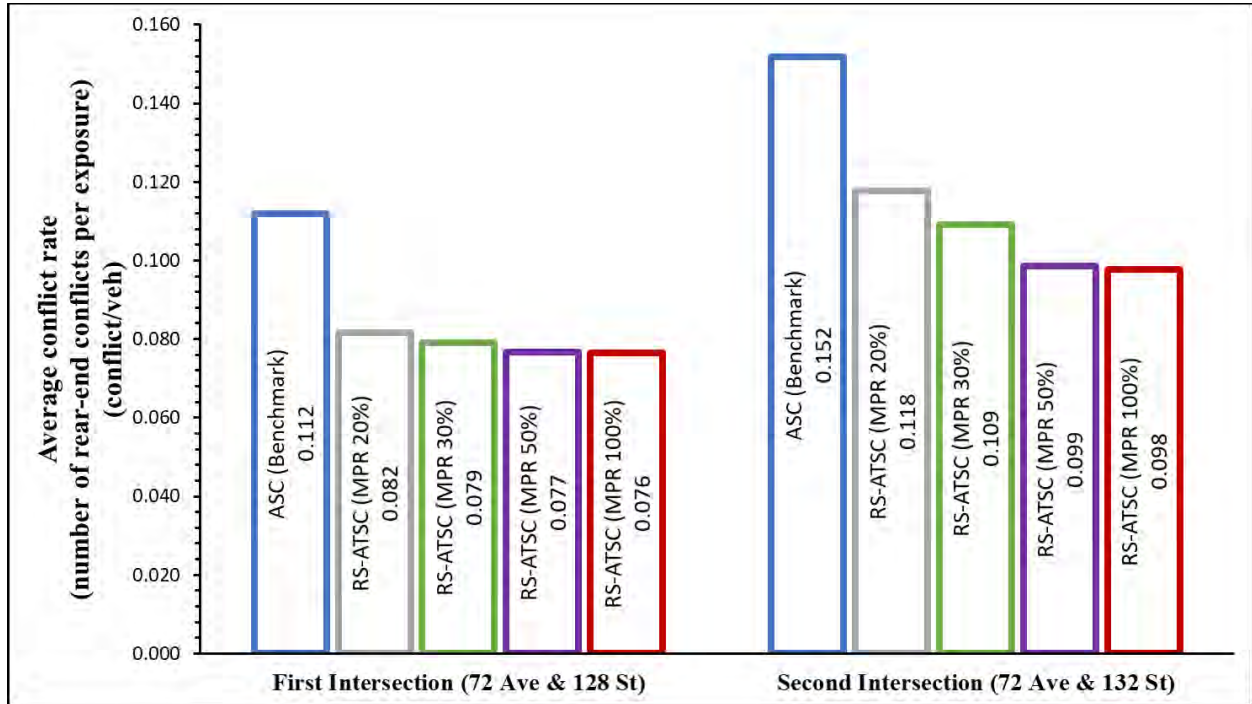
FIGURE 5.16: The effect of the CVs MPR value on the average conflict rate at the selected intersections when implementing the proposed RS-ATSC

Overall, the proposed RS-ATSC algorithm can be very effective when the MPR of CVs is equal to or higher than 20%. The higher the MPR value, the more the safety effectiveness of the algorithm. MPR values less than 20% may not lead to significant safety benefits, since the algorithm cannot define the environment state with a reasonable accuracy due to the lack of real-time information on vehicle positions and speeds.

CHAPTER 6: SUMMARY AND CONCLUSIONS

6.1   Summary and Conclusions

In the era of connected vehicles (CVs), a considerable amount of high-resolution data on vehicle positions and trajectories will be generated in real time. These data can be used for real-time safety and mobility optimization of traffic signals. Using CVs data for mobility optimization at signalized intersections has been investigated in several studies. Various procedures have been proposed in the literature to adapt traffic signal controllers in real time to minimize delays using vehicle-to-infrastructure (V2I) and vehicle-to-vehicle (V2V) communications. However, real-time safety optimization of traffic signals has not been considered in existing research.

This study has several contributions toward optimizing safety and mobility of signalized intersections in real time using CVs data. First, new models for real-time safety evaluation of signalized intersections were developed using real-world traffic data from several intersections in British Columbia and Alberta. Second, for wider application of the developed models, their transferability to other jurisdictions was investigated. Third, a novel self-learning adaptive traffic signal control (ATSC) algorithm was proposed to optimize the safety of signalized intersections in real time. These three contributions are presented in chapters 3, 4, and 5 of this report. The following paragraphs provide a summary of these chapters.

Chapter 3 describes the development of real-time safety models for signalized intersections. Traffic video-data were recorded for six signalized intersections located in two cities in Canada. Rear-end conflicts and various traffic variables at each signal cycle were extracted from the recorded videos. The traffic variables include: traffic volume, maximum queue length, shock wave characteristics (e.g. shock wave speed and shock wave area), and the platoon ratio. The models were developed using the generalized linear models (GLM) approach. The results show that all models have good fit and almost all the explanatory variables are statistically significant leading to better prediction of conflict occurrence beyond what can be expected from the traffic volume only. Furthermore, space-time conflict heat maps were developed to investigate the distribution of the traffic conflicts. The heat maps illustrate graphically the association between rear-end conflicts and various traffic parameters. The developed models can give insight about how changes in the signal cycle design affect the safety of signalized intersections. The overall goal is to use the developed models for the real-time optimization of signalized intersection safety by changing the signal design.

Chapter 4 presents the transferability of the developed real-time safety models to new jurisdictions. Two corridors of signalized intersections in California and Atlanta were used in the analysis as destination jurisdictions. Detailed vehicle trajectories for these corridors were obtained from the Next Generation Simulation (NGSIM) data. Various transferability analysis approaches were applied. The transferability of the real-time safety models was evaluated with and without a local calibration for the model parameters at the new jurisdictions. Several goodness-of-fit measures were examined to assess the ability of the developed models to predict traffic conflicts.

University of British Columbia
Department of Civil Engineering

Overall, the results showed that the real-time safety models are transferable, which confirms the validity of using them for real-time safety evaluation of signalized intersections.

Chapter 5 explains the proposed ATSC algorithm. The algorithm was developed using the Reinforcement Learning (RL) approach and was trained using the simulation platform VISSIM. The trained algorithm was then validated using real-world traffic data obtained from two signalized intersections in the City of Surrey, British Columbia. Compared to the traditional actuated signal control system, the proposed algorithm reduces shock waves, traffic conflicts, and vehicle delays by approximately 71%, 31%, and 44%, respectively. Moreover, the proposed ATSC algorithm was tested under various market penetration rates (MPRs) of CVs. The results showed that 98% and 60% of the algorithm's safety benefits can be achieved at MPR values of 50% and 20%, respectively. To the best of the authors' knowledge, this is the first self-learning ATSC algorithm that optimizes traffic safety in real time.

6.2   Future Research

For further improvement of the proposed ATSC's performance and feasibility, several areas of future research are suggested. First, the state space can be expanded by applying extra discretization (i.e., the number of ranges of the queue-arrival factor) or by considering a continuous state space by converting the Q-matrix to a neural network (i.e., deep reinforcement learning). Second, it is suggested to investigate the results' sensitivity to various parameters, such as the discount factor, the update time-interval, and the V2I DSRC domain. Third, incorporating other conflict types, such as crossing and merging conflicts, is recommended. Moreover, safety measures other than traffic conflicts, such as the risk of collision or the predicted number of crashes (Zheng et al. 2019a; 2019b), can be used to represent real-time traffic safety and define the reward function in the RS-ATSC. Lastly, it is worthwhile to develop a multi-objective RL ATSC algorithm that includes both safety and mobility as two primary objectives in the real-time signal optimization.

BIBLIOGRAPHY

AASHTO, 2000. *Highway Capacity Manual.* Washington, D.C.: Transportation Research Board.

AASHTO, 2010. *Highway Safety Manual.* Washington, D.C.: Transportation Research Board.

Abdel-Aty, M., Dilmore, J. & Dhindsa, A., 2006. Evaluation of variable speed limits for real-time freeway safety improvement. *Accident analysis & prevention,* 38(2), pp. 335-345.

Abdulhai, B. & Kattan, L., 2003. Reinforcement learning: Introduction to theory and potential for transport applications. *Canadian Journal of Civil Engineering,* 30(6), pp. 981-991.

Abdulhai, B., Pringle, R. & Karakoulas, G., 2003. Reinforcement learning for true adaptive traffic signal control. *Journal of Transportation Engineering,* 129(3), pp. 278-285.

Ahmed, M. & Abdel-Aty, M., 2013. A data fusion framework for real-time risk assessment on freeways. *Transportation Research Part C: Emerging Technologies,* Volume 26, pp. 203-213.

Akaike, H., 1974. A new look at the statistical model identification. *Selected Papers of Hirotugu Akaike. Springer, New York, NY.,* pp. 215-222.

Al Islam, S. & Hajbabaie, A., 2017. Distributed coordinated signal timing optimization in connected transportation networks. *Transportation Research Part C: Emerging Technologies,* Volume 80, pp. 272-285.

Amundsen, F. & Hydén, C., 1977. *Proceedings of First Workshop on traffic Conflicts,* Oslo: Institute of Economics.

Anon., 2017. *Planning for Connected and Automated Vehicles,* Michigan: Public Sector Consultants and Center for Automative Research.

Arel, I., Liu, C., Urbanik, T. & Kohls, A., 2010. Reinforcement learning-based multi-agent system for network traffic signal control. *IET Intelligent Transport Systems,* 4(2), pp. 128-135.

Balaji, P., German, X. & Srinivasan, D., 2010. Urban traffic signal control using reinforcement learning agents. *IET Intelligent Transport Systems,* 4(3), pp. 177-188.

Barth, M. A. F. Y. T. et al., 2000. *Comprehensive Modal Emission Model (CMEM), version 2.0 user's guide..* Riverside: University of California.

Brimley, B., Saito, M. & Schultz, G., 2012. Calibration of Highway Safety Manual safety performance function: development of new models for rural two-lane two-way highways. *Transportation Research Record: Journal of the Transportation Research Board,* Volume 2279, pp. 82-89.

Brys, T., Pham, T. & Taylor, M., 2014. Distributed learning and multi-objectivity in traffic light control. *Connection Science,* 26(1), pp. 65-83.

Cafiso, S., Di Silvestro, G. & Di Guardo, G., 2012. Application of Highway Safety Manual to Italian divided multilane highways. *Procedia-Social and Behavioral Sciences,* Volume 53, pp. 910-919.

Camponogara, E. & Kraus, W., 2003. Distributed learning agents in urban traffic control. *In Portuguese Conference on Artificial Intelligence,* pp. 324-335.

Chatterjee, I. & Davis, G., 2016. Analysis of rear-end events on congested freeways by using video-recorded shock waves. *Transportation Research Record: Journal of the Transportation Research Board,* Volume 2583, pp. 110-118.

Chen, Y., Persaud, B. & Sacchi, E., 2012. Improving transferability of safety performance functions by Bayesian model averaging. *Transportation Research Record,* 2280(1), pp. 162-172.

Chin, H. & Quek, S., 1997. Measurement of traffic conflicts. *Safety Science ,* Volume 26, p. 169–185.

Chong, J., 2016. *Automated and Connected Vehicles: Status of the Technology and Key Policy Issues for Canadian Governments,* s.l.: Library of Parliament.

Cunto, Flávio & Frank F. Saccomanno, 2008. Calibration and validation of simulated vehicle safety performance at signalized intersections. *Accident Analysis & Prevention,* 40(3), pp. 1171-1179.

Cunto, F., Sobreira, L. & Ferreira, S., 2014. Assessing the transferability of the Highway Safety Manual predictive method for urban roads in Fortaleza City, Brazil. *Journal of transportation engineering,* 141(1), p. 04014072.

D'agostino, C., 2014. Investigating transferability and goodness of fit of two different approaches of segmentation and model form for estimating safety performance of Motorways. *. Procedia Engineering,* Volume 84, pp. 613-623.

Dijkstra, Atze, Paula Marchesini & Frits Bijleveld, 2010. Do calculated conflicts in microsimulation model predict number of crashes?. *Transportation Research Record,* 1(2147), pp. 105-112.

Dutta, U., Lynch, J., Dara, B. & Bodke, S., 2010. *Safety Evaluation of the SCATS Control System (No. RC-1545K).,* Detroit: Michigan Ohio University Transportation Center.

El-Basyouny, K. & Sayed, T., 2009a. Accident prediction models with random corridor parameters. *Accident Analysis & Prevention,* 41(5), pp. 1118-1123.

El-Basyouny, K. & Sayed, T., 2009b. Urban arterial accident prediction models with spatial effects. *Transportation Research Record: Journal of the Transportation Research Board,* Volume 2102, pp. 27-33.

El-Basyouny, K. & Sayed, T., 2009c. Collision prediction models using multivariate Poisson-lognormal regression. *Accident Analysis & Prevention,* 41(4), pp. 820-828.

El-Basyouny, K. & Sayed, T., 2013. Safety performance functions using traffic conflicts. *Safety Science,* 51(1), pp. 160-164.

El-Basyouny, K. & Sayed, T., 2013. Safety Performance Functions using Traffic Conflicts. *Safety Science,* 51(1), p. 160–164.

Elmitiny, N. et al., 2010. Classification analysis of driver's stop/go decision and red-light running violation. *Accident Analysis & Prevention,* 42(1), pp. 101-111.

El-Tantawy, S., Abdulhai, B. & Abdelgawad, H., 2013. Multiagent reinforcement learning for integrated network of adaptive traffic signal controllers (MARLIN-ATSC): methodology and large-scale application on downtown Toronto. *IEEE Transactions on Intelligent Transportation Systems,* 14(3), pp. 1140-1150.

El-Tantawy, S., Abdulhai, B. & Abdelgawad, H., 2014. Design of reinforcement learning parameters for seamless application of adaptive traffic signal control. *Journal of Intelligent Transportation Systems,* 18(3), pp. 227-245.

Elvik, R., Erke, A. & Christensen, P., 2009. Elementary units of exposure. *Transportation Research Record: Journal of the Transportation Research Board,* Issue 2103, pp. 25-31.

Essa, M. & Sayed, T., 2015a. Simulated Traffic Conflicts: Do They Accurately Represent Field-Measured Conflicts?. *Transportation Research Record: Journal of the Transportation Research Board,* Volume 2514, pp. 48-57.

Essa, M. & Sayed, T., 2015b. Transferability of calibrated microsimulation model parameters for safety assessment using simulated conflicts. *Accident Analysis & Prevention,* Volume 84, pp. 41-53.

Essa, M. & Sayed, T., 2016. A comparison between PARAMICS and VISSIM in estimating automated field-measured traffic conflicts at signalized intersections. *Journal of Advanced Transportation,* 50(5), pp. 897-917.

Farid, A., Abdel-Aty, M. & Lee, J., 2018. Transferring and calibrating safety performance functions among multiple states. *Accident Analysis & Prevention,* Volume 117, pp. 276-287.

Farid, A. et al., 2016. Exploring the transferability of safety performance functions. *Accident Analysis & Prevention,* Volume 94, pp. 143-152.

Farid, A., Abdel-Aty, M., Lee, J. & Eluru, N., 2017. Application of Bayesian informative priors to enhance the transferability of safety performance functions. *Journal of safety research,* Volume 62, pp. 155-161.

Feng, Y., Head, K., Khoshmagham, S. & Zamanipour, M., 2015. A real-time adaptive signal control in a connected vehicle environment. *Transportation Research Part C: Emerging Technologies,* Volume 55, pp. 460-473.

Fink, J., Kwigizile, V. & Oh, J., 2016. Quantifying the impact of adaptive traffic control systems on crash frequency and severity: Evidence from Oakland County, Michigan. *Journal of safety research,* Volume 57, pp. 1-7.

Fyfe, M. & Sayed, T., 2017. Safety Evaluation of Connected Vehicles for a Cumulative Travel Time Adaptive Signal Control Microsimulation Using the Surrogate Safety Assessment Model. *Transportation Research Board 96th Annual Meeting,* Issue 17-01651.

Gartner, N. H., 1983. OPAC: A demand-responsive strategy for traffic signal control. *Transportation Research Record: Journal of the Transportation Research Board,* Issue 906, pp. 75-81.

Gettman, Douglas & Head, L., 2003. Surrogate safety measures from traffic simulation models. *Transportation Research Record,* Issue 1840, pp. 104-115.

Gettman, et al., 2008. *Surrogate safety assessment model and validation: Final Report,* s.l.: FHWA-HRT-08-051.

Gong, Y., Abdel-Aty, M., Cai, Q. & Rahman, M., 2019. Decentralized network level adaptive signal control by multi-agent deep reinforcement learning. *Transportation Research Interdisciplinary Perspectives,* Volume 1, p. 100020.

Goodall, N., Smith, B. & Park, B., 2013. Traffic signal control with connected vehicles. *Transportation Research Record: Journal of the Transportation Research Board,* Issue 2381, pp. 65-72.

Guler, S., Menendez, M. & Meier, L., 2014. Using connected vehicle technology to improve the efficiency of intersections. *Transportation Research Part C: Emerging Technologies,* Volume 46, pp. 121-131.

Guo, F., Wang, X. & Abdel-Aty, M., 2010. Modeling signalized intersection safety with corridor-level spatial correlations. *Accident Analysis & Prevention,* 42(1), pp. 84-92.

Hadayeghi, A., Shalaby, A., Persaud, B. & Cheung, C., 2006. Temporal transferability and updating of zonal level accident prediction models. *Accident Analysis & Prevention,* 38(3), pp. 579-589.

Harding, J. et al., 2014. *Vehicle-to-vehicle communications: Readiness of V2V technology for application (Report No. DOT HS 812 014),* Washington, DC:: United States Department of Transportation [U.S DOT], National Highway Traffic Safety Administration [NHTSA].

Hayward, J., 1968. Near-miss determination through use of a scale of danger. *Highway Research Record,* Volume 384, pp. 24-34.

Hayward, J. C., 1972. Near-miss determination through use of a scale of danger. *Highway Research Record,* Issue 384.

Head, K. L., Mirchandani, P. B. & Sheppard, D., 1992. Hierarchical framework for real-time traffic control. *Transportation Research Record. Journal of the Transportation Research Board,* Issue 1360, pp. 82-88.

Hossain, M. & Muromachi, Y., 2012. A Bayesian network based framework for real-time crash prediction on the basic freeway segments of urban expressways. *Accident Analysis & Prevention,* pp. 373-381.

Huang, et al., 2013. Identifying if VISSIM simulation model and SSAM provide reasonable estimates for field measured traffic conflicts at signalized intersections. *Accident Analysis & Prevention,* Issue 50, pp. 1014-1024.

Hunt, P., Robertson, D., Bretherton, R. & Winton, R., 1981. *SCOOT-a traffic responsive method of coordinating signals (No. LR 1014 Monograph),* Crowthorne, England: Transport and Road Research.

ICBC, 2018. *newsroom.* [Online]
Available at: http://www.icbc.com/about-icbc/newsroom/Pages/2018-Jan28.aspx
[Accessed November 2018].

Ismail, K., Sayed, T. & Saunier, N., 2010. Automated Analysis of Pedestrian-vehicle Conflicts: A Context For Before-and-after Studies. *Transportation Research Record: Journal of the Transportation Research Board,* Issue 2198, pp. 52-64.

Ismail, K., Sayed, T. & Saunier, N., 2011. Methodologies for aggregating indicators of traffic conflict. *Transportation Research Record: Journal of the Transportation Research Board,* Volume 2237, pp. 10-19.

ITS Canada, 2017. *ITS Canada.* [Online]
Available at: https://www.itscanada.ca/about/index/index.html
[Accessed 10 May 2017].

Jahangiri, A., Rakha, H. & Dingus, T., 2016. Red-light running violation prediction using observational and simulator data. *Accident Analysis & Prevention,* Issue 96, pp. 316-328.

Jiang, H. et al., 2017. Eco approaching at an isolated signalized intersection under partially connected and automated vehicles environment. *Transportation Research Part C: Emerging Technologies,* Volume 79, pp. 290-307.

Kamal, M. et al., 2015. A vehicle-intersection coordination scheme for smooth flows of traffic without using traffic lights. *IEEE Transactions on Intelligent Transportation Systems,* 16(3), pp. 1136-1147.

Khattak, Z., Magalotti, M. & Fontaine, M., 2018. Estimating safety effects of adaptive signal control technology using the Empirical Bayes method. *Journal of safety research,* Volume 64, pp. 121-128.

Khazraeian, S., Hadi, M. & Xiao, Y., 2017. Safety Impacts of Queue Warning in a Connected Vehicle Environment. *Transportation Research Record: Journal of the Transportation Research Board,* Issue 2621, pp. 31-37.

Koppelman, F. & Wilmot, C., 1982. Transferability analysis of disaggregate choice models. *Transportation Research Record,* Volume 895, pp. 18-24.

Lee, C., Hellinga, B. & Saccomanno, F., 2003. Real-time crash prediction model for application to crash prevention in freeway traffic. *Transportation Research Record: Journal of the Transportation Research Board,* Volume 1840, pp. 67-77.

Lee, J., Abdel-Aty, M. & Cai, Q., 2017. Intersection crash prediction modeling with macro-level data from various geographic units.. *Accident Analysis & Prevention,* Issue 102, pp. 213-226.

Lee, J. & Park, B., 2012. Development and evaluation of a cooperative vehicle intersection control algorithm under the connected vehicles environment. *IEEE Transactions on Intelligent Transportation Systems,* 13(1), pp. 81-90.

Lee, J., Park, B., Malakorn, K. & So, J., 2013. Sustainability assessments of cooperative vehicle intersection control at an urban corridor. *Transportation Research Part C: Emerging Technologies,* Volume 32, pp. 193-206.

Lee, J., Park, B. & Yun, I., 2013. Cumulative travel-time responsive real-time intersection control algorithm in the connected vehicle environment. *Journal of Transportation Engineering,* 139(10), pp. 1020-1029.

Li, W. et al., 2017. Development and Evaluation of High-Speed Differential Warning Application Using Vehicle-to-Vehicle Communication. *Transportation Research Record: Journal of the Transportation Research Board,* Issue 2621, pp. 81-91.

Li, Z., Elefteriadou, L. & Ranka, S., 2014. Signal control optimization for automated vehicles at isolated signalized intersections. *Transportation Research Part C: Emerging Technologies,* Volume 49, pp. 1-18.

Lodes, M. & Benekohal, R., 2013. *Safety benefits of implementing adaptive signal control technology: Survey results (FHWA-ICT-12-020),* Urbana, Illinois: Illinois Center for Transportation.

Luyanda, F. et al., 2003. ACS-Lite algorithmic architecture: applying adaptive control system technology to closed-loop traffic signal control systems. *Transportation Research Record,* 1856(1), pp. 175-184.

Lyon, C., Haq, A., Persaud, B. & Kodama, S., 2005. Safety performance functions for signalized intersections in large urban areas: Development and application to evaluation of left-turn priority treatment. Transportation Research Record: Journal of the. *Transportation Research Record: Journal of the Transportation Research Board,* Volume 1908, pp. 165-171.

Machiani, S. & Abbas, M., 2016. Safety surrogate histograms (SSH): A novel real-time safety assessment of dilemma zone related conflicts at signalized intersections. *Accident Analysis & Prevention,* Volume 96, pp. 361-370.

Ma, J. et al., 2016. Estimation of crash modification factors for an adaptive traffic-signal control system. *Journal of Transportation Engineering,* 142(12), p. 04016061.

Mehta, G. & Lou, Y., 2013. Calibration and development of safety performance functions for Alabama: Two-lane, two-way rural roads and four-lane divided highways. *Transportation Research Record: Journal of the Transportation Research Board,* Volume 2398, pp. 75-82.

Miaou, S. & Lord, D., 2003. Modeling traffic crash-flow relationships for intersections: dispersion parameter, functional form, and Bayes versus empirical Bayes methods. *Transportation Research Record: Journal of the Transportation Research Board,* Volume 1840, pp. 31-40.

MOVES, 2018. *Motor Vehicle Emission Simu-lator (MOVES).* [Online]
Available at: https://www.epa.gov/moves
[Accessed May 2018].

NCHRP, 2015. *Signal Timing Manual - Second Edition,* Washington DC: The National Academies Press.

Oh, J., Oh, C., Ritchie, S. & Chang, M., 2005. Real-time estimation of accident likelihood for safety enhancement. *Journal of transportation engineering,* 131(5), pp. 358-363.

Olia, A., Abdelgawad, H., Abdulhai, B. & Razavi, S., 2016. Assessing the potential impacts of connected vehicles: mobility, environmental, and safety perspectives. *Journal of Intelligent Transportation Systems,* 20(3), pp. 229-243.

Paikari, E., Tahmasseby, S. & Far, B., 2014. A simulation-based benefit analysis of deploying connected vehicles using dedicated short range communication. *Intelligent Vehicles Symposium Proceedings, IEEE,* pp. 980-985.

Pande, A. & Abdel-Aty, M., 2006. Comprehensive analysis of the relationship between real-time traffic surveillance data and rear-end crashes on freeways. *Transportation Research Record: Journal of the Transportation Research Board,* Volume 1953, pp. 31-40.

Papaioannou, P., 2007. Driver behaviour, dilemma zone and safety effects at urban signalised intersections in Greece. *Accident Analysis & Prevention,* 39(1), pp. 147-158.

Pearson, K., 1900. X. On the criterion that a given system of deviations from the probable in the case of a correlated system of variables is such that it can be reasonably supposed to have arisen from random sampling. *The London, Edinburgh, and Dublin Philosophical Magazine and Journal of Science,* 302(50), pp. 157-175.

Persaud, B., Lan, B., Lyon, C. & Bh, R., 2010. Comparison of empirical Bayes and full Bayes approaches for before–after road safety evaluations. *Accident Analysis & Prevention,* 42(1), pp. 38-43.

Persaud, B., Lord, D. & Palmisano, J., 2002. Calibration and transferability of accident prediction models for urban intersections. *Transportation Research Record: Journal of the Transportation Research Board,* Volume 1784, pp. 57-64.

Persaud, B. et al., 2012. *Adoption of Highway Safety Manual Predictive Methodologies for Canadian Highways.* s.l., s.n.

Poch, M. & Mannering, F., 1996. Negative binomial analysis of intersection-accident frequencies. *Journal of transportation engineering,* 122(2), pp. 105-113.

PTV, 2015a. *PTV VISSIM 7 User Manual,* Karlsruhe, Germany: PTV AG.

PTV, 2015b. *PTV VISSIM 7 INTRODUCTION TO THE COM API,* Karlsruhe, Germany: PTV Planung Transport Verkehr AG.

Ren, Y. et al., 2016. Influential factors of red-light running at signalized intersection and prediction using a rare events logistic regression model. *Accident Analysis & Prevention,* Issue 95, pp. 266-273.

Richter, S., Aberdeen, D. & Yu, J., 2007. Natural actor-critic for road traffic optimisation. *Advances in neural information processing systems,* pp. 1169-1176.

Sabra, Z. et al., 2010. *Balancing safety and capacity in an adaptive signal control system—Phase 1 (No. FHWA-HRT-10-038),* Mclean, United States: Federal Highway Administration..

Sabra, Z., Gettman, D., Henry, R. & Nallamothu, V., 2013. *Enhancing safety and capacity in an adaptive signal control system—Phase 2. Rep. No. FHWA-PROJ-10-0037,* Washington, DC.: Federal Highway Administration.

Sacchi, E., Persaud, B. & Bassani, M., 2012. Assessing international transferability of highway safety manual crash prediction algorithm and its components. *Transportation Research Record: Journal of the Transportation Research Board,* Volume 2279, pp. 90-98.

Sacchi, E. & Sayed, T., 2016a. Conflict-Based Safety Performance Functions for Predicting Traffic Collisions by Type. *Transportation Research Record. Journal of the Transportation Research Board,* Volume 2583, pp. 50-55.

Sacchi, E. & Sayed, T., 2016b. Bayesian estimation of conflict-based safety performance functions. *Journal of Transportation Safety & Security,* 8(3), pp. 266-279.

Sacchi, E., Sayed, T. & DeLeur, P., 2013. A Comparison of Collision-Based and Conflict-Based Safety Evaluations: The Case of Right-Turn Smart Channels. *Accident Analysis and Prevention,* Volume 59, pp. 260-266.

SAE International, 2014. *AUTOMATED DRIVING LEVELS OF DRIVING AUTOMATION ARE DEFINED IN NEW SAE INTERNATIONAL STANDARD J3016.* [Online]
Available at: https://www.sae.org/misc/pdfs/automated_driving.pdf
[Accessed 10 May 2017].

Salkham, A., Cunningham, R., Garg, A. & Cahill, V., 2008. A collaborative reinforcement learning approach to urban traffic control optimization. *In Proceedings of the 2008 IEEE/WIC/ACM International Conference on Web Intelligence and Intelligent Agent Technology. IEEE Computer Society,* pp. 560-566.

Sawalha, Z. & Sayed, T., 2001. Evaluating safety of urban arterial roadways. *Journal of Transportation Engineering,* 127(2), pp. 151-158.

Sawalha, Z. & Sayed, T., 2006a. Transferability of accident prediction models. *Safety science,* 44(3), pp. 209-219.

Sawalha, Z. & Sayed, T., 2006b. Traffic accident modeling: some statistical issues. *Canadian Journal of Civil Engineering,* 33(9), pp. 1115-1124.

Sayed, T. & de Leur, P., 2007. Evaluation of intersection safety camera program in Edmonton, Canada. *Transportation Research Record: Journal of the Transportation Research Board,* Volume 2009, pp. 37-45.

Sayed, T. & Zein, S., 1999. Traffic Conflict Standards for Intersections. *Transportation Planning and Technology,* Issue 22, pp. 309-323.

Shabestary, S. & Abdulhai, B., 2018. Deep Learning vs. Discrete Reinforcement Learning for Adaptive Traffic Signal Control. *21st International Conference on Intelligent Transportation Systems (ITSC),* pp. 286-293.

Shahdah, Usama, Saccomanno, F. & Bhagwant , P., 2014. Integrated traffic conflict model for estimating crash modification factors. *Accident Analysis & Prevention,* Issue 71, pp. 228-235.

Shi, Q. & Abdel-Aty, M., 2015. Big data applications in real-time traffic operation and safety monitoring and improvement on urban expressways. *Transportation Research Part C: Emerging Technologies,* Volume 58, pp. 380-394.

Shoufeng, L., Ximin, L. & Shiqiang, D., 2008. Q-Learning for adaptive traffic signal control based on delay minimization strategy. *IEEE International Conference on Networking, Sensing and Control,* pp. 687-691.

Sikder, S., Augustin, B., Pinjari, A. R. & Eluru, N., 2014. Spatial Transferability of Tour-Based Time-of-Day Choice Models. *Transportation Research Record: Journal of the Transportation Research Board,* 1(2429), pp. 99-109.

Sims, A., 1979. *SCAT-The Sydney coordinated adaptive traffic system.* Pacific Grove, California, USA, Engineering Foundation Conference on Research Directions in Computer Control of Urban Traffic Systems.

So, J. et al., 2015. Development and evaluation of an enhanced surrogate safety assessment framework. *Transportation research part C: emerging technologies,* Volume 50, pp. 51-67.

Songchitruksa, P. & Tarko, A. P., 2006. The extreme value theory approach to safety estimation. *Accident Analysis & Prevention,* 38(4), pp. 811-822.

Srinivasan, R. & Carter, D., 2011. *Development of safety performance functions for North Carolina (No. FHWA/NC/2010-09),* Chapel Hill, NC: North Carolina Department of Transportation, Research and Analysis Group.

Srinivasan, R. et al., 2016. Estimation of calibration functions for predicting crashes on rural two-lane roads in Arizona. *Transportation Research Record: Journal of the Transportation Research Board,* Volume 2583, pp. 17-24.

Stevanovic, A., Kergaye, C. & Haigwood, J., 2011. *Assessment of surrogate safety benefits of an adaptive traffic control system.* Indianapolis, 3rd International Conference on Road Safety and Simulation.

Stevanovic, A., Stevanovic, J. & Kergaye, C., 2013. Optimization of traffic signal timings based on surrogate measures of safety. *Transportation research part C: emerging technologies,* Volume 32, pp. 159-178.

Stevanovic, A., Stevanovic, J., So, J. & Ostojic, M., 2015. Multi-criteria optimization of traffic signals: Mobility, safety, and environment. *Transportation Research Part C: Emerging Technologies,* Volume 55, pp. 46-68.

Sun, C. et al., 2014. *Calibration of the HSM's SPFs for Missouri. Publication CMR14-007,* Missouri: Missouri Department of Transportation.

Sutton, R. S. & Barto, A. G., 1998. *Reinforcement Learning: An Introduction.* s.l.:The MIT Press.

Tageldin, A., Sayed, T., Zaki, M. & Azab, M., 2014. A Safety Evaluation of an Adaptive Traffic Signal Control System using Computer Vision. *Advances in Transportation Studies,* 2(Special Issue), pp. 83-96.

The Ontario Centers of Excellence, 2017. *Connected Vehicle/Automated Vehicle (CVAV) Program. "How it Works?".* [Online]
[Accessed 8 May 2017].

Theofilatos, A., 2017. Incorporating real-time traffic and weather data to explore road accident likelihood and severity in urban arterials. *Journal of safety research,* Volume 61, pp. 9-21.

Thorpe, T. & Anderson, C., 1996. *Traffic light control using sarsa with three state representations,* s.l.: Technical report, Citeseer.

Transport Canada, 2016. *Canadian Motor Vehicle Traffic Collision Statistics 2014.* [Online]
Available at: https://www.tc.gc.ca/media/documents/roadsafety/cmvtcs2014_eng.pdf
[Accessed 17 May 2017].

Treiber, M., Hennecke, A. & Helbing, D., 2000. Congested traffic states in empirical observations and microscopic simulations. *Physical review E,* 62(2), p. 1805.

U.S. Department of Transportation, 2015. *ITS Research 2015-2019: Connected Vehicle (Connected Vehicles: Benefits, Roles, Outcomes).* [Online]
Available at: https://www.its.dot.gov/research_areas/WhitePaper_connected_vehicle.htm
[Accessed 12 May 2017].

U.S. Department of Transportation, 2017. *How Connected Vehicels Work.* [Online]
Available at: https://www.its.dot.gov/factsheets/pdf/JPO_HowCVWork_v3.pdf
[Accessed 15 May 2017].

US DOT, 2018. *Next Generation Simulation (NGSIM) Vehicle Trajectories and Supporting Data.* [Online]
Available at: https://data.transportation.gov/Automobiles/Next-Generation-Simulation-NGSIM-Vehicle-Trajector/8ect-6jqj
[Accessed March 2018].

van der Horst, R. & Hogema, J., 1993. *Time-to-collision and collision avoidance systems.* s.l., s.n.

Vogt, A. & Bared, J., 1998. Accident models for two-lane rural segments and intersections. *Transportation Research Record: Journal of the Transportation Research Board,* Volume 1635, pp. 18-29.

Wang, X. & Abdel-Aty, M., 2008. Modeling left-turn crash occurrence at signalized intersections by conflicting patterns. *Accident Analysis & Prevention,* 40(1), pp. 76-88.

Wang, X., Abdel-Aty, M. & Brady, P., 2006. Crash estimation at signalized intersections: significant factors and temporal effect.. *Transportation Research Record: Journal of the Transportation Research Board,* Volume 1953, pp. 10-20.

University of British Columbia
Department of Civil Engineering

Watkins, C., 1989. *Learning from delayed rewards (Doctoral dissertation).* Cambridge: King's College, .

Watkins, C. & Dayan, P., 1992. Q-learning. *Machine learning,* pp. 279-292.

Wiedemann, R., 1974. Simulation des Straßenverkehrsflusses. *Schriftenreihe des Instituts für Verkehrswesen der Universität Karlsruhe, Heft 8.*

Wiedemann, R., 1991. Modeling of RTI-Elements on multi-lane roads. *Advanced Telematics in Road Transport edited by the Commission of the European Community, DG XIII, Brussels .*

Wiering, M., 2000. Multi-agent reinforcement learning for traffic light control. *Machine Learning: Proceedings of the Seventeenth International Conference (ICML'2000),* pp. 1151-1158.

Wong, S. C., Sze, N. N. & Li, Y. C., 2007. Contributory factors to traffic crashes at signalized intersections in Hong Kong. *Accident Analysis & Prevention,* 39(6), pp. 1107-1113.

Wu, Y. et al., 2017a. Comparison of proposed countermeasures for dilemma zone at signalized intersections based on cellular automata simulations. *Accident Analysis & Prevention.*

Wu, Y., Abdel-Aty, M. & Lee, J., 2017b. Crash risk analysis during fog conditions using real-time traffic data. *Accident Analysis & Prevention,* Volume 114, pp. 4-11.

Xie, F., Gladhill, K., Dixon, K. & Monsere, C., 2011. Calibration of highway safety manual predictive models for Oregon state highways. *Transportation Research Record: Journal of the Transportation Research Board,* Volume 2241, pp. 19-28.

Xu, B. et al., 2017. V2I based cooperation between traffic signal and approaching automated vehicles. *Intelligent Vehicles Symposium (IV). IEEE,* pp. 1658-1664.

Xu, C., Tarko, A., Wang, W. & Liu, P., 2013. Predicting crash likelihood and severity on freeways with real-time loop detector data. *Accident Analysis & Prevention,* Volume 57, pp. 30-39.

Yang, K., Guler, S. & Menendez, M., 2016. Isolated intersection control for various levels of vehicle technology: Conventional, connected, and automated vehicles. *Transportation Research Part C: Emerging Technologies,* Volume 72, pp. 109-129.

Young, J., Park, P. & Eng, P., 2012. *Comparing the Highway Safety Manual's Safety Performance Functions with Jurisdiction-Specific Functions for Intersections in Regina.* Fredericton, New Brunswick, In Annual Conference of the Transportation Association of Canada.

Zhang, X. et al., 2014. Modeling the Frequency of Opposing Left-Turn Conflicts at Signalized Intersections Using Generalized Linear Regression Models. *Traffic injury prevention,* 15(6), pp. 645-651.

Zheng, L., Saayed, T., Essa, M. & Guo, Y., 2019c. *Do Simulated Traffic Conflicts Predict Crashes? An Investigation Using the Extreme Value Approach.* Auckland, New Zealand, IEEE Intelligent Transportation System Conference.

Zheng, L., Sayed, T. & Essa, M., 2019a. Bayesian hierarchical modeling of the non-stationary traffic conflict extremes for crash estimation. *Analytic Methods in Accident Research,* Volume 23, p. 100100.

Zheng, L., Sayed, T. & Essa, M., 2019b. Validating the bivariate extreme value modeling approach for road safety estimation with different traffic conflict indicators. *Accident Analysis & Prevention,* Volume 123, pp. 314-323.

Zheng, Z., Ahn, S. & Monsere, C., 2010. Impact of traffic oscillations on freeway crash occurrences. *Accident Analysis & Prevention,* 42(2), pp. 626-636.